Modeling plant biomass partitioning: responses to environmental conditions and disturbance

Gianni Boris Pezzatti

A thesis submitted in
fulfillment of the requirement for the award of the
Degree of Doctor of Philosophy

Università degli Studi di Napoli Federico II

Supervisor: Prof. Stefano Mazzoleni
Co-Supervisor: PhD. Marco Conedera
Co-Supervisor: PhD. Francesco Giannino

November 30, 2011

Ad Anna*, che fino all'ultimo è quasi riuscita a non sostenermi in questa tesi,*

a Zeno*, che chiede se il "dottorato" sia come il "Dottor Hudson",*

e a chi, senza mai vedere il sole, é rimasto nel mio cuore.

Acknowledgments

I want to warmly thank all the people that supported me during this thesis. It has been a great experience, both from a professional and human perspective. I really enjoyed the hospitality and willingness of the people I met in Naples, in particular of all the staff of the Laboratorio di Ecologia Applicata in Portici. A big thank also to the WSL staff in Bellinzona, for their help and welcoming atmosphere.

In particular I would like to thank

Stefano, for sharing his incredible enthusiasm, wise suggestions and for being a skillful guide through the process of model development, aiming at unveiling the essential processes able to reproduce the observed, emerging complexity

Francesco, for effectively teaching me the technical aspects of system dynamics and the basics of the Naples' way of life (e.g. how to cross a street without being run over)

Marco, for his fundamental contribution in the revision of the manuscript and for his advises on sampling design and dendrometric details

Eric, for his incredible work during the field campaign and his master thesis, contributing considerably to the present work

Patrik, for his experienced support in scanning parameterization and digital image analysis

Franco, for his help in the field work.

And last but not list, I wish to thank my family, *Anna*, *Zeno* and my parents, for sharing with me the good and the bad, the funny and the difficult moments of this period, *supporting* the idea of this thesis and *"sopporting"* when I was away from home for it.

Gianni Boris Pezzatti,

Portici, lì 30.11.2011

Abstract

The aim of the present thesis is to contribute to the understanding of the plant phenotypic responses to environmental conditions and disturbances. In particular, the value of the pipe model theory as a measure of morphological plasticity of chestnut tree (*Castanea sativa* Mill.) in relation to the site conditions was assessed, and the main physiological mechanisms underlying biomass allocation were theoretically explored using modeling technics.

The constancy of the leaf to sapwood area slope coefficient *(LASA)* in *C. sativa* was confirmed at the intra-branch level, but showed a considerable variability among branches within a tree. In particular the *LASA* changed according to branch type (crown branches vs. epicormic shoots) and declined with height. With a generalized linear mixed modeling approach, a new reference parameter (*Ground-level LASA*), corresponding to a theoretical value of *LASA* for a branch at ground level, was proposed and validated on an independent dataset. The variation of this measure was investigated in different environmental conditions, confirming that the sweet chestnut is able to greatly vary the allocation patterns. In particular, the *Ground-level LASA* was high for trees growing in sites with good water supply (concave sites) and low in water poor convex sites. The analysis of the stool uprooting phenomena in over-aged coppice stands provided an indirect evidence of the role of microtopography and water availability in the allocation patterns between above and below ground biomass.

In order to further theoretically explore the key issue of biomass partitioning in plants, a fairly simple model of allocation was developed, based on the interactions between water and carbon transport processes with assimilation and growth. The model is able to reproduce consistent deviations from the allometric trajectory, showing qualitatively correct responses in a range of different environmental conditions (light and water) and during recovery from unbalanced biomass removal (e.g. recover after pruning or fire damages). In this respect this model has the potential to be a good instrument for theoretical investigation of relations between anatomical (e.g. sclerophylly) and functional (e.g. transport resistances) characters and allocation patterns.

Contents

List of Tables

List of Figures

Chapter 1

Biomass allocation and plasticity in plants

Introduction

Allocation is a concept of crucial importance in life history theory (Stearns, 1992), and the individual strategies of partitioning play a central role in shaping species distribution and dominance in diverse environments. The extreme variety of life forms, which evolved under the natural selection, is astonishing. Plants for instance had to adapt to extreme conditions regarding water (e.g. deserts), temperature (e.g. boreal forests) and radiation (e.g. sites at high altitudes). While in the last two cases, evolution led to the development of either secondary metabolites or protective tissues, water availability has been a major driver for shaping form and in the development of organs for both water storage and transpiration reduction.

Along a gradient of decreasing water resources we can classify vascular plants into hydro-, meso- and xerophytes, which gradually display an higher relative allocation to roots compared to the above ground organs (Kramer, 1983), an increased stomatal control (Raven, 2002; Brodribb & McAdam, 2011; Ruszala *et al.* , 2011) and more frequent cases of sclerophylly. Although this last adaptation may be also related to promoting leaf longevity in resource-poor environments (Turner, 1994), rather than directly to water relations (Salleo & Lo Gullo, 1990; Salleo *et al.* , 1997). Aquatic plants and cacti are extreme examples on this gradient, reaching absence of either root or shoot biomass respectively (Figure 1.1).

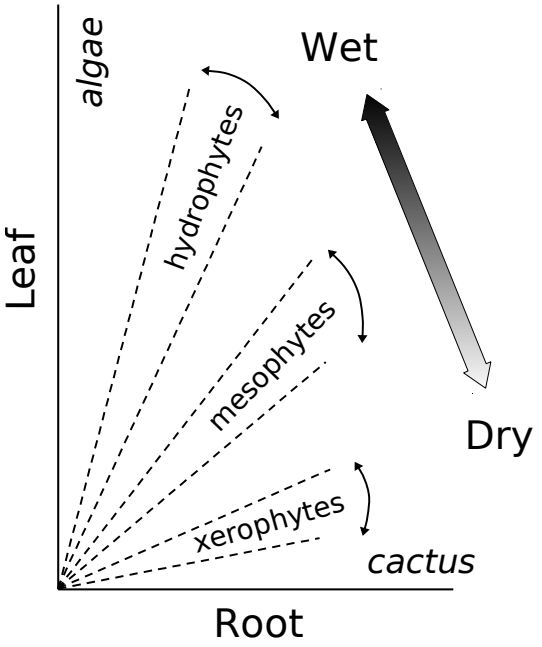

Figure 1.1: General representation of different biomass allocation patterns in plants along a gradient of water availability. Dashed lines represent limits of phenotypic plasticity within each life form to balance for variable environmental conditions (redrawn and adapted from Mazzoleni & Spada, 1992).

Moreover, plants, being sessile organisms, have to cope with environmental changes and disturbances through exogenous factors. The ability of an organism to dynamically change its strategies (phenotypic plasticity, Fordyce, 2006) is a key issue for survival and for the potential colonization of adjacent areas (Figure 1.1). In this respect, the ongoing climate

change phenomena will have a major impact in many ecosystems, with increasing temperatures (Kattenberg, 1996) and water becoming even more a limiting factor (García-Fayos *et al.* , 2000; Maherali *et al.* , 2004; Bochet *et al.* , 2007). In this scenario, a better understanding of ecological plasticity is of paramount importance to predict plant responses and possible adaptations (Weiher *et al.* , 1999; Parmesan, 2006; Ghalambor *et al.* , 2007).

However, the underlying mechanisms of the phenotypic variation (physiological, morphological and functional plasticity) are still largely unknown, even if the diverse responses to various environments have been characterized in many studies (Sultan, 2004). In particular, also the formulation of allocation in models remains a weak point of current plant modeling (Roux *et al.* , 2001; Minchin & Lacointe, 2005), with the phenomena often formulated with simple empirical terms or teleonomic approaches. Although these goal-seeking models may be appealing and useful, Thornley (1998) categorized them as a "cul-de-sac", since in a progressive modeling endeavour only a mechanistic framework should be properly considered.

Pipe model theory

The study of organism shapes and allometry has a long tradition (e.g. Thompson, 1917; Huxley, 1932; Niklas, 2004). Regarding tree structures, already Leonardo Da Vinci (1452-1519), observing the branching patterns of a tree, postulated the theory that *"the sum of cross-sectional areas of branches at any height equals to the cross-sectional area of the trunk"* (Richter, 1970), later known as the Da Vinci's rule (Figure 1.2). In the last century, Huber (1928) found a constancy of the sapwood cross-section (or the branch cross-section) divided by the leaf dry weight (or area) distal to the branch (known as the Huber value HV, Zimmermann, 1983), adding a functional concept to the branching rules of Leonardo. Supposing a conservative relation between structure and functioning,

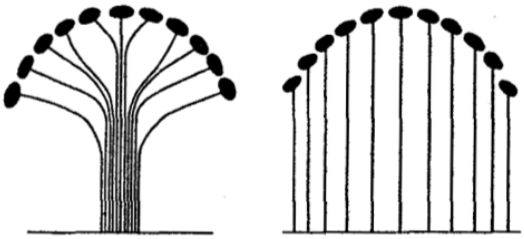

Figure 1.3: Diagrams representing the pipe model theory, at the tree (*left*) or stand (*right*) level (image copied and reversed from the original publication of Shinozaki *et al.* , 1964a). Vertical lines are unit pipes, and filled circles are unit amounts of leaves.

Shinozaki *et al.* (1964a,b) observed that *"the amount of leaves existing in and above a certain horizontal stratum in the plant community is directly proportional to the amount of the stems and branches existing in that horizon"*. This rule is also known as "pipe model theory": the xylem conductive tissue of woody plants is assumed to correspond to an assemblage of pipe units supporting a correspondent sector of leaves each, which results in a constant ratio between leaf area (LA) and sapwood area (SA) within a single branch, a tree or a stand (Figure 1.3).

This hypothesis has been supported by many studies (e.g. Kaufmann & Troendle, 1981; Waring *et al.* , 1982; Mazzoleni & Schirone, 1990; Bartelink, 1997; Infante *et al.* , 2001; Sone *et al.* , 2009), and some authors (e.g. Mazzoleni, 1990; White *et al.* , 1998; Gotsch *et al.* , 2010) reported its variation according to the site conditions (e.g. water and nutrients availability), highlighting the potential usefulness of the $\frac{LA}{SA}$ ratio for environmental research.

This measure gives, indeed, an insight into the plant water relations, bridging the evaporative surface with the conducting tissues. However the value in some species was found to decrease with tree height (e.g. Mencuccini & Grace, 1996a; McDowell *et al.* , 2002a) and age, and to change according to management practices (Aussenac & Granier, 1988; Pothier & Margolis, 1991). The use of $\frac{LA}{SA}$ ratios

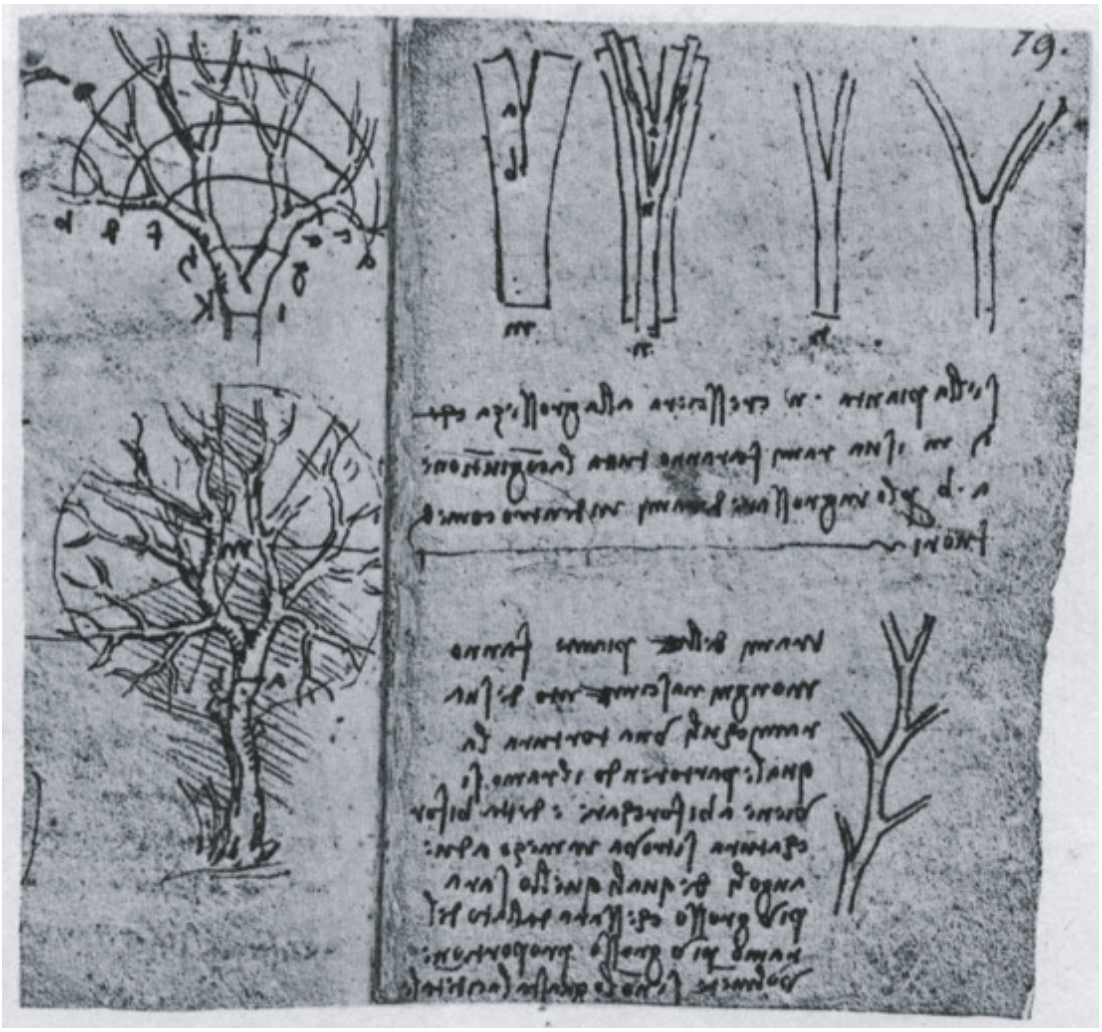

Figure 1.2: Sketches of Leonardo Da Vinci (1452-1519) for branching rules, from Richter (1970).

for environmental studies need therefore some precautions (Cruiziat *et al.* , 2002) and the investigation of the species specific behaviour of this allometric measure.

Understanding the relation of the $\frac{LA}{SA}$ ratio of a given species with the site conditions by means of empirical models with regression analysis should already allow useful applications at the stand level, like the mapping of potential drought sensibility or uprooting danger. However, the validity of these predictions are often limited to conditions similar of those of the sampling region, while only a mechanistic understanding of the involved processes can eventually capture the full complexity of the phenomena, allowing for a broader application. To this scope process-based models represent a useful instrument, allowing the qualitative testing of the underlying mechanisms of the observed phenomena.

Models of partitioning

As already stated, the implementation of allocation processes still remains a weak point of current plant modeling (Roux *et al.* , 2001; Minchin & Lacointe, 2005). Different approaches have been used to represent biomass partitioning in plant models (Wilson, 1988a; Dewar, 1993; Cannell & Dewar, 1994; Lacointe, 2000; Mäkelä *et al.* , 2000; Prusinkiewicz *et al.* , 2007), including empirical coefficients, functional balance, allometric relationships, transport resistance (TR) and source-sink models (Roux *et al.* , 2001).

Allocation models based on fixed coefficients, functional balance, and allometry are of empirical nature. They have been mostly used in models with yearly timesteps, while TR and source-sink models, with their more mechanistic basis of the dynamics of carbon and water transport pathways, usually have been applied at daily timesteps (Roux *et al.* , 2001). In fact, the mass flow described by Münch (1927, 1930) is now widely accepted to be the mechanism of assimilate transfer and allocation (Lacointe, 2000; Minchin & Lacointe, 2005). To this respect, TR models represent a better process-based approach, with explicit (more or less simplified) mechanical functioning of the assimilate flows, by differences of potentials (or concentrations), conducting areas, transport resistance and pathway length. On the other hand, source-sink approaches in part implicitly include those processes, by relating the transport to the sink-strength (or sink ability) of an organ, considered as an estimate of potential differences between sources and sinks. Because of this simplification, the source-sink approach has been more widely used in the case of models with fine-grained organs scale (plant models with an explicit architecture, e.g. L-system-based models), while the more mechanistic TR design has been applied with bulk-compartments, presumably due to the difficulty of estimating local transport parameters (Roux *et al.* , 2001; Minchin & Lacointe, 2005).

However, more recently the TR approach has been successfully applied also to more fine-grained models, using analogies with electrical circuits. Examples are the work by Daudet (2002) that developed a model coupling allocation to a detailed representation of the Munch flow and Da Silva *et al.* (2010) that included a water circuit into L-Peach, in order to link water stress effects to carbon partitioning. Nonetheless the high computational needs of these models do not allow applications at the community scale.

To this purpose, an approach with larger modules or with a simplification of the mechanistic process is still needed (Minchin & Lacointe, 2005). At this scale, only few models have been focused on the response of biomass allocation to water stress (e.g. see Dewar, 1993; Chen & Reynolds, 1997), being more focused on interactions of growth and nutrient availability (e.g. Thornley, 1972a,b).

Furthermore, the specific effects of disturbance on biomass allocation in plants has not been sufficiently understood and, so far, never included in dynamic representation of partitioning models. This is a critical issue to be considered for both the-

oretical understanding and applications of allocation models in ecology. For instance, complex responses arising from the interaction of disturbance and particular climatic events, like increased drought susceptibility after fire (Mazzoleni & Pizzolongo, 1990) or cut (Mazzoleni & Dickmann, 1988), may become of crucial importance in light of the ongoing climate change.

A specific comment can be done about the plant models used as modules of larger integrated models applied in the analysis of global change issues. The current state of the art is quite poor, with the use of empirically derived allometric relationships being applied at global scale (Friedlingstein *et al.* , 1999; Barnes *et al.* , 2007), and still producing large variations in estimates of global carbon flux and storage (Ise *et al.* , 2010). Still there is little understanding of the underlying processes (Litton *et al.* , 2007; Ise *et al.* , 2010) and little capability of capturing eventual feedbacks on emergent properties at ecosystem levels, mediated by the dynamics of the allocation behaviour of plants.

Aims

The present thesis has two major aims: to better understand the morphological plasticity of *C. sativa* related to environmental variability, and with modeling technics to develop a theoretical exploration of the main physiological mechanisms underlying biomass allocation. A particular focus has been laid on plant water relations, being the role of water availability a major driver of plant form at the local scale. To this purpose the following two parallel research paths were covered:

- The pipe model theory of Shinozaki *et al.* (1964a) applied on small branches of *C. sativa* was investigated, assessing its value as a measure of plant phenotypic response in relation to site conditions, first by testing its suitability (Chapter 2) and secondly by finding the main environmental determinants of its variation (Chapter 3). This findings were then compared to a dataset on stool uprooting in over-aged coppice stands (Chapter 4), in order to derive some practical implications of the pipe model regarding tree stability.
- In Chapter 5 an absolutely generic individual plant model with dynamic biomass allocation was developed, based on an explicit representation of phloematic transport by Munch flow and of water relations, implemented as diffusive processes in a porous medium, according to Darcy's law. The model is aimed to a dynamic representation of allocation behaviours, targeting the integration as a partitioning module in large integrated models (e.g. Barnes *et al.* , 2007). Despite its minimal representation of the crucial processes involved in above and below-ground resource partitioning, it still captures the qualitatively correct responses to environmental conditions (light and water availability) and disturbances (e.g. post-fire regrowth, recover after pruning or pathogenous attack).

References

Aussenac, Gilbert, & Granier, André. 1988. Effects of thinning on water stress and growth in douglas-fir. *Canadian journal of forest research*, **18**(1), 100–105.

Barnes, Belinda, Mokany, Karel, & Roderick, Michael. 2007. Allocation within a generic scaling framework. *Ecological modelling*, **201**(2), 223–232.

Bartelink, H. H. 1997. Allometric relationships for biomass and leaf area of beech (fagus sylvatica l). *Annales des sciences forestières*, **54**(1), 12–12.

Bochet, E., García-Fayos, P., Alborch, B., & Tormo, J. 2007. Soil water availability effects on seed germination account for species segregation in semiarid roadslopes. *Plant and soil*, **295**(1 - 2), 179 – 191.

Brodribb, Tim J., & McAdam, Scott A. M. 2011. Passive origins of stomatal control in vascular plants. *Science*, **331**.

Cannell, M. G. R., & Dewar, R. C. 1994. Carbon allocation in trees: a review of concepts for modelling. *Advances in ecological research*, **25**, 59–104.

Chen, JL, & Reynolds, JF. 1997. A coordination model of whole-plant carbon allocation in relation to water stress. *Annals of botany*, **80**(1), 45–55.

Cruiziat, P., Cochard, H., & Ameglio, T. 2002. Hydraulic architecture of trees: main concepts and results. *Annals of forest science*, **59**(7), 723–752.

Da Silva, D, Favreau, R, Auzmendi, I, & DeJong, T. 2010 (September 12-17). Linking water stress effects on carbon partitioning by introducing a xylem circuit into l-peach. *In: Proceedings of the 6th international workshop on functional-structural plant models*. University of California, Davies.

Daudet, F. 2002. Generalized münch coupling between sugar and water fluxes for modelling carbon allocation as affected by water status. *Journal of theoretical biology*, **214**(3), 498, 481.

Dewar, R. C. 1993. A root-shoot partitioning model based on carbon-nitrogen-water interactions and munch phloem flow. *Functional ecology*, 356–368.

Fordyce, J. A. 2006. The evolutionary consequences of ecological interactions mediated through phenotypic plasticity. *Journal of experimental biology*, **209**(12), 2377 – 2383.

Friedlingstein, P., Joel, G., Field, C. B., & Fung, I. Y. 1999. Toward an allocation scheme for global terrestrial carbon models. *Global change biology*, **5**(7), 755–770.

García-Fayos, P., García-Ventoso, B., & Cerdà, A. 2000. Limitations to plant establishment on eroded slopes in southeastern spain. *Journal of vegetation science*, **11**(1), 77 – 86.

Ghalambor, C. K., Mckay, J. K., Carroll, S. P., & Reznick, D. N. 2007. Adaptive versus nonadaptive phenotypic plasticity and the potential for contemporary adaptation in new environments. *Functional ecology*, **21**(3), 394 – 407.

Gotsch, Sybil G., Geiger, Erika L., Franco, Augusto C., Goldstein, Guillermo, Meinzer, Frederick C., & Hoffmann, William A. 2010. Allocation to leaf area and sapwood area affects water relations of co-occurring savanna and forest trees. *Oecologia*, **163**(Jan.), 291–301.

Huber, Bruno. 1928. Weitere quantitative untersuchungen über das wasserleitungssystem der pflanzen. *Jahrb. wiss. bot.*, **67**, 877–959.

Huxley, Julian S. 1932. *Problems of relative growth*. London: Methuen and Co.

Infante, Juan Manuel, Mauchamp, André, Fernández-Alés, Rocío, Joffre, Richard, & Rambal, Serge. 2001. Within-tree variation in transpiration in isolated evergreen oak trees: evidence in support of the pipe model theory. *Tree physiology*, **21**(6), 409–414.

Ise, Takeshi, Litton, Creighton M., Giardina, Christian P., , & Ito, Akihiko. 2010. Comparison of modeling approaches for carbon partitioning: Impact on estimates of global net primary production and equilibrium biomass of woody vegetation from modis gpp. *Journal of geophysical research*, **115**, 1–11.

Kattenberg, A. 1996. Climate models: Projections of future climate.

Kaufmann, Merrill R., & Troendle, Charles A. 1981. The relationship of leaf area and foliage biomass to sapwood conducting area in four subalpine forest tree species. *Forest science*, **27**(Sept.), 477–482.

Kramer, Paul Jackson. 1983. *Water relations of plants*. Academic P.,U.S.

Lacointe, André. 2000. Carbon allocation among tree organs: A review of basic processes and representation in functional-structural tree models. *Annals of forest science*, **57**(5-6), 13 pages.

Litton, CM, Raich, JW, & Ryan, MG. 2007. Carbon allocation in forest ecosystems. *Global change biology*, **13**, 2089–2109.

Maherali, H., Pockman, W. T., & Jackson, R. B. 2004. Adaptive variation in the vulnerability of woody plants to xylem cavitation. *Ecology*, **85**(8), 2184 – 2199.

Mazzoleni, S., & Spada, F. 1992. *Responses of forest ecosystems to environmental changes*. Elsevier Applied Science,London and New York. Chap. Deciduous broadleaved versus evergreen sclerophyllous forests. Disturbance and local shifting dominance in Mediterranean environments., page 839?840.

Mazzoleni, Stefano. 1990. Relazioni tra aree fogliari e superfici di conduzione nel fusto nell'analisi di gradienti ambientali. *Linea ecologica*, 27–30.

Mazzoleni, Stefano, & Dickmann, Donald I. 1988. Differential physiological and morphological responses of two hybrid populus clones to water stress. *Tree physiol*, **4**(1), 61–70.

Mazzoleni, Stefano, & Pizzolongo, Paolo. 1990. *Post-fire regeneration patterns of mediterranean shrubs in the Campania region, Southern Italy*. SPB Academic Publishing bv. Pages 43–51.

Mazzoleni, Stefano, & Schirone, B. 1990. Allometric estimations of woody and foliar biomass. applications on quercus cerris sprouts and mediterranean shrubs. *Annali di botanica*, **XVIII**.

McDowell, N., Barnard, H., Bond, B., Hinckley, T., Hubbard, R., Ishii, H., i, B. Kästner, Magnani, F., Marshall, J., Meinzer, F., Phillips, N., Ryan, M., & Whitehead, D. 2002a. The relationship between tree height and leaf area: sapwood area ratio. *Oecologia*, **132**(1), 12–20.

Mencuccini, M., & Grace, J. 1996a. Developmental patterns of above-ground hydraulic conductance in a scots pine (pinus sylvestris l.) age sequence. *Plant, cell and environment*, **19**(8), 939 – 948.

Minchin, P. E. H., & Lacointe, A. 2005. New understanding on phloem physiology and possible consequences for modelling long-distance carbon transport. *New phytologist*, **166**(3), 771–779.

Mäkelä, Annikki, Landsberg, Joe, Ek, Alan R., Burk, Thomas E., Ter-Mikaelian, Michael, Agren, Goran I., Oliver, Chadwick D., & Puttonen, Pasi. 2000. Process-based models for forest ecosystem management: current state of the art and challenges for practical implementation. *Tree physiol*, **20**(5-6), 289–298.

Münch, E. 1927. Dynamik der saftströmungen. *Bericht der deutschen botanischen gesellschaft*, **44**, 69–71.

Niklas, Karl J. 2004. Plant allometry: is there a grand unifying theory? *Biol. rev.*, **79**, 871–889.

Parmesan, C. 2006. Ecological and evolutionary responses to recent climate change. *Annual review of ecology evolution and systematics*, **37**, 637 – 669.

Pothier, D., & Margolis, A. 1991. Analysis of growth and light interception of balsam fir and white birch saplings following precommercial thinning. *Annales des sciences forestières*, **48**(2), 10–10.

Prusinkiewicz, P, Allen, M, Escobar-Gutierrez, A, & DeJong, TM. 2007. *Functional-structural plant modelling in crop production*. Wageningen: Frontis. Chap. Numerical methods for transport- resistance sink-source allocation models, pages 123–138.

Raven, JA. 2002. Selection pressures on stomatal evolution. *New phytologist*, **153**(3), 371–386.

Richter, J.P. 1970. *The notebooks of leonardo da vinci*. Dover, New York: Dover.

Roux, XL, Lacointe, A, Escobar-Gutiérrez, A, & Dizès, SL. 2001. Carbon-based models of individual tree growth: A critical appraisal. *Annals of forest science*, **58**, 469–506.

Ruszala, Elizabeth M., Beerling, David J., Franks, Peter J., Chater, Caspar, Casson, Stuart A., Gray, Julie E., & Hetherington, Alistair M. 2011. Land plants acquired active stomatal control early in their evolutionary history. *Current biology*, **21**, 1030–1035.

Salleo, S., & Lo Gullo, M. A. 1990. Sclerophylly and plant water relations in three mediterranean quercus species. *Annals of botany*, **65**(3), 259–270.

Salleo, S., Nardini, A., & Lo Gullo, M. A. 1997. Is sclerophylly of mediterranean evergreens an adaptation to drought? *New phytologist*, **135**, 603–612.

Shinozaki, K, Yoda, K, Hozumi, K, & Kira, T. 1964a. A quantitative analysis of plant form – the pipe model theory i. basic analyses. *Japanese journal of ecology*, **14**(3), 97–105.

Shinozaki, K, Yoda, K, Hozumi, K, & Kira, T. 1964b. A quantitative analysis of plant form – the pipe model theory ii. further evidence of the theory and its application in forest ecology. *Japanese journal of ecology*, **14**(4), 133–139.

Sone, Kosei, Suzuki, Alata Antonio, Miyazawa, Shin-Ichi, Noguchi, Ko, & Terashima, Ichiro. 2009. Maintenance mechanisms of the pipe model relationship and leonardo da vinci-s rule in the branching architecture of acer rufinerve trees. *Journal of plant research*, **122**(Aug.), 41–52.

Stearns, SC. 1992. *The evolution of life histories*. Oxford: Oxford University Press.

Sultan, SE. 2004. Promising directions in plant phenotypic plasticity. *In: Perspectives in plant ecology, evolution and systematics*.

Thompson, D'Arcy W. 1917. *On growth and form*. Cambridge: Cambridge University Press.

Thornley, J. H. M. 1972a. A balanced quantitative model for root: Shoot ratios in vegetative plants. *Ann bot*, **36**(2), 431–441.

Thornley, J. H. M. 1972b. A model to describe the partitioning of photosynthate during vegetative plant growth. *Ann bot*, **36**(2), 419–430.

Thornley, JHM. 1998. Modelling shoot [ratio] root relations: the only way forward? *Annals of botany*, **81**(2), 165.

Turner, I. M. 1994. Sclerophylly: primarily protective? *Functional ecology*, **8**, 669–675.

Waring, R.H., Schroeder, P.E., & Oren, R. 1982. Application of the pipe model theory to predict canopy leaf-area. *Canadian journal of forest research*, **12**(3), 556–560.

Weiher, E., der Werf, A. Van, Thompson, K., Roderick, M., Garnier, E., & Eriksson, O. 1999. A common core list of plant traits for functional ecology. *Journal of vegetation science*, **10**(5), 609 – 620.

White, D., Beadle, Chris, Worledge, Dale, Honeysett, John, & Cherry, Maria. 1998. The influence of drought on the relationship between leaf and conducting sapwood area in eucalyptus globulus and eucalyptus nitens. *Trees - structure and function*, **12**(7), 406–414.

Wilson, J. Bastow. 1988a. A review of evidence on the control of shoot: Root ratio, in relation to models. *Ann bot*, **61**(4), 433–449.

Zimmermann, M. H. 1983. *Xylem structure and the ascent of sap*. Germany: Springer-Verlag.

Chapter 2

Applicability of the pipe model theory on chestnut tree *(Castanea sativa* Mill.*)*

With Gehring Eric[1], Krebs Patrik[1], Mazzoleni Stefano[2], Conedera Marco[1]

[1]WSL Swiss Federal Research Institute, Insubric Ecosystem Research Group. Via Belsoggiorno 22, CH-6500 Bellinzona, Switzerland

[2]University of Naples Federico II, Dip. di Arboricoltura, Botanica e Patologia vegetale, via Università 100 I-80055 Portici, Naples Italy

Keywords: leaf to sapwood area ratio, biomass allocation

Abstract

The pipe model theory postulates the constancy in the relationship between leaf to sapwood area for a whole tree and for its single parts. Variation of this relationship was investigated in 67 chestnut trees (*Castanea sativa* Mill.), analysing 183 crown branches and 41 reiterations (*sensu* Hallé) in order to test the correctness of this postulate for the chestnut tree. Results confirm the constancy of the leaf to sapwood area slope coefficient *(LASA)* at the intra-branch level but show a variability among branches within a tree. The *LASA* of crown branches declines with height, while for reiterations no clear patterns have been observed. Reiterations have enhanced sturdiness in respect to crown branches. A model for intra-tree *LASA* variability of crown branches is presented with a generalized linear mixed modelling approach and it is validated on an independent dataset, targeting the decrease of the variability within trees with respect to the variability among trees. The results are discussed in a physiological and practical application context.

Introduction

Physiology-related research topics are of paramount importance in understanding and preventing problems connected with global change such as plant adaptation to warming climate, competition with alien species, ecology and safe environment, plant productivity for food supply and bioresources (e.g. Le Maitre, 2004; Berger *et al.* , 2007; Kawachi *et al.* , 2007; Enquist *et al.* , 2007). Among them, analysis of tree structures is an important approach for understanding tree physiology and the related adaptation mechanisms to different ecological conditions and environmental stress factors (Schulze *et al.* , 1977; Cannell *et al.* , 1983; Ford, 1992).

Since the early decades of the 20th century plant architecture have had a determining influence on tree ecology and physiology (Arber, 1928, 1950). Starting from

the pioneer work of Hallé (e.g. Hallé & Oldeman, 1970; Hallé *et al.* , 1978; Hallé, 1981) different architectural empirical models and tree crown structure adaptation patterns have been defined (Tomlinson, 1982, 1987b) and studied in relation to water supply and adaptation to external factors (Ito *et al.* , 1995; Ishii *et al.* , 2007; Otoda & Ishii, 2008). The hydraulic architecture approach (Zimmermann, 1983), in particular, tries to link the plant architecture to physiological processes. In this modeling approach, the tree is viewed as an assembly of pipes where the water flows are driven and regulated by physical processes (Tyree & Ewers, 1991) as for instance electrical principles based on the Ohm's law such as resistance, capacitance, water potential, flow (Cruiziat *et al.* , 2002). Among the different approaches which have been worked out to get a better understanding of the building of this vascular system and of the relationship between roots, stem and leaves, many allometric relationships have been postulated basing on the relationship between the conducting pipes and the photosynthetic biomass (McDowell *et al.* , 2002a; Wright *et al.* , 2006; Gould & Harrington, 2008). Some are of static nature such as the Leonardo da Vinci's rule, assuming that the sum of cross-sectional branch area above a node is equal to the area of the stem below this node (Richter, 1970; Sone *et al.* , 2009), or the Huber value (HV), defined as the sapwood cross-section (or the branch cross-section) divided by the leaf area (or sometimes the leaf dry weight) distal to the branch (Huber, 1928; Zimmermann, 1983).

Supposing a conservative relation between structure and functioning, Shinozaki *et al.* (1964a,b,) proposed linking architecture and physiological processes of terrestrial plant forms in order to interpret and quantitatively analyze the resulting dynamic tree structure (Cruiziat *et al.* , 2002). According to the authors, *"the amount of leaves existing in and above a certain horizontal stratum in the plant community is directly proportional to the amount of the stems and branches existing in that horizon"* (Shinozaki *et al.* , 1964a). In practical terms, the xylem conductive tissue of woody plants is assumed to correspond to an assemblage of pipe units supporting a correspondent sector of leaves each (pipe model) what results in a constant ratio between leaf area (A_l) and sapwood area (A_s) within a single branch or a tree (Shinozaki *et al.* , 1964a,b).

Many following studies and experimental results supported the pipe model hypothesis (e.g. Waring *et al.* , 1982; Bartelink, 1997; Infante *et al.* , 2001; Sone *et al.* , 2009), founding evidences for the leaf to sapwood area relationship (e.g. Kaufmann & Troendle 1981; Mazzoleni & Schirone 1990; Waring & Gholz 1977; Whitehead *et al.* 1984) and encouraging the application of the pipe model approach for understanding processes of water conduction and storage (Mäkelä, 1986; Ewers & Zimmermann, 1984a,b; Yamamoto & Kobayashi, 1993), of the canopy conductance (Novick *et al.* , 2009), of the resource allocation within a tree and the resulting branching structure and tree architecture (Chiba, 1990; Kershaw *et al.* , 1990; Chiba, 1991; Nikinmaa, 1992; Chiba, 1998), and of the above ground forest productivity Magnani *et al.* (2000) or for indirectly estimate the leaf area, leaf mass or resource allocations using an easy-to-measure parameter such as the stem or sapwood cross section (Snell & Brown, 1978; Whitehead, 1978; Waring *et al.* , 1982). On the other hand, a number of studies exist highlighting that the $\frac{A_l}{A_s}$ ratio is not always consistent and may be influenced by several factors (Cruiziat *et al.* 2002). So, the $\frac{A_l}{A_s}$ ratio has been found to taper in a non-linear way along the trunk of a tree from the stump level to the crown break (Dean & Long, 1986; Waring *et al.* , 1982; White *et al.* , 1998), to decrease with tree height when applying hydraulic models based on the Darcy's law (e.g. Mencuccini & Grace, 1996a; McDowell *et al.* , 2002a), to be influenced by thinning practice (Aussenac & Granier, 1988; Pothier & Margolis, 1991) and to vary depending on site conditions (e.g. water and nutrients availability, Maz-

zoleni & Schirone, 1990; White *et al.* , 1998; Gotsch *et al.* , 2010).

Furthermore, the pipe model is subject to some basic criticisms. It is for instance observed that the conductive surface of a trunk or branch is a variable portion of the whole section and that the vessel diameter may greatly vary within the stem and branch systems (Zimmermann, 1978). When finally considering that the flux of a capillary is proportional to the fourth power of the radius, this all claims for a much more accurate sapwood area measurement approach as usually applied in pipe model studies. In addition, the pipe model misses considering some important physiological aspects, such as the different pathways length from soil to leaves that water has to go through to reach the leaves (Tyree & Ewers, 1991) or the branch autonomy paradigm stipulating that photosynthates produced in a branch are rarely transported to its neighboring branches (Sprugel *et al.* , 1991; Miyazaki *et al.* , 2002; Hasegawa *et al.* , 2003). Finally age and environment modify the inherited structural model of a plant on which the pipe model theory is based. It is thus possible that branches like crown suckers, which show different hydraulic behavior (Ishii *et al.* , 2007; Otoda & Ishii, 2008), display very different $\frac{A_l}{A_s}$ ratios with respect to normal structural branches.

From this short review one gets the impression that the pipe model may be a very useful tool for environmental research, but only if applied with some restrictions (Brix & Mitchell, 1983; Mencuccini & Grace, 1994; Cruiziat *et al.* , 2002) aiming to prevent oversimplifications of the model approach and misinterpretation of the related data. The overall aim of this paper is to verify the consistency and constancy of the model within branches and trees, using the European chestnut (*Castanea sativa* Mill.) as a case species. We in particular examined the model postulates at three different levels:

A within single branches;

B between different branch types, that is structural crown branches vs. reiterations.

C within a tree, including the analysis of factors influencing variations in the $\frac{A_l}{A_s}$ ratios

We finally discussed the results in the light of practical applications in the frame of environmental studies.

Material and methods

Study site

The sampled trees were located in the chestnut forests of the Insubric region of canton Ticino, Switzerland (Figure 2.1). It is an insubric region, with a moist warm temperate climate (annual mean precipitation: 1876 mm, annual mean temperature 11.3°C in Locarno-Monti; Spinedi & Isotta, 2004). The soils are generally classified as haplic podzol (cryptopodzol) on crystalline bedrock. The chestnut was introduced by the Romans nearly 2000 years ago (Tinner *et al.* , 1999) and became on acid soils the dominant tree species in the so called chestnut belt that stretches from 200 to 700-1000 m a.s.l. depending on the aspect. The chestnut tree is nowadays still present on different microtopographic conditions (from hump to mountain bottom and from extreme buttress to extreme depression).

Sampling design

A total of 224 branches belonging to 67 trees were sampled at locations with varying elevation, exposition, slope, and microtopography and at different tree heights and aspects. The branches were classified in two different types: normal (structural) crown branches and reiterations *sensu* Hallé *et al.* (1978) (epicormic shoots). Reiterations on chestnut tree are mainly due to damages caused by animals, fall of branches or crown parts and environmental stresses. If a chestnut with rough bark is considered, reiterations are distinguishable from crown branches because they usually have smooth bark, are located close to a

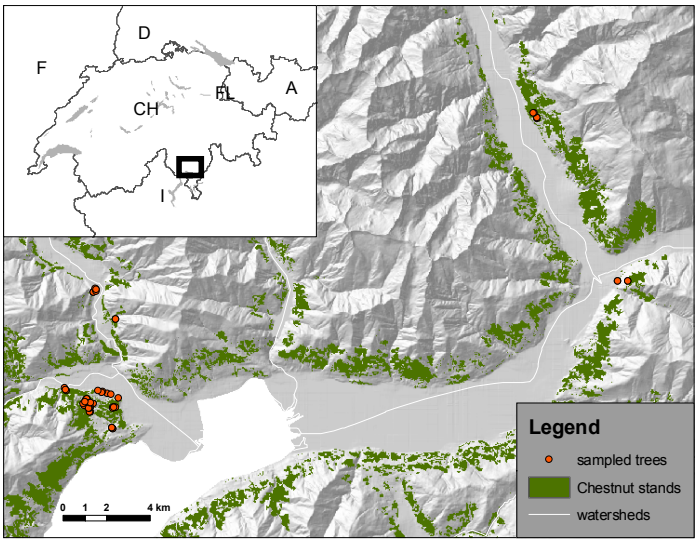

Figure 2.1: Study site

broken branch and are inserted in a different manner in the main trunk (Figure 2.2).

The sampled material was then differently used as function of the specific questions to be answered (Table 2.1):

A Constancy of the $\frac{A_l}{A_s}$ ratio within the single branch: the whole dataset (224 branches from 67 trees) was used.

B Consistency of the $\frac{A_l}{A_s}$ ratio between structural crown branches and reiterations *sensu* Hallé within the same tree (1 case with 4 crown branches and 13 reiterations *sensu* Hallé) or among trees growing in similar site conditions (22 crown branches belonging to 14 trees and 34 reiterations belonging to 15 trees located on humps.

C Analysis of factors influencing variations in the $\frac{A_l}{A_s}$ ratios of single branches within a tree. Two sub-samples were formed using crown branches only in order to avoid the influence of the difference in branch type: a *training dataset* consisting of 93 crown branches collected at different heights and aspects from 11 different trees (on average 8.45 branches per trees with a minimum and a maximum number of 4 and 12, respectively) and a *validation dataset* consisting of 65 crown branches from 32 trees, that is two branches from different heights and aspects per tree.

Data collection and processing

Data were collected during two sampling periods: from 7th June to 13th August 2009 and from 16th June to 22th July in 2010. In these periods all the leaves were fully developed and hadn't endured too many damages from climate, parasites and phytophagous insects. Branches were accessed by climbing the sampled trees using tree-climbing techniques. Once collected, they were carefully lowered to the ground with a rope. For the analysis of possible factors influencing the constancy of the $\frac{A_l}{A_s}$ ratio of single branches within a tree (question C), specific branch parameters were considered as reported in Table 2.2.

The collected branches were processed in the same day of the cutting in order to preserve the original form and colour of the leaves. Branches were divided up to 10 sections and their structural order noted, allowing the reconstruction of the branch structure and the calculation of the leaf area (A_l) for each possible section (Figure 2.3). For each section, minimum and maximum diameters were measured with a caliber, possibly on smooth bark 1 to 3 cm from the branching. The sapwood areas (A_s) were calculated from the 2 diameters using the ellipse formula, assuming that for the small branches sampled all the branch section has a conductive function (when present heartwood should be

Table 2.1: Site, trees and branches per dataset

Dataset		Site				Trees					Branches				
		Elevation [masl]		Slope [%]		Number	Height [m]		DBH [cm]		Number	Length [cm]		ϕ at cutting point [mm]	
		mean	*max* *min*	*mean*	*max* *min*		*mean*	*max* *min*	*mean*	*max* *min*		*mean*	*max* *min*	*mean*	*max* *min*
A	Overall	370.44	591 237	29.15	100 0	67	12.44	26.6 1.5	49.64	112 8	224	60.11	301 2	9.86	40.5 1.7
B	Crown	440.55	591 266	51.63	100 20	14	4.67	11 1.5	13.38	22 8	22	46.59	216 2	9.18	29.8 2.5
	Reiteration	426.17	510 301	34.18	100 0	15	10.28	18.1 1.5	50	50 50	34	70.2	301 4	9.52	26.8 1.9
C	Training	309.34	415 237	17.49	50 0	11	14.19	18.5 7.99	55.6	112 18	93	57.91	291 2	9.49	33.8 1.9
	Validation	391.85	513 237	35.09	90 0	32	13.58	26.6 2.5	46.79	96 14	65	61.31	251 2	10.77	40.5 2.3

Table 2.2: Branch parameters considered.

Parameter	Unit	Model*	Coll.**	Relevance	Notes
Branch parameters					
Branch height at cutting point	m	t	a	hydraulic property	
Branch height at main trunk insertion	m	t		hydraulic property	
Branch diameter at main trunk insertion	cm	(t)	bc	xylematic resistance at the trunc node	
Total length from main trunk	cm	t	b	xylematic resistance	
Structural order from main trunk to the branch end		t	c	xylematic resistance (number of bifurcations)	
Presence/absence of blight	*0/1*	t		radial growth	
Branch angle	$^\circ$	t		branch vigour	from trigonometry
Branch aspect transformed		t		transpirational demand (exposition to light)	according to Beers *et al.* (1966)
Intra-branch parameters (samples)					
Structural order		(b)	e	xylematic resistance (number of bifurcations)	
Branch length	cm				
Number of cupulae		b	d	sink for photosynthates	
Number of flowers		b		sink for photosynthates	
Age at each section	y	b		xylematic resistance (number of nodes related to the yearly growth)	
Stem mass	gr				
Minimum diameter	mm				
Maximum diameter	mm				
Number of leaves		(b)	e	could interfere with branch growth	
Leaf area	m^2				
Leaf colour ratio (Red/Green)		b	t	leaf light conditions	from RGB colour, ratio Red/Green
Mean leaf area	m^2		(t) ad	transpirational demand (leaf type)	
Section eccentricity	ratio	b		xylematic resistance (reaction wood)	ratio of branch section vertical diameter to horizontal diameter
Sapwood area	cm^2	b	e		calculated from the 2 diameters with the ellipse formula

* *tested as explaining variable in the intra-branch model (b) or the intra-tree model (t). Brackets indicate that the variable was excluded due to colllinearity with other variables*

** *collinearity among the model candidate variables: same letters represents correlated variables (Pearson* $R > 0.5$*)*

Figure 2.2: Examples of epicormic shoots (crown suckers) in chestnut (reiterations *sensu* Hallé).

considered calculating the functional relationships under the pipe model theory; Berthier *et al.* , 2001; Gould & Harrington, 2008).

All the leaves were then detached and digitalized with a scanner (*Xerox 9001* machine: resolution 200 dpi, contrast +1, coloured photo quality) in order to be analyzed with the image processing programs *Image Pro plus 6.0 (IPP)*. Table 2.2 shows all the intra-branch parameters measured and computed that may influence the constancy of the $\frac{A_l}{A_s}$ ratio at branch level.

All the measured and processed parameters were stored in a relational database *(PostGreSQL)* and ad hoc *pgSql* functions were developed to compute the parameters according to the hierarchical structure of the data.

For additional details of the methods see Appendix A.

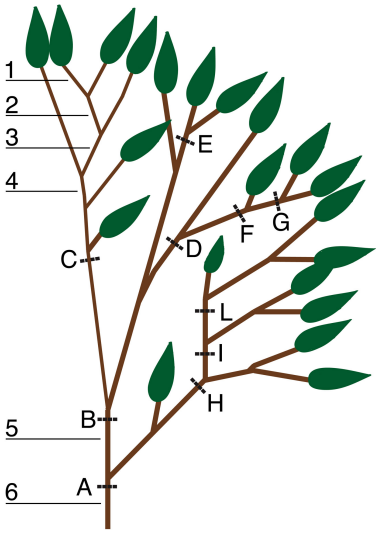

Figure 2.3: Schematical representation of a branch. Capital letters represent the 10 sapwood sections. A is the parent section of B and H. B is the parent section of C, D and E and so on. Leaf area (A_l) of section A is the sum of the A_l of all the sections (A-L). A_l of sections B is the sum of the A_l of sections from B to G, etc. Numbers represent the structural order of the branch. The youngest sprig is labelled with number 1. The number increases at each branching having circa the same sapwood diameter. The pathway having the highest score is considered.

Data analysis

Sapwood area and other measured intra-branch variables were tested for their relationship to leaf area within a branch (Table 2.2). This was done following a Generalized Linear Mixed Model approach, because the sampled data were not independent (random effects were the sampled sites, trees and branches). Section data within branches were not independent (hierarchical structure). Terminal branch sections (n=711), and a subset of higher hierarchical level sections (n=183) have been considered in the analysis. According to its position, each section could be defined by its hierarchical level as either parent of

child in relation to other sections (consequently, terminal sections could be only "child", Figure 2.3). In order to ensure data independence, for the parent sections a net sapwood area was calculated, as the difference between its total area and the cumulated sapwood areas of associated child sections (Figure 2.4). For the analysis only sections with a net sapwood area at least the half of the sapwood area were selected. From the set of the considered explanatory variables, only the uncorrelated ones were retained (Pearson $R \leq 0.5$). Using REML (restricted maximum likelihood) estimation on the model with all variables *(beyond optimal model)*, the optimal random configuration was determined (intercept random model or slope and intercept random model). Using the R package *glmulti*, all the combinations of explanatory variables were evaluated (no interactions or polynomial terms have been considered). The models were ranked on the base of the AICc coefficient (Akaike information criterion with a second order correction for small sample size), calculated using the maximum likelihood estimation (ML). The estimates of best model were finally recalculated using REML estimation (Zuur *et al.* , 2009). Although there is no universally recognized way to calculate an R^2 for mixed models, we computed two estimates proposed: the Cox-R^2 (Nagelkerke, 1991) and the Xu-R^2 (Xu, 2003). The model was then compared to the postulate of the pipe model theory and discussed.

In a second step, for each branch the distribution of leaf and sapwood area was fitted with a simple linear regression ($A_l = a \cdot A_s + b$), this time using sapwood areas and aggregated leaf areas of all sections. Although the linear models were based on not independent data (hierarchical branch sections), this allowed us to get a weighted estimate for the leaf to sapwood area relationship, accounting also for the possibility to have an non-zero intercept in the linear regressions. In fact the leaf to sapwood area slope coefficient ($LASA = a = \frac{A_l - b}{A_s}$) may be a more robust indicator of the allometric relationship, partially overcoming the influence of branch specific characteristics other than sapwood area.

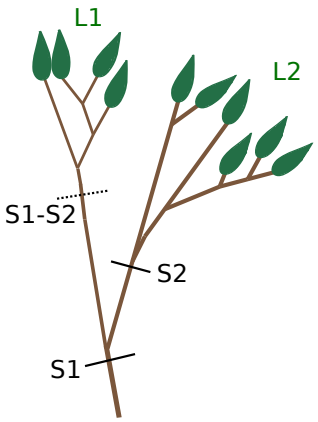

Figure 2.4: Schematic representation of association between sapwood areas and associated leaf variables: S1 with L1+L2, S2 with L2, S1-S2 with L1

An analogous mixed modeling approach was used for the analysis of the variables influencing the leaf to sapwood area relationship within a tree (Table 2.2), on a restricted dataset (question C). The random effects were represented by the sampled sites and trees. The estimates of the fixed effects of the selected model (marginal model) were then applied to an independent validation dataset (32 trees, with 2 branches each) and the discrepancies between the predicted and the observed $LASA$ coefficients were analysed in the light of their suitability in minimizing the inter-branch differences within a tree with respect to the variability among trees, and thus potentially better highlighting the inter-tree differences due to the environment.

The analysis were performed using the R statistical package version 2.14.0 (R Development Core Team, 2011).

Results

Branch level

As expected from the pipe model theory, for the intra-branch model the best random factor configuration was a slope and intercept random model on sapwood area.

This confirms that different branches, trees or sites may have a linear relationship between leaf and sapwood area with different intercepts and slopes. The best intra-branch model selected (among 64 generated models) included *net sapwood area*, *age order* (section age) and *Red/Green ratio* as explaining variables (Table 2.3), and gave the best results in terms of AICc, likelihood and explained variance. Both the R^2 estimates show a very high performance of the model. The residuals were normally distributed, no particular pattern could be recognized when plotting the residuals against the fitted values or the explaining variables, and no high correlation between the slope estimates was found (data not shown).

Most of the model variance was explained by the random slope effect of sapwood area, mainly at the branch (48%) and the tree (42 %) level (Table 2.4), thus confirming the importance of this factor in relationship with leaf area. Section age and the Red/Green ratio were also found to be related to the leaf area value, but with negative estimates (Table 2.4).

The physiological balance between leaf and sapwood area is confirmed by the strength of the correlations for each branch (Figure 2.5 *top right*): the R^2 of 97.3 % of the branches were higher than 0.94. Figure 2.5 *(top left)* shows as example the regression lines form 3 selected branches in different trees.

LASA slope coefficients were always significantly different from 0, and Figure 2.5 *(bottom left)* shows its range, that varies by a factor of 13 (0.1 to 1.35) for the branches with an R^2 greater than 0.94, highlighting a great variability.

Intercepts were significantly different from 0 in 14.3 % of the branches, and showed a skewness towards negative values (Figure 2.5 *bottom right*).

Only branches with R^2 regressions greater than 0.94 were considered for further analysis (218 branches), and the *LASA* slope coefficient was considered instead of the $\frac{A_l}{A_s}$ ratio.

Branch type

For trees growing in similar conditions, the *LASA*'s of the reiterations *sensu* Hallé were significantly higher than those of crown branches (Figure 2.6 *left*; non-parametric Wilcoxon test with p=2e-10), although the sampling heights for the two branch types were not differing (non-parametric Wilcoxon test with p=0.42). In fact regarding crown branches, a clear inter-branch tendency is present: $LASA$ declines with increasing height (Pearson R of -0.41 for all sampled crown branches). No tendencies were found for reiterations (Pearson R of 0.25), as shown also in Figure 2.6 *(right)* for the case of a single tree. No significant difference was found in the intercepts of the branch linear models.

Tree level

For the intra-tree analysis, among the 128 generated models, the model with *branch height* and *branch structural order from main trunk* gave the best result, in terms of AICc, likelihood, and explained variance (Table 2.5). The estimated R^2 indicated a clear relationship between the *LASA* and the fixed effects. The residuals were normally distributed, no particular pattern could be recognized when plotting the residuals against the fitted values or the explaining variables, and no high correlation between the slope estimates was found (data not shown). *LASA* was found to be negatively correlated with the branch height (at cutting point) and branch structural order from the trunk insertion. The best model was significantly better that with one fixed term (p-value 0.034), although the gain in terms of R^2 were minimal.

The estimated p-values (Table 2.6) of both fixed effects were found to be significant, nonetheless for the branch structural order the HPD interval was crossing 0, highlighting a doubtful importance of this factor. The model with branch height only as fixed effects was thus considered more robust and was retained for the vali-

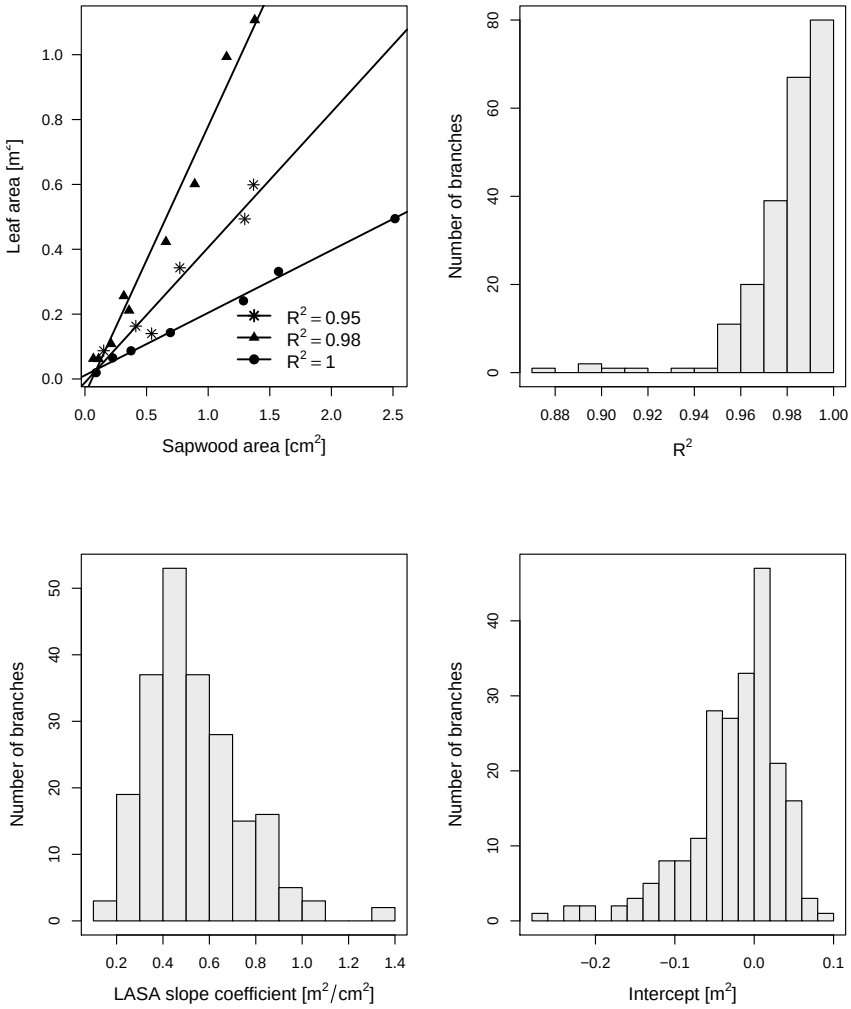

Figure 2.5: Linear regressions of leaf and sapwood area at the branch level: example of 3 selected linear regressions *(top left)* , histogram of the R^2 coefficients of the linear regressions for the whole dataset *(top right)*; and histograms of the $LASA$ slope coefficients *(bottom left)* and of the intercepts *(bottom right)* for the branches with an R^2 greater than 0.94.

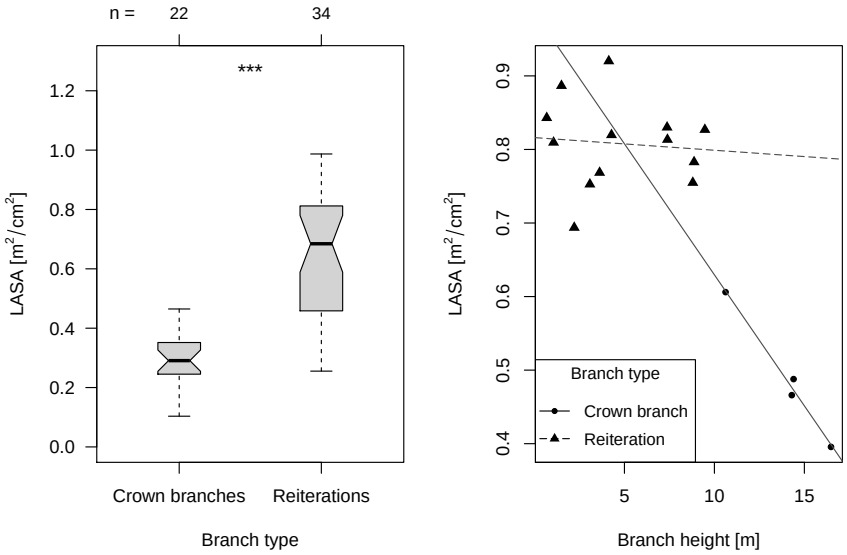

Figure 2.6: Differences in *LASA* between crown branches and reiterations *sensu* Hallé, among trees growing in similar conditions *(left)* or in a single tree *(right)* . The *left* figure shows the boxplots of the *LASA* of branches not higher than 10 m from trees growing in similar conditions (the distributions are significantly different ($p<0.001$), according to the non-parametric Wilcoxon test). Labels on the top *(n)* represent the number of sampled branches in each category. The *right* plot shows the LASA values of the branches of a single tree, and the lines represent the linear correlations (continuous line for crown branches, dashed line for reiterations).

Table 2.3: Best linear mixed models of intra-branch variability of *LASA* (with ML estimation). Model 1 is the best AICc ranking model, model 2 the best one with only 2 explaining variables, model 3 the best model with one explaining variable and model 4 is the null model with random intercept only (*SA=net sapwood area, RG=Red/Green ratio, AO=age order*, $\beta_{0...3}$*=fixed effects, N(0,d)=random term*).

	Model terms	log_{Lik}	s^2_{resid}	s_{resid}	AIC_c	$\bar{R}^2_{Cox}$	$\bar{R}^2_{Xu}$
1	$\beta_0 + \beta_1 SA + \beta_2 RG + \beta_3 AO + N(0,d)$	1340.37	0.00178	0.04222	-2652.26	1.000	0.927
2	$\beta_0 + \beta_1 SA + \beta_2 RG + N(0,d)$	1334.12	0.00178	0.04222	-2641.82	1.000	0.927
3	$\beta_0 + \beta_1 SA + N(0,d)$	1322.35	0.00179	0.04236	-2620.35	1.000	0.927
4	$\beta_0 + N(0,d)$	344.81	0.02458	0.15678	-679.55	0.000	0.000

Table 2.4: Estimates of the fixed effects *(left)* and variance of the random effects *(right)* for the best model of intra-branch variability of *LASA* (with REML estimation).

	Estimate	S.E.	stat
(Intercept)	0.0723	0.0102	7.114
Sapwood area (SA)	0.3661	0.0209	17.485
Age order (AO)	-0.0037	0.0009	-4.085
Red/Green ratio (RG)	-0.1954	0.0335	-5.829

Random	*Component*	s^2	$\%_{s^2}$
$Site_{id}$	(Intercept)	0.00005	0.002
$Site_{id}$	Sapwood area (SA)	0.00016	0.006
$Tree_{id}$	(Intercept)	0.00052	0.019
$Tree_{id}$	Sapwood area (SA)	0.01168	0.424
$Branch_{id}$	(Intercept)	0.00021	0.008
$Branch_{id}$	Sapwood area (SA)	0.01315	0.477
Residuals		0.00179	0.065
Total		0.02757	1.000

dation.

From a biological point of view, the value of the intercept in model 2 (*Equation 2.1* in Table 2.7) should correspond to a mean *LASA* of a branch at ground-level, without any effect of the height. Solving the equation for the intercept term (Equation 2.2 in Table 2.7) we obtain that the intercept value and its variation in the population of branches among sites and trees is equivalent to the difference between the *LASA* and the branch height component.

Using the estimate of model 2 for the slope effect of branch height (Table 2.6 in Table 2.7) and the extracted values of *LASA* from a validation dataset, we can then calculate the *Ground-level LASA* ($LASA_{ground}$, Equation 2.3 in Table 2.7). The $LASA_{ground}$ should then be a measure which, compared to the *LASA*, minimizes the intra-tree differences, allowing probably a better discrimination among trees.

The analysis of variance (ANOVA) on the validation dataset confirmed that *LASA* did not differ among the 32 trees ($F_{31,33} = 1.09, P = 0.4$), while $LASA_{ground}$ did ($F_{31,33} = 6.87, P = 0$). This supports the fact that the $LASA_{ground}$ may be a better parameter in discriminating among trees, allowing to focus on the environmental determinants of biomass partitioning. In fact 24 of the 31 coefficient estimates of the model underlying the ANOVA were significant for $LASA_{ground}$, while none was for *LASA*. Also the Tukey's honestly significant difference test confirmed the presence of 62 significant pairwise differences among trees (out of 496 possible combinations) in $LASA_{ground}$, and none for *LASA*.

Figure 2.7 shows that also the intra-tree ratios between the values of the branch with the lower value and the branch with the higher one, revealed a singnificant approaching to the identity value of 1 for the $LASA_{ground}$ compared to the *LASA* (non-parametric Wilcoxon test with $p<0.001$).

This higher power in discriminating among trees was further verified on environmental data, that is according to the fraction of rocks visible at the soil surface, which should be a factor influencing water availability in the soil. Figure 2.8 shows how with the $LASA_{ground}$ a signif-

Table 2.5: Best linear mixed models of variability of *LASA* within trees (with ML estimation). Model 1 is the best AICc ranking model, model 2 the best one with only 1 fixed effect and model 3 is the null model with intercept only (*H=branch height at cutting point, SO=structural order from the main trunk to branch end,* $\beta_{0...2}$*=fixed effects, N(0,d)=random term*).

	Model terms	log_{Lik}	s^2_{resid}	s_{resid}	AIC_c	$\bar{R}^2_{Cox}$	$\bar{R}^2_{Xu}$
1	$\beta_0 + \beta_1 H + \beta_2 SO + N(0,d)$	88.66	0.00688	0.08297	-164.34	0.616	0.657
2	$\beta_0 + \beta_1 H + N(0,d)$	86.42	0.00743	0.08622	-162.14	0.597	0.630
3	$\beta_0 + N(0,d)$	44.15	0.02008	0.14169	-79.84	0.000	0.000

Table 2.6: Estimates of the fixed effects for the best models of variability of *LASA* within trees (with REML estimation).

Model	Fixed.effect	Estimate	MCMCmean	HPD95lower	HPD95upper	pMCMC	Pr(>|t|)
1	Intercept	0.9106	0.8908	0.7709	1.0038	0.0001	0.0000
1	Branch height (H)	-0.0279	-0.0274	-0.0319	-0.0227	0.0001	0.0000
1	Structural order (SO)	-0.0140	-0.0120	-0.0243	0.0015	0.0682	0.0289
2	Intercept	0.8092	0.8063	0.7355	0.8731	0.0001	0
2	Branch height (H)	-0.0275	-0.0273	-0.0320	-0.0224	0.0001	0

Table 2.7: Equations of the empirical model of *LASA* according to branch height. $N(0,d)_{site_{id}/tree_{id}}$ is the intercept random factor on sites and trees.

$$LASA = 0.8092 - 0.0275 \cdot height_{branch} + N(0,d)_{site_{id}/tree_{id}} \quad (2.1)$$

$$0.8092 + N(0,d)_{site_{id}/tree_{id}} = LASA + 0.0275 \cdot height_{branch} \quad (2.2)$$

$$LASA_{ground} = LASA_{measured} + 0.0275 \cdot height_{branch} \quad (2.3)$$

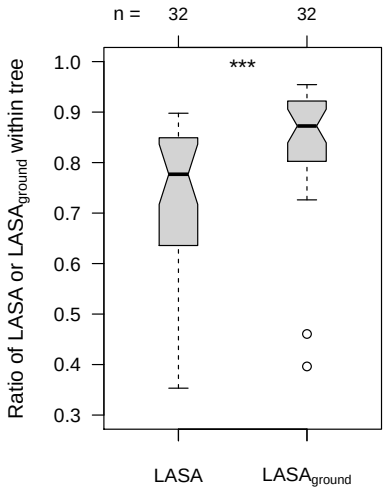

Figure 2.7: Boxplots of the ratios between couple of branches within trees of the validation dataset (lower branch value to higher branch value), according to $LASA$ and $LASA_{ground}$. The distributions are different (p<0.001) according to the non-parametric Wilcoxon test. Labels on the top (n) represent the number of computed ratio between couple of branches within each tree.

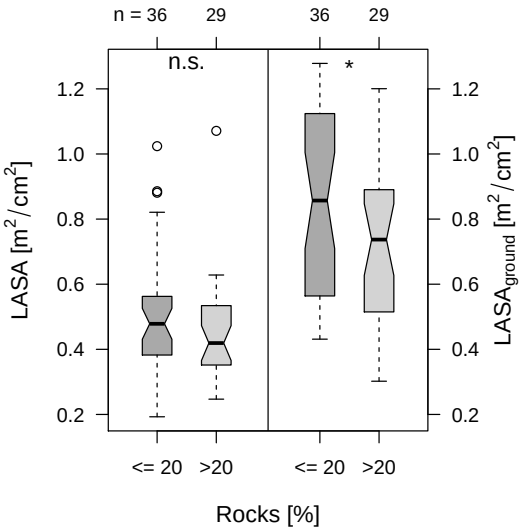

Figure 2.8: Boxplots of the $LASA$ and $LASA_{ground}$ of the branches of the validation dataset, according to the percentage of rocks visible at the soil surface. Significance codes are according the non-parametric Wilcoxon test. Labels on the top (n) represent the number of sampled branches in each category.

icant difference between the groups could be detected, while not with $LASA$. This was also confirmed by the analysis of variance (nested ANOVA on rock category and tree), displaying an highly significant difference between the rock categories with $LASA_{ground}$ ($F_{1,33} = 18.4, P = 0$), and not with $LASA$ ($F_{1,33} = 1.04, P = 0.31447$).

Discussion

Branch level

Pipe Model rules such as the allometric relationships between A_l and A_s are present in *C. sativa,* especially at the intra-branch level. Our results are consistent with other studies (e.g. Grier & Waring, 1974; Waring & Gholz, 1977; Rogers & Hinckley, 1979; Kaufmann & Troendle, 1981), confirming that a physiological balance exists between these two parameters (Shinozaki *et al.* , 1964a,b; Cruiziat *et al.* , 2002). In fact even if the sample size is relatively small and trees vary in height and age, regressions based on A_l and A_s always show very high R^2 coefficients.

The best intra-branch model according to the AICc also considers the age of the branch section as a factor inversely influencing this allometric relationship. This may be explained by a reduction of the xylematic conductivity along the increasing number of annual nodes (Larson & Isebrands, 1978; Rust & Huttl, 1999), thus older branches may support, in similar conditions and comparable sapwood area, a reduced leaf area compared to younger ones. This could also partially explain the observation that the significant intercepts in the A_l to A_s regressions were found to be correlated to the branch sapwood areas (Pearson R of -0.71), highlighting a probable decrease of the $\frac{A_l}{A_s}$ ratio regarding the marginal sections of a branch (towards branch tip).

Our study suggests that the red/green ratio of the leaf colour is another parameter influencing the LASA. Many different pigments give the colour of leaves.

The multitude of photosynthetic pigments varies in proportion and composition between sun and shade leaves (e.g. Gamon *et al.* , 1997; Lichtenthaler *et al.* , 2007). Being an organ specialised for photosynthesis, colour is mainly related to spectral properties of photosynthetic pigments. But this is not always true, in fact in certain cases, other molecules are responsible for the colour of the leaves. For example in red leaves, colours are principally due to anthocyanins or betalains molecules (Manetas, 2006), which are non-photosynthetic pigments. Moreover the complexation of anthocyanins with other polyphenols seems to be one of the major factors affecting the colour of plant tissues (Brouillard, 1988). The exact function of anthocyanins molecules is unclear. Many hypothesis have been done (for a review: Manetas, 2006) and despite literature on this subject remains controversial anthocyanins, in associations with other molecules, have been proposed to act as sunscreens, attenuating the penetration of sun radiation in order to reduce photoinhibition under high irradiances (Gould *et al.* , 1995, 2002; Manetas *et al.* , 2002; Neill *et al.* , 2002; Steyn *et al.* , 2002) and have a powerful anti-oxidative capacity (Wang *et al.* , 1997; Tsuda *et al.* , 1996; Yamasaki *et al.* , 1996). The major anthocyanin found in leaves is the red cyaniding-3-glycoside (Harborne, 1976). Anthoycianins are present in different species of *Fagaceae* (Yoshitama *et al.* , 1972; Wheldale, 1916). *C. sativa* belonging to this family, it allows us to assume that theses pigments are present in this species. The amount of anthocyanins pigments can be estimated by the $\frac{R_{red}}{R_{green}}$ ratio (where R refers to reflectance and the subscripts refer to red band (600-699 nm) and green band (500-599 nm); Gamon & Surfus, 1999). An analogy could be thus done with our Red/-Green ratio. If we assume that this analogy holds, the Red/Green ratio should reflect the average amount of light received by branches and discriminate thus sun and shade leaves, with respectively higher or lower values. In this view the Red/Green ratio is more likely to be a proxy for sun exposition, with higher values for the leaves inside the branch being more exposed to sun, and thus to transpiration. The same area of such a sun leaf constitues an higher evaporative demand compared to a shaded leaf, and branches with a comparable diameter should support more leaf area when in a shaded position, as supported by the negative estimate of this effect in our model (Table 2.4). In the model this may have become relevant particularly for branches displaying a gradient in the light environment.

However, although the best mixed model was significantly better than that with two (p-value 4e-04) or one fixed term (p-value 2e-08), no consistent increase in residual variance or decrease in R^2 was found, which led us to think that the age of the branch section and the Red/Green ratio play a secondary role in the leaf to sapwood area relationship, also confirmed by the low t-values associated.

Branch type

Reiterations *sensu* Hallé display a higher *LASA* than crown branches, confirming that plants are able to redistribute unequally the water flow (Zimmermann, 1978, 1983). Moreover no tendencies (e.g. with branch height) were found within the same tree. Similarly, Hallé (1986) described that spatial distribution of reiterated branches is neither regular nor predictable. Our result concerning the higher vigour of reiterations is in concordance with several studies (e.g. Ito *et al.* , 1995; Otoda & Ishii, 2008). The enhanced vigour of reiterated branches seems to be due to different factors. Generally, the hydraulic conductivity is reduced by the additional number of annual node and junctions (Larson & Isebrands, 1978; Rust & Huttl, 1999) and therefore decreases with increasing distance from the trunk (Ewers & Zimmermann, 1984a,b). Ishii *et al.* (2007) suggests that reiterations are able to maintain higher hydraulic conductivity countering these trends. Reiterations alter the hydraulic architecture, shortening water path

lengths to new foliage and connecting directly to lower order axis as the main trunk (Briand & Larson, 1992; Rust & Huttl, 1999; Ishii *et al.* , 2002, 2007; Otoda & Ishii, 2008) which have high hydraulic conductivity (Tyree & Ewers, 1991; Kozlowski & Pallardy, 1996). From an ecological point of view, different hypothesis have been formulated to explain this phenomena. Reiteration appears normally after an injury or a change in environmental conditions (Bryan & Lanner, 1981; DelTredici, 2001). This ability to resprout enhances the possibility for young woody plants to survive in disturbed habitats (DelTredici, 2001). Instead, in mature trees the reiterative ability could be a mechanism allowing the individual to restore his original architecture (Begin & Filion, 1999), maintain leaf area in the inner crown (Briand & Larson, 1992; Nicolini *et al.* , 2001; Ishii *et al.* , 2007) and respond to disturbance quickly (Sakai *et al.* , 1995; Ito *et al.* , 1999), in order to ensure longevity (Gerrish, 1990; Ishii *et al.* , 2007). It has also been proposed that this mechanism could enable plants to occupy adjacent areas (DelTredici, 2001) and allow species to exploit the surrounding niche. Regarding chestnut trees, reiterations are a response to injury due to pruning and damages as drought or blight attacks. Moreover, having higher *LASA* the hypothesis of crown productivity maintenance and enhancement of longevity (Bryan & Lanner, 1981; Ishii *et al.* , 2002) seems to be in concordance with our results.

Tree level

The decline of the LASA with tree height as been highlighted by other studies regarding other tree species (e.g. Magnani *et al.* , 2000; **?**; McDowell *et al.* , 2002a; Sellin & Kupper, 2006). Different hypothesis have been formulated regard to this tendency, e.g. being a way for trees to support growing hydraulic constrictions with height (Meinzer *et al.* , 1997; Becker *et al.* , 2000; McDowell *et al.* , 2002a), like decreasing conductivity of xylem tissue (Tyree & Ewers, 1991; Mencuccini, 2003; Phillips *et al.* , 2003a). Besides this, the decline with height of the leaf to sapwood area ratio ($\frac{A_l}{A_s}$) seems to play an important role in plant-atmosphere water exchange. For example, $\frac{A_l}{A_s}$ should be related to stomatal conductance (Becker *et al.* , 2000; Mencuccini & Bonosi, 2001; Delzon *et al.* , 2004; Novick *et al.* , 2009) and more generally water conductance constraints (Becker *et al.* , 2000; Mencuccini & Bonosi, 2001; Ewers *et al.* , 2005). Increasing sapwood area with respect to leaf area should be thus a homeostatic way to cope the increasing hydraulic constraints with height and allow canopy conductance to be maintained (Becker *et al.* , 2000). It is important to specify that this hypothesis is still controversial. Although some experiments pointed out that reduction in the $\frac{A_l}{A_s}$ ratio could fully mitigate hydraulic limitations (e.g. Barnard & Ryan, 2003), the majority of studies suggest that this compensatory shift in the $\frac{A_l}{A_s}$ ratio just partially alleviate the problem(Mencuccini & Grace, 1996b; Mencuccini & Magnani, 2000; Ryan *et al.* , 2000; McDowell *et al.* , 2002a; Novick *et al.* , 2009) and other mechanisms like changes in tree water storage with height (Phillips *et al.* , 2003b) and increased hydraulic redistributed water (Brooks *et al.* , 2002) could significantly contribute to the water balance.

This reduction of *LASA* with height could be also related to abiotic stress. Mazzoleni (1990) and Waring & Schlesinger (1985)found that a larger surface of sapwood area for a given leaf area is necessary in environments more exposed to stress compared to more protected sites. Similarly a branch situated in the higher part of a tree is more exposed to stress regard to branches situated in the lower part. Moreover the average size of leaves decrease with tree height in our study (Pearson R of -0.69 for the model dataset) and it has been proposed that it is advantageous to present a smaller leaf to the wind to enhance convective cooling (e.g. De Soyza & Kinkaid, 1991; Smith *et al.* , 1997). The decreasing of the *LASA* with height should be thus also indirectly

due to the increase of certain stresses like wind or evaporative demand.

The fact that also branch structural order was retained in the best AICc model confirms the probable decrease of xylematic conductivity along the branches, from the main trunk towards branch tips (Ewers & Zimmermann, 1984a,b), probably reduced by the number of junctions and annual nodes (Larson & Isebrands, 1978; Rust & Huttl, 1999).

In conclusion, the *LASA* is closely related to the hydraulic system of a plant. In the presented analysis the main parameter influencing this index is branch height, being directly related to the hydraulic constrains due to height and a good proxy for to the evaporative demand due to wind and exposition to sun. The suitability of this parameter was confirmed by the validation of the model. The proposed notion of *Ground-level LASA* ($LASA_{ground}$) proved to be effective in reducing the interbranch variation within a tree, allowing then a better discrimination among trees and environmental conditions.

Conclusion

The leaf area to sapwood area relationship is an useful index to understand hydraulic architecture of trees. Moreover it is also used to understand plant response to an environmental gradient (Mazzoleni, 1990) and as an indicator of plant vigour and relative competitive ability (Bacon & Zedaker, 1986; Rogers & Hinckley, 1979).

The *LASA* in *C. sativa* vary at the inter-branch level and between branch types (reiteration *sensu* Hallé versus crown branches). Depending on the branch sampled, the index could be greater or smaller. For environmental studies it is thus very important to select crown branches (carefully avoiding reiterations) and to standardize branch selection, e.g. with a constant branch height. The notion of *Ground-level LASA* ($LASA_{ground}$) with the formula suggested in our model allowed to partially mitigate differences due the sampling height. This could help to better discriminate variations due to environmental parameters in studies comparing trees in different environmental conditions.

References

Arber, A. 1928. Tree habit in angiosperms: Its origin and meaning. *New phytologist*, **27**(2), 69 – 84.

Arber, A. 1950. *The natural philosophy of tree form.* Cambridge: Cambridge University Press.

Aussenac, Gilbert, & Granier, André. 1988. Effects of thinning on water stress and growth in douglas-fir. *Canadian journal of forest research*, **18**(1), 100–105.

Bacon, CG, & Zedaker, SM. 1986. Leaf-area prediction equations for young southeastern hardwood stems. *Forest science*, **32**(Sept.), 818–821.

Barnard, H. R., & Ryan, M. G. 2003. A test of the hydraulic limitation hypothesis in fast-growing Eucalyptus salign. *Plant, cell and environment*, **26**(8), 1235 – 1245.

Bartelink, H. H. 1997. Allometric relationships for biomass and leaf area of beech (fagus sylvatica l). *Annales des sciences forestières*, **54**(1), 12–12.

Becker, P., Meinzer, F. C, & Wullschleger, S. D. 2000. Hydraulic limitation of tree height: a critique. *Functional ecology*, **14**(1), 4–11.

Beers, T. W., Dress, P. E., & Wensel, L. C. 1966. Aspect transformation in site productivity research. *Journal forestry*, **64**, 691 – 692.

Begin, C., & Filion, L. 1999. Black spruce (Picea marianna) architecture. *Canadian journal of botany*, **77**(5), 664 – 672.

Berger, Susanne, Sinha, Alok K., & Roitsch, Thomas. 2007. Plant physiology meets phytopathology: plant primary metabolism and plant–pathogen interactions. *Journal of experimental botany*, **58**(15-16), 4019–4026.

Berthier, S., Kokutse, A. D., Stokes, A., & Fourcaud, T. 2001. Irregular heartwood formation in Maritime pine (Pinus pinaster Ait.): Consequences for biomechanical and hydraulic tree functioning. *Annals of botany*, **87**(1), 19 – 25.

Briand, C. H. P., & Larson, D. W. 1992. Differential axis architecture in Thuja occidentalis (eastern white cedar). *Canadian journal of botany*, **70**(2), 340 – 348.

Brix, H., & Mitchell, A. K. 1983. Thinning and nitrogen fertilization effects on sapwood development and relationships of foliage quantity to sapwood area and basal area in Douglas-fir. *Canadian journal of forest research*, **13**, 384 – 389.

Brooks, R. J., Meinzer, C. F., Coulombe, R., & Gregg, J. 2002. Hydraulic redistribution of soil water during summer drought in two contrasting Pacific Northwest coniferous forests. *Tree physiology*, **22**(15 - 16), 1107 – 1117.

Brouillard, R. 1988. *The flavonoids-advances in research since 1980.* London: Chapman and Hall.

Bryan, J. A., & Lanner, R. M. 1981. Epicormic branching in Rocky Mountain Douglas-fir. *Journal of forest research*, **11**(2), 190 – 199.

Cannell, M. G. R., Sheppard, L. J., Ford, E. D., & Wilson, R. H. F. 1983. Clonal differences in dry matter distribution, wood specific gravity and foliage "efficiency" in Picea sitchensis and Pinus contorta. *Silvae genetica*, **32**(5 - 6), 195 – 202.

Chiba, Y. 1990. Plant form analysis based on the pipe model theory. I. A statical model within the crown. *Ecology research*, **5**(2), 207 – 220.

Chiba, Y. 1991. Plant form analysis based on the pipe model theory. II. Quantitative analysis of ramification in morphology. *Ecology research*, **6**(1), 21 – 28.

Chiba, Yukihiro. 1998. Architectural analysis of relationship between biomass and basal area based on pipe model theory. *Ecological modelling*, **108**(1-3), 219–225.

Cruiziat, P., Cochard, H., & Ameglio, T. 2002. Hydraulic architecture of trees: main concepts and results. *Annals of forest science*, **59**(7), 723–752.

De Soyza, A. M., & Kinkaid, D. T. 1991. Patterns in leaf morphology and photosynthesis in shoots of sassafras albidum (lauraceae). *American journal of botany*, **78**(1), 89 – 98.

Dean, T. J., & Long, J. N. 1986. Variation in sapwood Area-Leaf area relations within two stands of lodgepole pine. *Forest science*, **32**(Sept.), 749–758.

DelTredici, P. 2001. Sprouting in temperate trees: A morphological and ecological review. *Botanical review*, **67**(2), 121 – 140.

Delzon, S., Sartore, M., Burlett, R., Dewar, R., & Loustau, D. 2004. Hydraulic responses to height growth in maritime pine trees. *Plant, cell & environment*, **27**(9), 1077–1087.

Enquist, B.J., Kerkhoff, A.J., Huxman, T.E, & Economo, E.P. 2007. Adaptive differences in plant physiology and ecosystem paradoxes: insights from metabolic scaling theory. *Global change biology*, **13**, 591–609.

Ewers, B. E., Gower, S. T., Bond-Lamberty, B., & Wang, C. K. 2005. Effects of stand age and tree species on canopy transpiration and average stomatal conductance of boreal forests. *Plant cell environment*, **28**(5), 660 – 678.

Ewers, F. W., & Zimmermann, M. H. 1984a. The hydraulic architecture of balsam fir (abies balsamea). *Physiologia plantarum*, **60**, 453 – 458.

Ewers, F. W., & Zimmermann, M. H. 1984b. The hydraulic architecture of eastern henlock (tsuga canadensis). *Canadian journal of botany*, **62**, 940 – 946.

Ford, E. D. 1992. The control of tree structure and productivity through the interaction of morphological development and physiological processes. *International journal of plant sciences*, **153**(3), 147 – 162.

Gamon, J. A., & Surfus, J. S. 1999. Leaf pigment content and activity with a reflectometer. *New phytologist*, **143**(1), 105 – 117.

Gamon, J. A., Serrano, L., & Surfus, J. S. 1997. The photochemical reflectance index: An optical indicator of photosynthetic radiation use efficiency across species, functional types, and nutrient levels. *Oecologia*, **112**(4), 492 – 501.

Gerrish, G. 1990. Relating carbon allocation patterns to tree senescence in metrosideros forests. *Ecology*, **71**(3), 1176 – 1184.

Gotsch, Sybil G., Geiger, Erika L., Franco, Augusto C., Goldstein, Guillermo, Meinzer, Frederick C., & Hoffmann, William A. 2010. Allocation to leaf area and sapwood area affects water relations of co-occurring savanna and forest trees. *Oecologia*, **163**(Jan.), 291–301.

Gould, K. S., Kuhn, D. N., Lee, D. W., & Oberbauer, S. F. 1995. Why leaves are sometimes red. *Nature*, **378**(6554), 241 – 242.

Gould, K. S., Neil, S., & Vogelmann, T. C. 2002. *A unified explanation for anthocyanins in leaves?* Vol. 37. London: Academic Press. Pages 167 – 192.

Gould, Peter J., & Harrington, Constance A. 2008. Extending sapwood : Leaf area relationships from stems to roots in coast douglas-fir. *Annals of forest science*, **65**(8), 8–8.

Grier, C., & Waring, R. H. 1974. Conifer foliage mass related to sapwood area. *Forest science*, **20**(3), 205 – 206.

Hallé, F. 1981. Crown construction in mature dipterocarps. *Malaysian forester journal*, **44**, 222 – 233.

Hallé, F. 1986. Modular growth in seed plants. *Philosophical transactions of the royal society of london. series b, biological sciences*, **313**(1159), 77 – 87.

Hallé, F., & Oldeman, R. A. A. 1970. *Essai sur l'architecture et la dynamique de croissance des arbres tropicaux.* Paris: Masson.

Hallé, F., Oldeman, R. A. A., & Tomlinson, P. B. 1978. *Tropical trees and forests: An architectural analysis.* Berlin: Springer Verlag.

Harborne, J. B. 1976. *The anthocyanin pigments.* London: Academic Press. Pages 1 – 36.

Hasegawa, S., Koba, K., & Tayasu, I. 2003. Carbon autonomy of reproductive shoots of siberian alder (alnus hirsuta var. sibirica). *Journal of plant research*, **116**(3), 183 – 188.

Huber, Bruno. 1928. Weitere quantitative untersuchungen über das wasserleitungssystem der pflanzen. *Jahrb. wiss. bot.*, **67**, 877–959.

Infante, Juan Manuel, Mauchamp, André, Fernández-Alés, Rocío, Joffre, Richard, & Rambal, Serge. 2001. Within-tree variation in transpiration in isolated evergreen oak trees: evidence in support of the pipe model theory. *Tree physiology*, **21**(6), 409–414.

Ishii, H. T., Ford, E. D., & Dinnie, C. E. 2002. The role of epicormic shoot production in maintaining foliage in old pseudotsuga menziesii (douglas-fir) trees ii. basal reiteration from older branch axes. *Canadian journal of botany*, **80**(9), 916 – 926.

Ishii, Hiroaki T., Ford, E. David, & Kennedy, Maureen C. 2007. Physiological and ecological implications of adaptive reiteration as a mechanism for crown maintenance and longevity. *Tree physiology*, **27**(3), 455–462.

Ito, K., Ito, S., Gyokusen, K., & Saito, A. 1999. Ecological roles of stem sprouts and creeping sprouts of aucuba japonica thunb. *Journal of forest research*, **4**(2), 137 – 143.

Ito, Satoshi, Sakuta, Kotaro, & Gyokusen, Koichiro. 1995. Distribution of hydraulic resistance in seedlings, sprouts and an adult tree ofpasania edulis makino. *Ecological research*, **10**(Aug.), 143–149.

Kaufmann, Merrill R., & Troendle, Charles A. 1981. The relationship of leaf area and foliage biomass to sapwood conducting area in four subalpine forest tree species. *Forest science*, **27**(Sept.), 477–482.

Kawachi, N., Fujimaki, S., Suzui, N., Ishii, S., Matsuhashi, S., Satoh, T., Watanabe S., Takeda, S., & Takahashi, T. 2007. Molecular imaging for plant physiology (2): Multitracer imaging system for the dynamics of nutrients and pollutants in intact plants. *Plant and cell physiology*, **48**, S226.

Kershaw, John A., Maguire, Douglas A., & Hann, David W. 1990. Longevity and duration of radial growth in douglas-fir branches. *Canadian journal of forest research*, **20**(11), 1690–1695.

Kozlowski, T. T., & Pallardy, S. G. 1996. *Physiology of woody plants.* San Diego: Academic Press.

Larson, P. R., & Isebrands, J. G. 1978. Functional significance of nodal constricted zone in populus deltoides. *Canadian journal of botany*, **56**(7), 801 – 804.

Le Maitre, D.C. 2004. Predicting invasive species impacts on hydrological processes: The consequences of plant physiology for landscape processes. *Weed technology*, **18**, 1408–1410.

Lichtenthaler, H. K., Ac, A., Marek, M. V., Kalina, J., & Urban, O. 2007. Differences in pigment composition, photosynthetic rates and chlorophyll fluorescence images of sun and shade leaves of four tree species. *Plant physiology and biochemistry*, **45**(8), 577 – 588.

Magnani, F., Mencuccini, M., & Grace, J. 2000. Age-related decline in stand productivity: the role of structural acclimation under hydraulic constraints. *Plant, cell & environment*, **23**(3), 251–263.

Manetas, Y. 2006. Why some leaves are anthocyanic and why most anthocyanic leaves are red? *Flora*, **210**(3), 163 – 177.

Manetas, Y., Drinia, A., & Petropoulou, Y. 2002. High contents of anthocyanins in young leaves are correlated with low pools of xanthophyll cycle components and low risk of photoinhibitation. *Photosynthetica*, **40**(3), 349 – 354.

Mazzoleni, Stefano. 1990. Relazioni tra aree fogliari e superfici di conduzione nel fusto nell'analisi di gradienti ambientali. *Linea ecologica*, 27–30.

Mazzoleni, Stefano, & Schirone, B. 1990. Allometric estimations of woody and foliar biomass. applications on quercus cerris sprouts and mediterranean shrubs. *Annali di botanica*, **XVIII**.

McDowell, N., Barnard, H., Bond, B., Hinckley, T., Hubbard, R., Ishii, H., i, B. Kästner, Magnani, F., Marshall, J., Meinzer, F., Phillips, N., Ryan, M., & Whitehead, D. 2002a. The relationship between tree height and leaf area: sapwood area ratio. *Oecologia*, **132**(1), 12–20.

Meinzer, F. C., Andrade, J. L., Goldstein, G., Holbrook, N. M., Cavelier, J., & Jackson, P. 1997. Control of transpiration from the upper canopy of a tropical forest: The role of stomatal, boundary layer and hydraulic architecture components. *Plant, cell and environment*, **20**(10), 1242 – 1252.

Mencuccini, M. 2003. The ecological significance of long-distance water transport: short-term regulation, long-term acclimation and the hydraulic costs of stature across plant life forms. *Plant, cell & environment*, **26**(1), 163–182.

Mencuccini, M., & Bonosi, L. 2001. Leaf/sapwood area ratios in scots pine show acclimation across europe. *Canadian journal of forest research*, **31**(3), 442 – 456.

Mencuccini, M., & Grace, J. 1996a. Developmental patterns of above-ground hydraulic conductance in a scots pine (pinus sylvestris l.) age sequence. *Plant, cell and environment*, **19**(8), 939 – 948.

Mencuccini, M., & Grace, J. 1996b. Hydraulic conductance, light interception and needle nutrient concentration in scots pine stands and their relations with net primary productivity. *Tree physiology*, **16**(5), 459 – 468.

Mencuccini, M., & Magnani, F. 2000. Comment on 'hydraulic limitation of tree height: A critique' by becker, meinzer and wullschleger. *Functional ecology*, **14**(1), 135–137.

Mencuccini, Maurizio, & Grace, John. 1994. Climate influences the leaf area/sapwood area ratio in scots pine. *Tree physiol*, **15**(1), 1–10.

Miyazaki, Y., Hiura, T., Kato, E., & Funada, R. 2002. Allocation of resources to reproduction in styrax obassia in a masting year. *Annals of botany*, **89**(6), 767 – 772.

Mäkelä, Annikki. 1986. Implications of the pipe model theory on dry matter partitioning and height growth in trees. *Journal of theoretical biology*, **123**(1), 103–120.

Nagelkerke, N. J. D. 1991. A note on a general definition of the coefficient of determination. *Biometrika*, **78**(3), 691 – 692.

Neill, S. O., Gould, K. S., Kilmartin, P. A., Mitchell, K. A., & Markham, K. R. 2002. Antioxidant capacities of green and cyanic leaves in the sun species, quintinia serrata. *Functional plant biology*, **29**(12), 1437 – 1443.

Nicolini, E., Chanson, B., & Bonne, F. 2001. Stem growth and epicormic branch formation in understory beech trees (fagus sylvatica l.). *Annals of botany*, **87**, 737 – 750.

Nikinmaa, E. 1992. *Analyses of the growth of scots pine; matching structure with function.* Thesis, Helsinki Univ.

Novick, Kimberly, Oren, Ram, Stoy, Paul, Juang, Jehn-Yih, Siqueira, Mario, & Katul, Gabriel. 2009. The relationship between reference canopy conductance and simplified hydraulic architecture. *Advances in water resources*, **32**(6), 809–819.

Otoda, Takashi, & Ishii, Hiroaki. 2008. Basal reiteration improves the hydraulic functional status of mature cinnamomum camphora trees. *Trees*, **23**(Oct.), 317–323.

Phillips, N., Bond, B. J, McDowell, N. G, Ryan, M. G, & Schauer, A. 2003a. Leaf area compounds height-related hydraulic costs of water transport in oregon white oak trees. *Functional ecology*, **17**(6), 832–840.

Phillips, N. G., Ryan, M. G., Bond, B. J., McDowell, N. G., Hinckley, T. M., & Ä?ermÃ¡k, J. 2003b. Reliance on stored water increases with tree size in three species in the pacific northwest. *Tree physiology*, **23**(4), 237–245.

Pothier, D., & Margolis, A. 1991. Analysis of growth and light interception of balsam fir and white birch saplings following precommercial thinning. *Annales des sciences forestières*, **48**(2), 10–10.

R Development Core Team. 2011. *R: A language and environment for statistical computing.* R Foundation for Statistical Computing, Vienna, Austria. ISBN 3-900051-07-0.

Richter, J.P. 1970. *The notebooks of leonardo da vinci.* Dover, New York: Dover.

Rogers, R, & Hinckley, TM. 1979. Foliar weight and area related to current sapwood area in oak. *Forest science*, **25**, 298–303.

Rust, S., & Huttl, R. F. 1999. The effect of shoot architecture on hydraulic conductance in beech (fagus sylvatica l.). *Trees-structure and function*, **14**(1), 39 – 42.

Ryan, M. G., Bond, B. J., Law, B. E., Hubbard, R. M., Woodruff, D., Cienciala, E., & Kucera, J. 2000. Transpiration and whole-tree conductance in ponderosa pine trees of different heights. *Biomedical and life sciences*, **124**(4), 553 – 560.

Sakai, A., Ohsawa, T., & Ohsawa, M. 1995. Adaptive significance of sprouting of euptelea polyandra, a deciduous tree growing on steep slopes with shallow soil. *Journal of plant research*, **108**(3), 377 – 386.

Schulze, E. D., Fuchs, M. I., & Fuchs, M. 1977. Spatial distribution of photosynthetic capacity and performance in a mountain spruce of northern germany. i. biomass distribution and daily co2 uptake in different crown layers. *Oecologia*, **29**(1), 43 – 61.

Sellin, Arne, & Kupper, Priit. 2006. Spatial variation in sapwood area to leaf area ratio and specific leaf area within a crown of silver birch. *Trees*, **20**(Jan.), 311–319.

Shinozaki, K, Yoda, K, Hozumi, K, & Kira, T. 1964a. A quantitative analysis of plant form – the pipe model theory i. basic analyses. *Japanese journal of ecology*, **14**(3), 97–105.

Shinozaki, K, Yoda, K, Hozumi, K, & Kira, T. 1964b. A quantitative analysis of plant form – the pipe model theory ii. further evidence of the theory and its application in forest ecology. *Japanese journal of ecology*, **14**(4), 133–139.

Smith, W. K., Vogelmann, C. T., DeLucia, E. H., Bell, D. T., & Shepherd, K. A. 1997. Leaf form and photosynthesis. *American institute of biological sciences*, **47**(11), 785 – 793.

Snell, J. A. Kendall, & Brown, James K. 1978. Comparison of tree biomass Estimators–DBH and sapwood area. *Forest science*, **24**(Dec.), 455–457.

Sone, Kosei, Suzuki, Alata Antonio, Miyazawa, Shin-Ichi, Noguchi, Ko, & Terashima, Ichiro. 2009. Maintenance mechanisms of the pipe model relationship and leonardo da vinci-s rule in the branching architecture of acer rufinerve trees. *Journal of plant research*, **122**(Aug.), 41–52.

Spinedi, F., & Isotta, F. 2004. Il clima del ticino. *Dati statistiche e società*, **2**, 5 – 39.

Sprugel, D. G., Hinckley, T. M., & Schaap, W. 1991. The theory and practice of branch autonomy. *Annual review of ecology and systematics*, **388**, 71 – 83.

Steyn, W. J., Wand, S. J. E., Holcroft, D. M., & Jacobs, G. 2002. Anthocyanins in vegetative tissues: A proposed unified function in photoprotection. *New phytologist*, **155**(3), 349 – 361.

Tinner, W., Hubschmid, P., Wehrli, M., Ammann, B., & Conedera, M. 1999. Long-term forest fire ecology and dynamics in southern switzerland. *Journal of ecology*, **87**, 273–289.

Tomlinson, P. B. 1982. Change and design in the construction of plants. *Acta biotheoretica*, **31A**(1-3), 162 – 183.

Tomlinson, PB. 1987b. Architecture of tropical plants. *Annual review of ecology and systematics*, 1–21.

Tsuda, T., Shiga, K., Ohshima, K., Kawakishi, S., & Osawa, T. 1996. Inhibition of lipid peroxidation and the active oxagen radical scavenging effect of anthocyanin pigments isolated from Phaseolus vulgaris L. *Biochemical pharmacology*, **52**(7), 1033 – 1039.

Tyree, Melvin T., & Ewers, Frank W. 1991. Tansley review no. 34. the hydraulic architecture of trees and other woody plants. *New phytologist*, **119**(3), pp. 345–360.

Wang, H., Cao, G. H., & Prior, R. L. 1997. Oxygen radical absorbing capacity of anthocyanins. *Journal of agricultural and food chemistry*, **45**(2), 304 – 309.

Waring, R. H., & Gholz, H. L. 1977. Evaluating stem conducting tissue as an estimator of leaf area in four woody angiosperms. *Canadian journal of botany*, **55**(11), 1474–1477.

Waring, R. H., & Schlesinger, W. H. 1985. *Forest ecosystems. concepts and management.* New York: Academic Press.

Waring, R.H., Schroeder, P.E., & Oren, R. 1982. Application of the pipe model theory to predict canopy leaf-area. *Canadian journal of forest research*, **12**(3), 556–560.

Wheldale, M. 1916. *The anthocyanin pigments of plants.* Cambridge: Cambridge Univeristy Press.

White, D., Beadle, Chris, Worledge, Dale, Honeysett, John, & Cherry, Maria. 1998. The influence of drought on the relationship between leaf and conducting sapwood area in eucalyptus globulus and eucalyptus nitens. *Trees - structure and function*, **12**(7), 406–414.

Whitehead, D. 1978. Estimation of foliage area from sapwood basal area in scots pine. *forestry*, **51**(2), 137–149.

Whitehead, D., Edwards, W. R. N., & Jarvis, P. G. 1984. Conducting sapwood area, foliage area, and permeability in mature trees of piceasitchensis and pinuscontorta. *Canadian journal of forest research*, **14**(6), 940–947.

Wright, Ian J, Falster, Daniel S, Pickup, Melinda, & Westoby, Mark. 2006. Cross-species patterns in the coordination between leaf and stem traits, and their implications for plant hydraulics. *Physiologia plantarum*, **127**(3), 445–456.

Xu, Ronghui. 2003. Measuring explained variation in linear mixed effects models. *Statistics in medicine*, **22**(22), 3527–3541.

Yamamoto, K., & Kobayashi, S. 1993. Analysis of crown structure based on the pipe model theory. *J. jpn. for. soc.*, **75**, 445–448.

Yamasaki, H., Uefuji, H., & Sakihama, Y. 1996. Bleaching of the red anthocyanin induced by superoxide radical. *Archives of biochemistry and biophysics*, **332**(1), 183 – 186.

Yoshitama, K., Ozaku, M., Hujii, M., & Hayashi, K. 1972. A survey of anthocyanins in sprouting leaves of some japanese angiosperms studies on anthocyanins, lxv. *Journal of plant research*, **85**(4), 303 – 306.

Zimmermann, M. H. 1978. Hydraulic architecture of some diffuse-porous trees. *Canadian journal of botany*, **56**(18), 2286 – 2295.

Zimmermann, M. H. 1983. *Xylem structure and the ascent of sap.* Germany: Springer-Verlag.

Zuur, A.F., Ieno, E.N., Walker, N., Saveliev, A.A, & Smith, G.M. 2009. *Mixed effects models and extensions in ecology with r.* Statistics for Biology and Health, vol. XXII. Springer.

Chapter 3

Influence of site water availability on leaf to sapwood area relationship in chestnut tree *(Castanea sativa* Mill.*)*

With Gehring Eric[1], Krebs Patrik[1], Mazzoleni Stefano[2] and Conedera Marco[1]

[1]WSL Swiss Federal Research Institute, Insubric Ecosystem Research Group. Via Belsoggiorno 22, CH-6500 Bellinzona, Switzerland

[2]University of Naples Federico II, Dip. di Arboricoltura, Botanica e Patologia vegetale, via Università 100 I-80055 Portici, Naples Italy

Keywords: chestnut autoecology, leaf area, tree physiology, pipe model, water availability

Abstract

The broad diffusion and active management by man of the sweet chestnut in past centuries has resulted in the establishment of the species at the limits of its potential ecological range in many European mountain areas. This raises the hypothesis that the chestnut tree has some mechanisms, enabling the species to adapt to very different sites and conditions. In order to test this hypothesis, we applied to single branches the pipe model approach, postulating the constancy of the leaf area to sapwood area relationship for single portions of a tree. Considering a correction for branch height (Chapter 2), we analysed the variation of the leaf to sapwood area slope coefficient ($LASA_{ground}$) among chestnut trees in different site conditions (e.g. convex vs. concave sites), in order to better understand the strategy used by the species to cope with water deficiency. The results confirm that the sweet chestnut is able to greatly vary the allocation of resources with respect to environmental conditions. In particular, $LASA_{ground}$ is high when trees are growing in sites with good water supply (concave sites) and low in water poor convex sites. Moreover, we confirmed the applicability of a simplified, non-destructive sampling procedure, which should allow the study of temporal (yearly) variations of $LASA_{ground}$ on selected trees. This may be a very useful measure for assessing the plasticity and the adaptation potential of plant species in the perspective of the ongoing global change.

Introduction

Ecological (i.e. physiological, morphological, and functional) plasticity is a key trait allowing species to adapt and organisms to cope with environmental condi-

tions (Fordyce, 2006). Ecological plasticity is a combination of genetic variability, environmental effects and their interactions (Schlichting, 1986; Martinez-Vilalta *et al.* , 2009). Anthropogenic and other exogenic drivers act as environmental filters, selecting individuals displaying suitable functional traits and characteristics. This on turn affects the ecological plasticity of the species (Valladares *et al.* , 2007). The broader the plasticity of a species, the highest is the probability of overcoming a given driver or limiting factor. The ability of an organism to respond to the surrounding environment is very important for its success, especially to explore and successfully colonize the potential area of diffusion.

Climate change will in future constitute an additional selecting factor for species. In particular it is believed that in the next century the water resource may become a even more limiting factor in many ecosystems (García-Fayos *et al.* , 2000; Bochet *et al.* , 2007; Maherali *et al.* , 2004). A rapid increase in global temperature and a consequently greater rate of evaporation for organisms are expected as a result of increased CO_2 emissions (Kattenberg, 1996). Understanding ecological plasticity is therefore of paramount importance to predict plant responses and possible adaptations to climate change (Weiher *et al.* , 1999; Parmesan, 2006; Ghalambor *et al.* , 2007).

In case of cultivated tree species, active management and diffusion masked the selection mechanisms, resulting in a population that may not be enough adapted for coping with future climate change. This may be the case of the chestnut tree (*Castanea sativa* Mill.) groves that have been created and maintained by man in many mountainous regions of Europe during more than 2000 years (Conedera *et al.* , 2004). In fact, the broad diffusion and active management by man of the sweet chestnut in past centuries has resulted in the establishment of the species at the limits of its potential ecological range in many European mountain areas (Pitte, 1986; Conedera *et al.* , 2004).

In recent times, abiotic (e.g. extreme summer droughts) and biotic (diseases such as the chestnut blight and the ink-disease; Waldboth & Oberhuber, 2009) stress factors, combined with the lack of active management, have locally caused the death of whole chestnut stands (Conedera *et al.* , 2001; Barthold *et al.* , 2004; Vettraino *et al.* , 2005; Conedera *et al.* , 2010a). For example the extreme drought of the Swiss summer 2003 caused damages in several chestnut stands in the Southern Alps showing that *C. sativa* could lack of a mechanism to protect against over-transpiration (Barthold *et al.* , 2004; Conedera *et al.* , 2011). This raises the hypothesis that climate change (e.g. extreme drought events) combined with extreme environmental conditions (e.g. water limited convex sites) may outrun the potential ecological range of the species, causing significant losses in chestnut forests.

It is thus of great interest and importance to assess the ability of adaptation to environmental constraints of a key species like *C. sativa,* providing ecosystem services, such as slope stability, and protection against landslides, as well as cultural and historical values (Bounous, 2005). To this purpose we applied the pipe model approach (Shinozaki *et al.* , 1964a,b), postulating constancy of the leaf to sapwood area ratio ($\frac{A_l}{A_s}$) relationship for single portions of a tree crown. This relationship should reflect the hydraulic traits of an individual, since it reflects the coordination between water conducting and transpiring tissues. It is in fact assumed, that variability of the $\frac{A_l}{A_s}$ ratio among individuals of a given plant species growing in different environmental conditions represents an indicator of the plasticity of the species (Mazzoleni & Dickmann, 1988). In fact, water and nutrient stress affects the growth of plants: organisms exposed to suboptimal environmental conditions need a larger area of sapwood for leaf area unit than those living on better conditions (having easier access to water and nutrients; Mencuccini & Grace, 1994). As a conse-

quence, plants living on poor and dry soil have a lower ratio between leaf surface and sapwood area or root dimension respectively (Grier & Running, 1977; Waring & Schlesinger, 1985; Mazzoleni, 1990; Li *et al.* , 2000). This leads to a low aerial part/root ratio and to a low slope coefficient of the $\frac{A_l}{A_s}$ regression line (Mazzoleni, 1990; Callaway *et al.* , 2000; Martinez-Vilalta *et al.* , 2009). The $\frac{A_l}{A_s}$ ratio could thus be used to predict the ability of a species to colonize and survive in different environmental conditions (sun exposure, nutriment, water).

This study intends to investigate the variation of the leaf to sapwood area relationship among chestnut trees subjected to different site conditions (e.g. convex vs. concave sites, different slope steepness), in order to determine the ability of chestnut trees to cope with environmental constraints such as water supply. We hypothesized that microtopography and slope are the main parameters influencing water availability at local scale.

Finally we tested the possibility to apply simplified non-destructive methods to analyse the leaf to sapwood area relationship. This would be of relevant importance for climate change studies, as a physiological integration of phenological observations, allowing a long term monitoring of selected trees.

Material and methods

Study site

Canton Ticino is a 2812 km^2 region located on the southern slope of the Alps in the Italian-speaking part of Switzerland (Figure 3.1). The area is characterized by a marked altitudinal gradient, ranging from 197 m a.s.l. around Lake Maggiore (Locarno) to 3402 m on the Adula Peak in northern Ticino. The geology of the area is dominated by siliceous rock with small spots of limestone, except in the very southern part where only limestone is present. Depending on the elevation and the geographical location, the mean annual precipitation ranges from 1,600 to 2,600 mm, and the mean annual temperature from 3 to 12 °C (Spinedi & Isotta, 2004). Summer rain is characteristic for the whole area, and there can be longer periods without rain or even drought in winter or spring times.

The distribution of the forest vegetation types follows the altitudinal gradient with different vegetation belts according to elevation. At low elevations (from 200 m up to 900–1100 m a.s.l.). forest vegetation is dominated by chestnuts *(Castanea sativa)*, which were first cultivated (and probably first introduced) in the area by the Romans nearly 2000 years ago (Tinner *et al.* , 1999). Chestnut forests are anthropogenic monocultures occasionally interrupted by the presence of other broadleaved species, such as *Tilia cordata, Quercus petraea, Q. pubescens, Alnus glutinosa, Prunus avium, Acer* spp., or *Fraxinus* spp.. The chestnut tree is nowadays still present on different microtopographic conditions (from hump to mountain bottom and from extreme buttress to extreme depression).

Sampling

A total of 93 trees were sampled from June 7th to August 13th in 2009, and from June 16th to July 22th in 2010, at locations with varying elevation, exposition, slope and microtopography (Table 3.1). Of the sampled trees, 32 were shared with the validation dataset of the preceeding study (Chapter 2), while the others were independent samples, which were selected with particular attention to the site microtopography and slope (Table 3.1). Trees' heights ranged from 1.5 to 26.6 m and diameters at breast height (1.3 m above ground) ranged from 5 to 112 cm. Each sampled tree has been characterized through different dendrometric and geo-physiographic parameters, as shown in Table 3.2. A synthetic index for microtopography was developed, in order to expressly define the interaction of the vertical and horizontal components. Since we could assume that soils from the sampling sites had a similar composition (Blaser, 1973), we did not consider additional soil specific factors playing a role in soil water storage capacity, and which

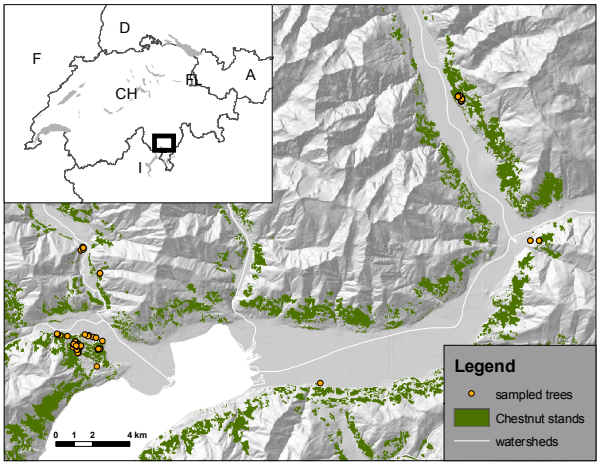

Figure 3.1: Study site.

Table 3.1: Sampled trees and branches.

	Variable	*Mean*	*Max* / *Min*
Trees (n=93)	Elevation [masl]	396.45	591 / 221
	Slope [%]	37.26	100 / 0
	Height [m]	11.2	26.6 / 1.5
	DBH [cm]	43.63	112 / 5
Branches (n=163)	Length [cm]	120.18	251 / 20
	ϕ at cutting point [mm]	18.64	40.5 / 7.9

would be required for a study on a larger area.

A total of 163 chestnut branches (Table 3.1) were collected when all the leaves were fully developed and hadn't endured too many damages from climate, parasites and phytophagous insects. Particular attention was paid to the choice of the sample branches. In fact epicormic shoots were avoided and only crown branches were taken in consideration. Moreover branches were collected in the top region of the trees, in order to minimize the potential difference in the leaf to sapwood area relationship due to branch type and abiotic factors like branch exposition to light. The same procedure used in the previous study (Chapter 2) for branch collection and processing was applied.

Table 3.3: Branch and intra-branch parameters considered.

Parameter	*Unit*
Branch height at cutting point	m
Section minimum diameter	mm
Section maximum diameter	mm
Sapwood area	cm^2
Leaf width	cm
Leaf length	cm
Leaf area	m^2
Mean leaf area	cm^2

Leaf width and length were also recorded from the digital image analysis, in order to evaluate the possibility to use simpler measures as a proxy for leaf area (Table 3.3).

Data analysis

Similar to the previous study (Chapter 2), simple linear regression ($A_l = a \cdot A_s + b$) was used to calculate the leaf to sapwood area slope coefficient ($LASA = a = \frac{A_l - b}{A_s}$). We analysed this coefficient instead of the $\frac{A_l}{A_s}$ ratio, accounting for the possibility to have an non-zero intercept in the linear regressions (see Chapter 2).

In order to standardize the $LASA$ and minimize the differences due to the branch height, the *ground-level* $LASA$ ($LASA_{ground}$) was computed, according to the model develped in the previous study

Table 3.2: Dendrometric and geo-physiograhic parameters considered.

Parameter	Unit / Values	Model*	Coll.**	Assessment/Notes
Dendrometric parameters				
Social position	Predominant (1) Dominant (2) Co-dominant (3) Dominated (4)	e		
DBH	*cm*		t	
Bark type	Incipient (1) Smooth(2) Wrinkled (3)		t	
Height	*m*		t	hypsometer VertexIII-60
Crown base height	*m*		t	
Crown exposure to light	*%*	e		
Leaf loss	*%*		t	
Number of suckers	$\frac{nr}{m}$		t	mean of observations on three 1m portions of trunk
Geo-physiographic parameters				
Geographic coordinates	CH1903_LV03 projected coordinate system [m]			GPS Trimble, Geoexplorer 2005 series GeoXh
Aspect	transformed (Beers *et al.* , 1966)	e		compass Meridian MG-3002
Elevation	*masl*	e		extracted from DEM
Slope	*%*	e		clinometer Meridian MG-3002
Rocks	*%*	e		cover of rocks visible on surface
Soil depth (cm)	*cm*	(e)	a	mean of 6 measures of depth assessed with a metal stick (Ø 13 mm) and hammer
Distance to waterbed	m	(e)	b	laser distance-meter Leica, Disto Classic
Vertical microtopography	Hump (-1) Slope (0) Slope bottom (1)	(e)	a	
Horizontal microtopography	Extreme convexity (-2) Convexity (-1) Slope (0) Concavity (1) Extreme concavity (2)	(e)	ab	
Composite microtopography	[-3,3]	e	ab	calculated as the sum of Horizontal micr. and Vertical microtopography: negative values for convexity, 0 for slope, positive values for concavity

* *tested as explaining variable in the model with environmental factors (e) or in the model with the tree characteristics (t). Brackets indicate the variable was excluded due to colllinearity with other variables*

** *collinearity among the model candidate variables: same letters represents correlated variables (Pearson $R > 0.5$)*

(Chapter 2: $LASA_{ground} = LASA + 0.0275 \cdot height_{branch}$). This should correspond to the theoretical $LASA$ value of a branch at ground level. A mean value has been calculated for trees with more than one sampled branch.

Linear regression analysis and model selection were used to understand the relationship between the physiographic and dendrometric variables with $LASA_{ground}$. In particular the explaining variables were tested in two separate groups (Table 3.2): variables defining the environmental conditions, which may influence $LASA_{ground}$ (potential causality), and tree specific characteristics, related to tree development (dimensions) or to plant responses emerging from possibly common physiological processes (e.g. number of suckers). According to those groups, two separate model selections have been performed. Only uncorrelated variables (*Pearson* $R \leq 0.5$) were tested in each model (Table 3.2). Using the R package *glmulti*, all models with all possible combinations of explaining variables were computed (16384 models for the environmental variables, 4096 for the dendrometric ones) with simple and quadratic terms (no interactions have been considered). The best models were chosen on the base of the AICc coefficient (Akaike information criterion with a second order correction for small sample size), and were compared to the models with reduced terms.

Additionally univariate comparative analysis were performed on the categorized explicative variables (non parametric Wilcoxon test), and the relevant results were plotted.

To test the possibility of simplifying the sampling methodology, the relationship between area, width and length of leaves has been analysed with linear regressions, at the leaf and the branch level. Also the use of the $\frac{A_l}{A_s}$ ratio instead of $LASA$ to compute $LASA_{ground}$ is evaluated by means of regression analysis.

The analysis were performed using the R statistical package version 2.14.0 (R Development Core Team, 2011).

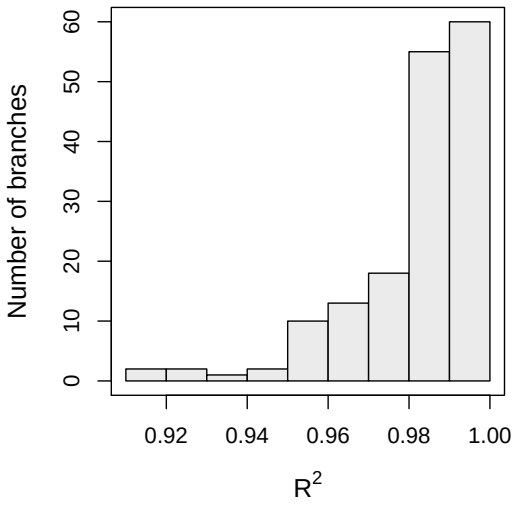

Figure 3.2: Histogram of the R^2 coefficients of $LASA$ linear regressions of the branches.

Results

A strong intra-branch correlation between leaf area and sapwood area was found for all branches, confirming that a physiological balance exists between these two parameters (all R^2 were above 0.91; Figure 3.2). Intercepts were significantly different from zero in 19.6 % of the branches.

The measured $LASA$ varied by a factor of 10.4 (0.1 to 1.07), while the calculated $LASA_{ground}$ varied by a factor of 4.2 (0.3 to 1.25), highlighting a considerable plasticity and the expected reduced range of the second term.

Out of the 16384 tested environmental variable combinations, the model formula with *microtopography*, *aspect* and *crown exposure to light* (the last two factors with both simple and quadratic terms) gave the best result in term of AICc. Table 3.4 reports the best model and the subsequent best models that consider less variables. In the best model only the estimates of intercept, micropotography and the quadratic term of aspect were significant (p-value < 0.05). The R^2 value was quite high (0.66), although the increase in $\bar{R}^2$ from the model with a single term to the best model was limited (Table 3.4).

Figure 3.3 shows how $LASA_{ground}$ relates to different site conditions. Signif-

Table 3.4: Best linear models with environmental variables. Model 1 is the best AICc ranking model, model 2 the best one with only two explaining variables, model 3 the best model with a single factor and model 4 is the null model with intercept only *(M=microtopography ; A=aspect ; C=crown exposure to light, $\beta_{0...5}$=coefficients).*

	Model terms	log_{Lik}	s^2_{resid}	s_{resid}	AIC_c	R^2	$\bar{R}^2$
1	$\beta_0 + \beta_1 M + \beta_2 A + \beta_3 A^2 + \beta_4 C + \beta_5 C^2$	50.50	0.02111	0.14528	-85.75	0.662	0.643
2	$\beta_0 + \beta_1 M + \beta_2 C + \beta_3 C^2$	48.00	0.02221	0.14903	-85.35	0.644	0.632
3	$\beta_0 + \beta_1 M$	45.56	0.02334	0.15278	-84.87	0.626	0.622
4	β_0	-2.58	0.06235	0.24970	9.29	0.000	0.000

icant differences were found for vertical and horizontal microtopography, slope, soil depth and distance to the next waterbed (non-parametric pairwise Wilcoxon test with Holm adjustment for p-values, differences were all with $p<0.001$, except for soil depth, with $p<0.05$ between the first two categories). Higher $LASA_{ground}$ were found in convex sites, with gentle slopes, deeper soils and in proximity of waterbeds. The same analysis performed on the measured $LASA$ instead of $LASA_{ground}$ highlighted much less significant correlations (data not shown).

Table 3.5 reports the best model based on dendrometric variables out of 4096 (including *tree height*, *crown base height* and *number of suckers*; the two factors with both simple and quadratic terms), the best models with reduced terms and the null model. The estimates of all terms of the best model were highly significant ($p < 0.001$). The R^2 value was quite high (0.71), and the best model was according to the $\bar{R}^2$ value considerably better that those with two or one explaining variables (Table 3.5).

A quite high correlation was found between $LASA_{ground}$ and tree height (Pearson R of 0.77) and also between $LASA_{ground}$ and tree DBH's up to 60 cm (Pearson R of 0.56, Figure 3.4). However $LASA_{ground}$ was decreasing from DBH's between 40 and 60 cm to DBH's above 60 cm.

Although an appreciable variation in leaf form was observed, with leaf area ranging approximately from the ellipse area to values 1/3 lower (Figure 3.5 *left*), the correlation at the branch level of leaf area and an estimation based on leaf length and width was very high (R^2 of 0.999, Figure 3.5 *right*). This was found to be 0.785 times the area calculated considering an ellipse form of the leaves ($length \cdot width \cdot \frac{\pi}{4}$). Figure 3.6 shows the high correlation between the measured $LASA$ and an estimate of $\frac{A_l}{A_s}$ based on the above mentioned approximation of the ellipse formula.

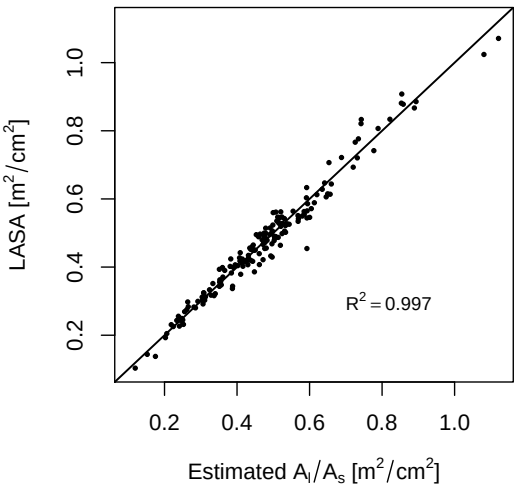

Figure 3.6: Relationship of the measured $LASA$ and the branch $\frac{A_l}{A_s}$ ratio, where leaf area is predicted with leaf width and height. The line represents the identity.

Repeating the regression analysis of the environmental and dendrometric factors with the proposed estimate of $\frac{A_l}{A_s}$ yielded the same results (data not shown), including the same significant terms in the best selected models. This confirms the validity of this approximation of $LASA$.

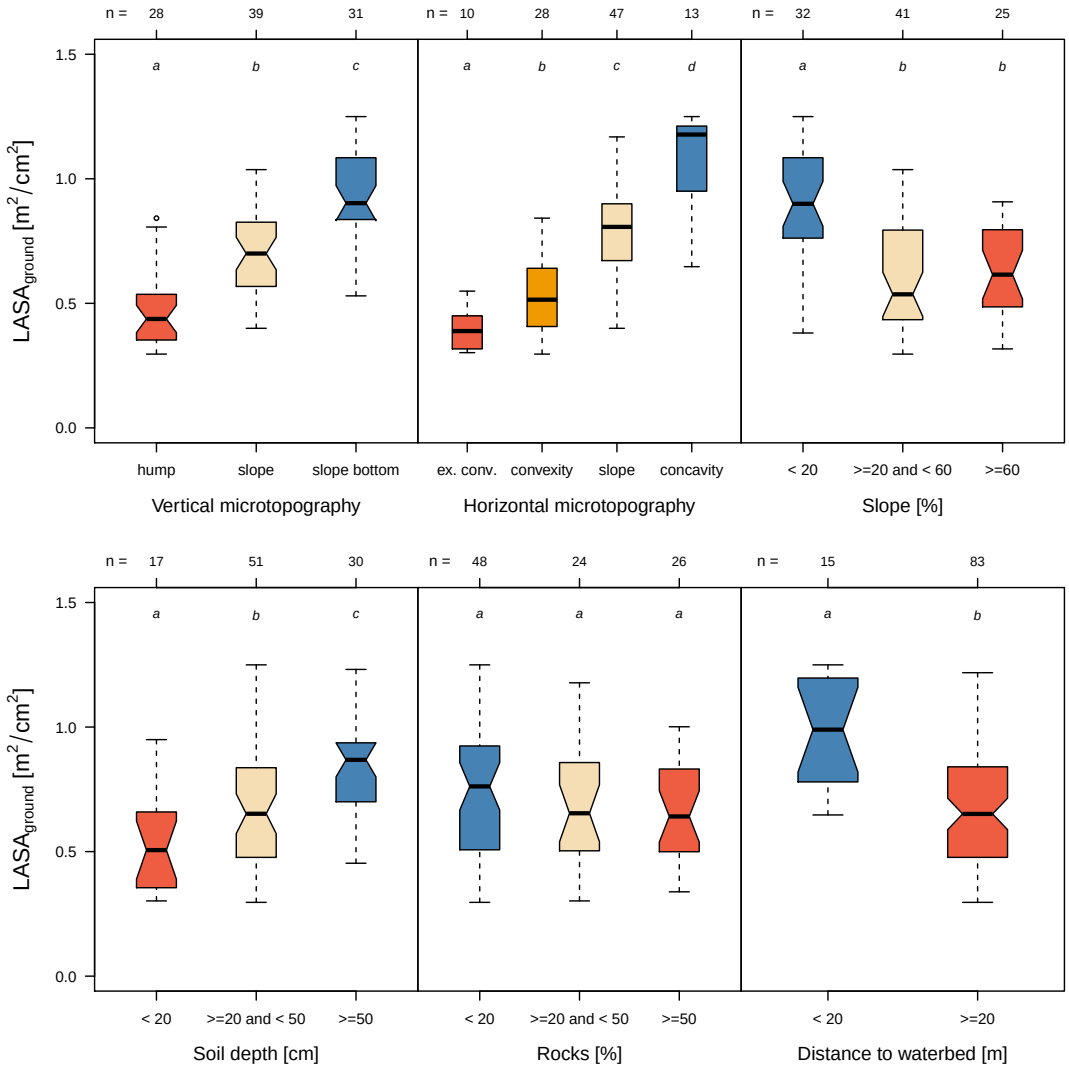

Figure 3.3: Boxplots of the mean $LASA_{ground}$ of the trees, according to different site conditions. Letters indicate significant differences (p<0.05), according to the non-parametric Wilcoxon test with Holm adjustement. Labels on the top *(n)* represent the number of sampled trees in each category.

Table 3.5: Best linear models with dendrometric variables. Model 1 is the best AICc ranking model, model 2 the best one with only 2 fixed effects, model 3 the best model with one fixed effect and model 4 is the null model with random intercept only (*H=tree height ; Cbh= crown base height ; S=number of suckers*, $\beta_{0...5}$=*coefficients*).

	Model terms	log_{Lik}	s^2_{resid}	s_{resid}	AIC_c	R^2	$\bar{R}^2$
1	$\beta_0 + \beta_1 H + \beta_2 Cbh + \beta_3 Cbh^2 + \beta_4 S + \beta_5 S^2$	54.87	0.01864	0.13653	-94.45	0.706	0.690
2	$\beta_0 + \beta_1 H + \beta_2 S$	43.71	0.02402	0.15499	-78.99	0.614	0.606
3	$\beta_0 + \beta_1 H$	40.57	0.02585	0.16077	-74.88	0.585	0.581
4	β_0	-2.58	0.06235	0.24970	9.29	0.000	0.000

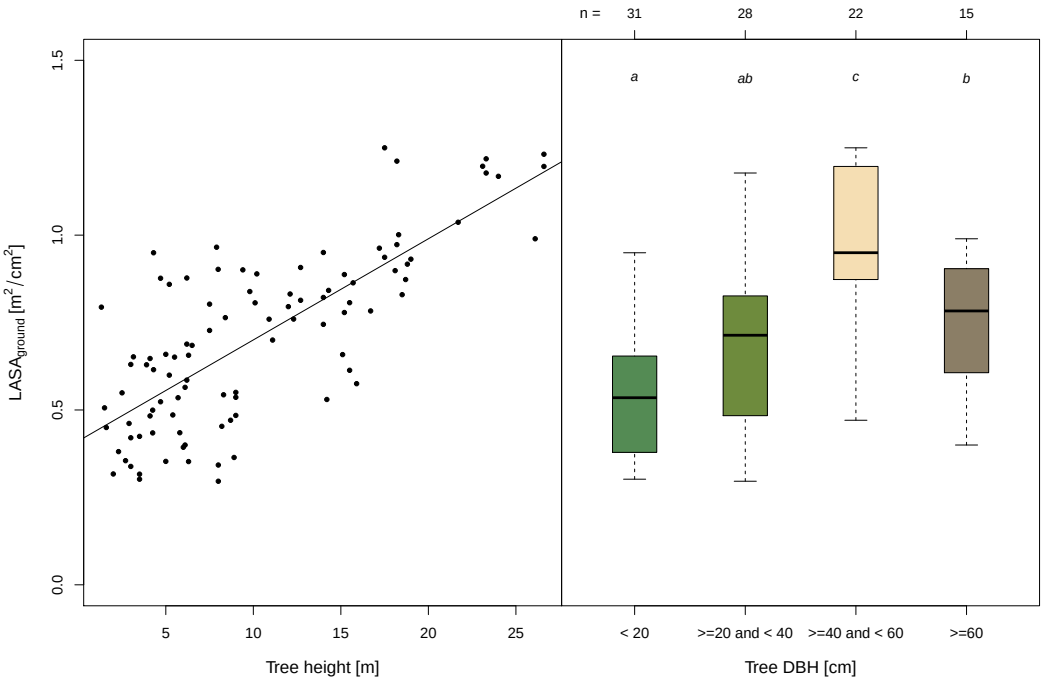

Figure 3.4: Relationship of the mean $LASA_{ground}$ of the trees with tree height *(left)* and DBH *(right)*. Letters indicate significant differences ($p<0.05$), according to the non-parametric Wilcoxon test with Holm adjustement. Labels on the top *(n)* represent the number of sampled trees in each category.

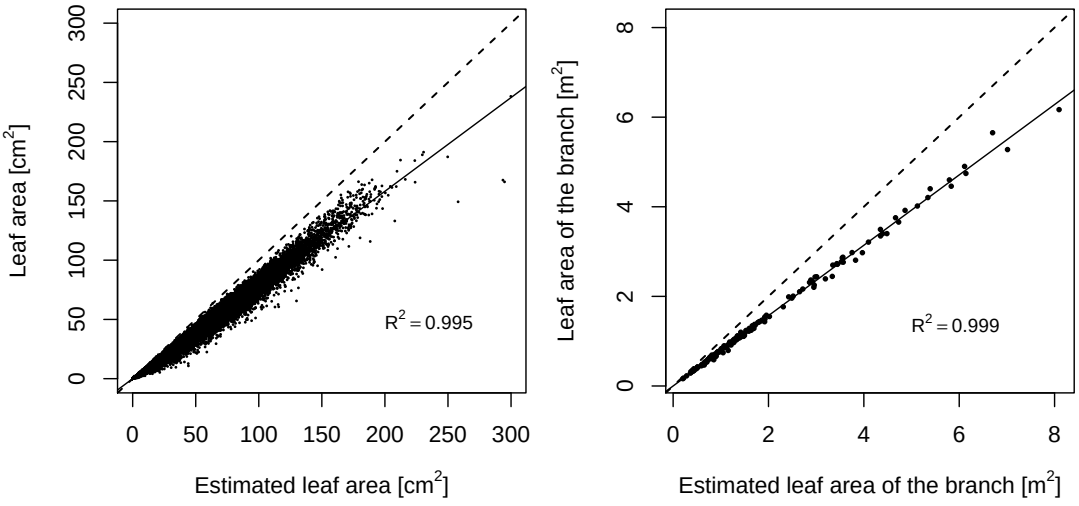

Figure 3.5: Relationship of leaf area calculated with the ellipse formula (from leaf width and length) and the effective leaf area, at leaf *(left)* and branch *(right)* level. Dashed lines represent the identity, while continuous ones the linear fit of the points with zero intercept.

Discussion

The R^2 linear regression coefficients of the intra-branch $LASA$ slope coefficient are very high, despite the considerable range of measured $LASA$ values, thus confirming the functional meaning of the allometric relationship among leaf and sapwood area (Shinozaki *et al.* , 1964a,b) in chestnut trees. The encountered variability of $LASA_{ground}$ was the double what Mazzoleni (1990) reports for *Populus euramericana*, highlighting the influence of specific site conditions. In particular, $LASA_{ground}$ decreases significantly from presumably water-rich (concave position, deeper soils and nearer to waterbeds) to water-poor sites (convex, steeper slopes). The remarkable correlation of the microtopography composite index with $LASA_{ground}$ confirms its importance in this potential water supply effect (R^2 of 0.63).

Our study additionally suggests the involvement of the evaporative demand, since aspect and portion of crown exposed to direct light were also involved in the best model. However according to their limited contribution to $\bar{R}^2$, they should play a secondary role compared to microtopography.

Castanea sativa seems thus to respond to lower water availability or increased evaporative demand by changing its biomass allocation. This findings are consistent with previous studies showing similar results (Mazzoleni, 1990; Mencuccini & Bonosi, 2001; Poyatos *et al.* , 2007; Martinez-Vilalta *et al.* , 2009) and other studies which found a decrease in the leaf to sapwood area ratio with increasing evaporative demand (Waring *et al.* , 1982; Mencuccini & Grace, 1994) and vapour pressure deficit (DeLucia *et al.* , 2000). In drier habitats a decrease in $LASA$ may contribute ensuring the water flow from root to leaves by supplying greater hydraulic capacity per unit of leaf area, pointing out the relationship between site water availability and the pipe model principle (Shinozaki *et al.* , 1964a,b). Moreover studies on poplar plants found that one of the first physiological processes affected by water deficiency is leaf growth (Kelliher & Tauer, 1980; Schulte *et al.* , 1986; Mazzoleni & Dickmann, 1988). It is therefore possible to assume that the balance between water availability and evaporative demand is one of the main factors influencing $LASA$ and the $\frac{A_l}{A_s}$ ratio.

In our study we supposed a similar mesoclimate for the study area, and we did not specifically consider differences in climatic variables such as summer water stress (including precipitation, temperature, net radiation, humidity and wind). Those factors also influence soil water availability and are known to be correlated with variations in plant traits (Grier & Running, 1977; Li *et al.* , 2000). In particular precipitation is known to occur with a certain variability at the local scale. Since summer rain (July) appears to be the main climatic variable controlling the growth of chestnut trees (Fonti & Garcia-Gonzalez, 2004), it is possible that local differences results in different allometric relationships. Similarly soil composition was assumed to be homogeneous in the study area, but local differences in soil properties also influence water availability. Considering that these factors all play a relevant role in the degree of unexplained variance of our model, the model fit is surprisingly high.

Regarding the dendrometric characteristics correlated with $LASA_{ground}$, and thus with the hydraulic properties of the tree, the most relevant parameter were individual height, number of suckers and crown base height. The model performed with an high coefficient of determination (R^2 of 0.71), despite no information on tree age was available. In fact, the ideal dataset would have required to have all the trees reaching their potential growth in the given environmental and stand-related situation (e.g. maximum tree height), condition that was not always met during the sampling.

Notwithstanding this potential bias, tree height shows a good correlation with $LASA_{ground}$, highlighting the fact that the better water conditions that determines an higher leaf to sapwood area ratio also allow an higher maximum tree height. This consistency holds only par-

tially when $LASA_{ground}$ is compared to the DBH, where the observed decreasing pattern of $LASA_{ground}$ for DBH's above 60 cm raises a question mark. This may be related specifically to the characteristics of the sampled trees with a DBH>60 cm, which had a well developed crown from the bottom up and were probably isolated individuals or in small groups (Figure 3.7), and thus exposed to an increased evaporative demand. Presumably those trees were subjected to a different management, nearer to an orchard structure (full crowns) than a coppice one.

While these correlations may be explained as the result of a similar effect of the environment on the considered variables, the observed decreasing pattern of $LASA_{ground}$ for DBH's above 60 cm raises a question mark. This may be related specifically to the characteristics of the sampled trees with a DBH>60 cm, which had a well developed crown from the bottom up and were probably isolated individuals or in small groups (Figure 3.7), and thus exposed to an increased evaporative demand.

Crown base height in our dataset was not collinear with tree height (*Pearson* R<0.5), and the coefficient estimates of the model (data not shown) showed a positive proportionality with the response variable. In this respect, crown base height can be considered as a proxy for crown shape and total leaf area, the latter being known to be related to site water availability (Grier & Running, 1977; Gholz, 1982; Nemani & Running, 1989; Jose & Gillespie, 1996).

Finally the number of suckers contributed to the best model with an inverse relationship, according to the coefficient estimates (data not shown). In fact the model predicts a lower $LASA_{ground}$ for individuals showing an higher density of suckers along the trunk, confirming the ability of chestnut trees to produce suckers when exposed to water stressed conditions. As already mentioned in the previous study (Chapter 2), this mechanism allows a quick response to disturbance (Sakai *et al.* , 1995; Ito *et al.* , 1999) and

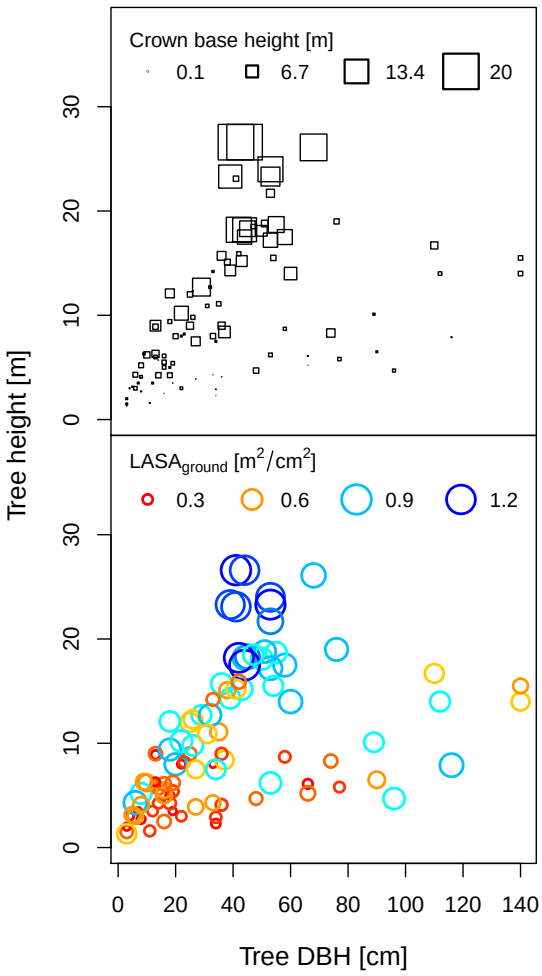

Figure 3.7: Relationship between tree DBH and tree height. The size of the squares and circles is proportional to crown base height and to mean $LASA_{ground}$, respectively.

restoration of the original architecture (Begin & Filion, 1999), maintaining leaf area (Briand & Larson, 1992; Nicolini *et al.* , 2001; Ishii *et al.* , 2007), crown productivity and promoting longevity (Bryan & Lanner, 1981; Ishii *et al.* , 2002; Gerrish, 1990).

Although *C. sativa* seems to be well adapted to dry conditions (Ellenberg, 1996), during the summer 2003, severe drought damages were observed (Barthold *et al.* , 2004). In case of sudden drops in water availability, plants have to face a situation were the transpirational surface is too large with respect to the existing water absorption and transport sys-

tem. However several years can be required for the adaptation of the proportions of the concerned functional parts, e.g. for the extension of the the root system or the reduction of canopy biomass. Therefore it is possible that *C. sativa* could lack an effective mechanism to protect the species against over-transpiration in extremely hot and dry weather conditions, such as stomata regulation or the ability to purge part of its foliage. If so, this may constitute an additional threat for the species in case of climatic change towards an increase in the frequency of summer hot spells. The specific strategies implemented to face such situations are key factors in survival and may impact interspecific competition, as hypothesized by Mazzoleni & Spada (1992) for water-stressed ecosystems underlying heavy disturbance regimes like the Mediterranean region (evergreen sclerophyllous vs. deciduous broadleaved species). Moreover the future decline of *C. sativa* with drought could be enhanced by the synergistic effect with parasite infection as for example the chestnut blight (*Cryphonectria parasitica*; Waldboth & Oberhuber, 2009; Conedera *et al.* , 2011).

Although the used methodology is quite time consuming, in particular the digitalization process of the leaves and the image analysis, a simplified procedure can be effectively applied, replacing $LASA$ with $\frac{A_l}{A_s}$ and estimating A_l from leaf width and length ($0.785 \cdot length \cdot width \cdot \frac{\pi}{4}$).

Conclusion

The relationship between leaf and sapwood area was confirmed to be a useful instrument to assess the ecological plasticity and thus the ability of species to establish in sites with different water availability. The determination of $LASA_{ground}$ of branch portions can provide a useful measure of the hydraulic conditions of the tree. To this respect the pipe model approach can improve our understanding of the ongoing phenomena in chestnut groves, such as the progressive decline of chestnut in abandoned chestnut orchards (e.g. Conedera *et al.* , 2000, 2001), the establishment of neophytes, and the stool uprooting in over-aged chestnut coppices (Pividori *et al.* , 2008; Conedera *et al.* , 2009), where $LASA_{ground}$ could be used as a proxy for the above and below ground biomass partitioning (Mazzoleni, 1990).

The analysis revealed also the practicability of a non-destructive sampling, allowing the monitoring of selected trees over several years. This could be of paramount interest in the frame of studies on climate change, integrating the phenological observations with a measure directly linked to the plant water relations. With increased temperatures and probable longer drought events, plant plasticity will be a key factor for coping with climate variation (Sultan, 1995; Cordell *et al.* , 1998; Joshi *et al.* , 2001; Lehmann & Rebele, 2005), driving species composition in future ecosystems.

References

Barthold, F., Conedera, M., Torriani, D., & Spinedi, F. 2004. Welkesymptome an edelkastanien im sommer 2003 auf der alpensüdseite der schweiz. *Schweizerische Zeitschrift für Forstwesen*, **155**(9), 392 – 399.

Beers, T. W., Dress, P. E., & Wensel, L. C. 1966. Aspect transformation in site productivity research. *Journal forestry*, **64**, 691 – 692.

Begin, C., & Filion, L. 1999. Black spruce (Picea marianna) architecture. *Canadian journal of botany*, **77**(5), 664 – 672.

Blaser, P. 1973. Die Bodenbildung auf Silikatgestein im südlichen Tessin. *Mitt. eidgenöss. forsch.anst. wald schnee landsch.*, **49**(3), 251–340.

Bochet, E., García-Fayos, P., Alborch, B., & Tormo, J. 2007. Soil water availability effects on seed germination account for species segregation in semiarid roadslopes. *Plant and soil*, **295**(1 - 2), 179 – 191.

Bounous, G. 2005. The chestnut: A multipurpose resource for the new millennium. *Acta horticulturae*, **693**, 33 – 40.

Briand, C. H. P., & Larson, D. W. 1992. Differential axis architecture in Thuja occidentalis (eastern white cedar). *Canadian journal of botany*, **70**(2), 340 – 348.

Bryan, J. A., & Lanner, R. M. 1981. Epicormic branching in Rocky Mountain Douglas-fir. *Journal of forest research*, **11**(2), 190 – 199.

Callaway, Ragan M., Sala, Anna, & Keane, Robert E. 2000. Succession may maintain high leaf area: Sapwood ratios and productivity in old-subalpine forests. *Ecosystems*, **3**(May), 254–268.

Conedera, M., Stanga, P., Lischer, C., & Stöckli, V. 2000. Competition and dynamics in abandoned chestnut orchards in southern switzerland. *Ecologia mediterranea*, **26**(1 - 2), 101 – 112.

Conedera, M., Stanga, P., Oester, B., & Bachmann, P. 2001. Different post-culture dynamics in abandoned chestnut orchards. *Forest snow and landscape research*, **76**(3), 487 – 492.

Conedera, M., Manetti, M. C., Giudici, F., & Amorini, E. 2004. Distribution and economic potential of the sweet chestnut (castanea sativa mill.) in europe. *Ecologia mededitterranea*, **30**(2), 179 – 193.

Conedera, M., Fonti, P., Nicoloso, A., Meloni, F., & Pividori, M. 2009. Ribaltamento delle ceppaie di castagno: Individuazione delle zone a rischio e proposte selvicolturali. *Sherwood*, **154**, 15 – 18.

Conedera, M., Barthold, F., Torriani, D., & Pezzatti, G.B. 2010a. Drought sensitivity of castanea sativa: Case study of summer 2003 in the southern alps. *Acta horticulturae (ishs)*, **866**, 297–302.

Conedera, Marco, Barthold, Frauke, Spinedi, Fosco, Ferrario, Federico, & Pezzatti, Gianni Boris. 2011. Siccità estiva e castagno. un'ulteriore minaccia dagli estremi climatici? *Sherwood*, **178**(November), 16–21.

Cordell, S., Goldstein, G., Mueller-Dombois, D., Webb, D., & Vitousek, P. M. 1998. Physiological and morphological variation in metrosideros polymorpha, a dominant hawaiian tree species, along an altitudinal gradient: The role of phenotypic plasticity. *Oecologia*, **113**, 188 – 196.

DeLucia, E. H., Maherali, H., & Carey, E. V. 2000. Climate-driven changes in biomass allocation in pines. *Global change biology*, **6**(5), 587 – 593.

Ellenberg, H. 1996. *Vegetation mitteleuropas mit den alpen*. 5th edn. edn. Stuttgart: Ulmer.

Fonti, P., & Garcia-Gonzalez, L. 2004. Suitability of chestnut earlywood vessel chronologies for ecological studies. *New phytologist*, **163**(1), 77 – 86.

Fordyce, J. A. 2006. The evolutionary consequences of ecological interactions mediated through phenotypic plasticity. *Journal of experimental biology*, **209**(12), 2377 – 2383.

García-Fayos, P., García-Ventoso, B., & Cerdà, A. 2000. Limitations to plant establishment on eroded slopes in southeastern spain. *Journal of vegetation science*, **11**(1), 77 – 86.

Gerrish, G. 1990. Relating carbon allocation patterns to tree senescence in metrosideros forests. *Ecology*, **71**(3), 1176 – 1184.

Ghalambor, C. K., Mckay, J. K., Carroll, S. P., & Reznick, D. N. 2007. Adaptive versus non-adaptive phenotypic plasticity and the potential for contemporary adaptation in new environments. *Functional ecology*, **21**(3), 394 – 407.

Gholz, H. L. 1982. Environmental limits on aboveground net primary production, leaf area, and biomass in vegetation zones of the pacific northwest. *Ecology*, **63**(2), 469 – 481.

Grier, Charles G., & Running, Steven W. 1977. Leaf area of mature northwestern coniferous forests: Relation to site water balance. *Ecology*, **58**(4), 893–899. ArticleType: primary_article / Full publication date: Jul., 1977 / Copyright © 1977 Ecological Society of America.

Ishii, H. T., Ford, E. D., & Dinnie, C. E. 2002. The role of epicormic shoot production in maintaining foliage in old pseudotsuga menziesii (douglas-fir) trees ii. basal reiteration from older branch axes. *Canadian journal of botany*, **80**(9), 916 – 926.

Ishii, Hiroaki T., Ford, E. David, & Kennedy, Maureen C. 2007. Physiological and ecological implications of adaptive reiteration as a mechanism for crown maintenance and longevity. *Tree physiology*, **27**(3), 455–462.

Ito, K., Ito, S., Gyokusen, K., & Saito, A. 1999. Ecological roles of stem sprouts and creeping sprouts of aucuba japonica thunb. *Journal of forest research*, **4**(2), 137 – 143.

Jose, S., & Gillespie, A. R. 1996. Aboveground production efficiency and canopy nutrient contents of mixed-hardwood forest communities along a moisture gradient in the central united states. *Canadian journal of forest research*, **26**(12), 2214 – 2223.

Joshi, J., Schmid, B., Caldeira, M. C., Dimitrakopoulos, P. G., Good, J., Harris, R., Hector, A., Huss-Danell, K., Jumpponen, A., Minns, A., Mulder, C. P. H., Pereira, J. S., Prinz, A., Lorenzen, M. S.-., Terry, A. C., Troumbis, A. Y., & Lawton, J. H. 2001. Local adaptation enhances performance of common plant species. *Ecology letters*, **4**(6), 536 – 544.

Kattenberg, A. 1996. Climate models: Projections of future climate.

Kelliher, F. M., & Tauer, C. G. 1980. Stomatal-resistance and growth of drought-stressed eastern cottonwood from a wet and dry site. *Silvae genetica*, **29**(5 - 6), 166 – 171.

Lehmann, C., & Rebele, F. 2005. Phenotypic plasticity in calamagrostis epigejos (poaceae): Response capacities of genotypes from different populations of contrasting habitats to a range of soil fertility. *Acta oecologica*, **28**(2), 127 – 140.

Li, C. Y., Berninger, F. K., & Sonninen, E. 2000. Drought responses of eucalyptus microtheca provenances depend on seasonality of rainfall in their place of origin. *Australian journal of plant physiology*, **27**(3), 231 – 238.

Maherali, H., Pockman, W. T., & Jackson, R. B. 2004. Adaptive variation in the vulnerability of woody plants to xylem cavitation. *Ecology*, **85**(8), 2184 – 2199.

Martinez-Vilalta, J., Cochard, H., Mencuccini, M., Sterck, F., Herrero, A., Korhonen, J. F. J., Llorens, P., Nikinmaa, E., Nole, A., Poyatos, R., Ripullone, F., Sass-Klaassen,

U., & Zweifel, R. 2009. Hydraulic adjustment of scots pine across europe. *New phytologist*, **184**(2), 353 – 364.

Mazzoleni, S., & Spada, F. 1992. *Responses of forest ecosystems to environmental changes.* Elsevier Applied Science,London and New York. Chap. Deciduous broadleaved versus evergreen sclerophyllous forests. Disturbance and local shifting dominance in Mediterranean environments., page 839?840.

Mazzoleni, Stefano. 1990. Relazioni tra aree fogliari e superfici di conduzione nel fusto nell'analisi di gradienti ambientali. *Linea ecologica*, 27–30.

Mazzoleni, Stefano, & Dickmann, Donald I. 1988. Differential physiological and morphological responses of two hybrid populus clones to water stress. *Tree physiol*, **4**(1), 61–70.

Mencuccini, M., & Bonosi, L. 2001. Leaf/sapwood area ratios in scots pine show acclimation across europe. *Canadian journal of forest research*, **31**(3), 442 – 456.

Mencuccini, Maurizio, & Grace, John. 1994. Climate influences the leaf area/sapwood area ratio in scots pine. *Tree physiol*, **15**(1), 1–10.

Nemani, R. R., & Running, S. W. 1989. Testing a theoretical climate-soil-leaf area hydrologic equilibrium of forests using satellite data and ecosystem simulation. *Agricultural and forest meteorology*, **44**(3 - 4), 245 – 260.

Nicolini, E., Chanson, B., & Bonne, F. 2001. Stem growth and epicormic branch formation in understory beech trees (fagus sylvatica l.). *Annals of botany*, **87**, 737 – 750.

Parmesan, C. 2006. Ecological and evolutionary responses to recent climate change. *Annual review of ecology evolution and systematics*, **37**, 637 – 669.

Pitte, J. R. 1986. Terres de castanide. hommes et paysages du châtaignier de l'antiquité à nos jours.

Pividori, M., Meloni, F., Nicoloso, A., Arienti, R., & Conedera, M. 2008. Ribaltamento delle ceppaie di castagno. due casi di studio in cedui invecchiati. *Sherwood*, **14**(149), 17 – 21.

Poyatos, R., Martinez-Vilalta, J., Cermak, J., Ceulemans, R., Granier, A., Irvine, J., Kostner, B., Lagergren, F., Meiresonne, L., Nadezhdina, N., Zimmermann, R., Llorens, P., & Mencuccini, M. 2007. Plasticity in hydraulic architecture of scots pine across eurasia. *Oecologia*, **153**(2), 245 – 259.

R Development Core Team. 2011. *R: A language and environment for statistical computing.* R Foundation for Statistical Computing, Vienna, Austria. ISBN 3-900051-07-0.

Sakai, A., Ohsawa, T., & Ohsawa, M. 1995. Adaptive significance of sprouting of euptelea polyandra, a deciduous tree growing on steep slopes with shallow soil. *Journal of plant research*, **108**(3), 377 – 386.

Schlichting, C. D. 1986. The evolution of phenotypic plasticity in plants. *Annual review of ecology and systematics*, **17**, 667 – 693.

Schulte, P. J., Hinckley, T. M., & Stettler, R. F. 1986. Stomatal response of populus to leaf water potential. *Canadian journal of botany*, **65**, 255 – 260.

Shinozaki, K, Yoda, K, Hozumi, K, & Kira, T. 1964a. A quantitative analysis of plant form – the pipe model theory i. basic analyses. *Japanese journal of ecology*, **14**(3), 97–105.

Shinozaki, K, Yoda, K, Hozumi, K, & Kira, T. 1964b. A quantitative analysis of plant form – the pipe model theory ii. further evidence of the theory and its application in forest ecology. *Japanese journal of ecology*, **14**(4), 133–139.

Spinedi, F., & Isotta, F. 2004. Il clima del ticino. *Dati statistiche e società*, **2**, 5 – 39.

Sultan, S. E. 1995. Phenotypic plasticity and plant adaptation. *Acta botanica neerlandica*, **44**(4), 363 – 383.

Tinner, W., Hubschmid, P., Wehrli, M., Ammann, B., & Conedera, M. 1999. Long-term forest fire ecology and dynamics in southern switzerland. *Journal of ecology*, **87**, 273–289.

Valladares, F., Gianoli, E., & Gomez, J. M. 2007. Ecological limits to plant phenotypic plasticity. *New phytologist*, **176**(4), 749 – 763.

Vettraino, A. M., Morel, O., Perlerou, C., Robin, C., Diamandis, S., & Vannini, A. 2005. Occurrence and distribution of phytophthora species in european chestnut stands, and their association with ink disease and crown decline. *European journal of plant pathology*, **111**(2), 169 – 180.

Waldboth, M., & Oberhuber, W. 2009. Synergistic effect of drought and chestnut blight (cryphonectria parasitica) on growth decline of european chestnut (castanea sativa). *Forest pathology*, **39**(1), 43 – 55.

Waring, R. H., & Schlesinger, W. H. 1985. *Forest ecosystems. concepts and management.* New York: Academic Press.

Waring, R.H., Schroeder, P.E., & Oren, R. 1982. Application of the pipe model theory to predict canopy leaf-area. *Canadian journal of forest research*, **12**(3), 556–560.

Weiher, E., der Werf, A. Van, Thompson, K., Roderick, M., Garnier, E., & Eriksson, O. 1999. A common core list of plant traits for functional ecology. *Journal of vegetation science*, **10**(5), 609 – 620.

Chapter 4

Relationship between biomass partitioning and stability of chestnut trees *(Castanea sativa* Mill.*)*

With Conedera Marco[1] and Gehring Eric[1]

[1]WSL Swiss Federal Research Institute, Insubric Ecosystem Research Group. Via Belsoggiorno 22, CH-6500 Bellinzona, Switzerland

Introduction

The root system provides two main functions: water uptake and mechanical anchorage (Coutts, 1987). Even if most applications of the pipe model theory have focused on above-ground allometric relationships, the same concepts can theoretically be extended to roots. For example Richardson & zu Dohna (2003) could confirm the Leonardo Da Vinci's area-preserving branching hypothesis for the root system of Douglas-fir.

Several studies reported a linear or exponential relationship between root and stem cross-sectional area, sapwood area or biomass (e.g. Carlson & Harrington, 1987; Kuiper & Coutts, 1992; Drexhage & Gruber, 1999; Tatarinov *et al.* , 2008), and more rarely a direct proportionality between leaves and roots (e.g. Drexhage & Gruber, 1999; Gould & Harrington, 2008). Gould & Harrington (2008) confirmed a clear allometric relationship between leaf area and the cross-sectional area of sapwood in roots of Coast Douglas-fir, although less strong than that with trunk sapwood area (r^2 of 0.81 instead of 0.98). However data on root biomass, especially of mature trees, are generally scarce, due to the complexity of the sampling techniques, involving a considerable effort (Tatarinov *et al.* , 2008).

Tree stability can thus represent an indirect evidence of the relation between the pipe model theory and the balance of above and below ground biomass. In this view a tree with an higher above to below ground biomass ratio ($\frac{B_{above}}{B_{below}}$) is statically less anchored and therefore less stable, and presumably displays also an higher leaf to sapwood area ratio ($\frac{A_l}{A_s}$).

Uprooting occurs when lateral forces applied to the tree overcome the root anchorage (Putz *et al.* , 1983). This may be driven by external factors like windthrows, by tree mechanical instability or by the concurrence of both. We may formulate following hypothesis regarding the factors influencing tree statics and falling probability:

A exposure to wind, that is higher on exposed sites on humps or for trees having an emerging crown (social position)

B tree height, which raise the tree center of gravity and also acts as a longer lever arm in case of strong wind

C terrain slope, since on steeper slopes the tree center of gravity tend to be more downhill than the stem basis

D small root system in comparison with above ground biomass (and related high $\frac{A_l}{A_s}$ ratio)

Vogt *et al.* (2006) and Conedera *et al.* (2009) already provided the evidence that uprooted chestnut stools are preferably located in concave microtopographic positions, where, according to our preceding study (Chapter 3), chestnut trees tend to display higher $LASA_{ground}$ (slope of the linear relationship between A_l and A_s, corrected for branch height, as described in Chapter 2).

In this study we focused on the discussion of the main factors influencing uprooting, comparing them to the findings of our previous studies.

Methods

The dataset of the study of Vogt *et al.* (2006), kindly provided by the Swiss Federal Institute of Forest, Snow and Landscape Research WSL in Bellinzona, has been reanalysed, after a partial adaptation of the environmental and dendrometric variables, in order to be more directly comparable with the results obtained in the study relating site water availability and the pipe model theory (Chapter 3).

Vogt *et al.* (2006) investigated the spatio-temporal dynamics of stool uprooting in abandoned chestnut coppice forests, a phenomena that is becoming increasingly relevant on the southern slopes of the Alps, and that is raising concern among forest managers. The main study area was composed by various abandoned forest plots (ca. 100 ha) belonging to the non-native chestnut forest belt of the Southern Swiss Alps, in southern Ticino (latitude 468020 0000 N, longitude 88510 5000 E), ranging from 330 to 820 m a.s.l., exposed prevailing east–northeast and with steep slopes (with half of the area exhibiting slopes above 30°). The forest is mainly constituted by chestnut coppices abandoned for more than half a century, building a closed single-layer canopy. Among the recently uprooted stools (live uprooted stools *sensu* Schaetzl *et al.* , 1989), 45 trees were randomly selected, and an equal number of standing coppice stools were picked up casually from a 50 m sampling grid. For each tree a set of topographic, stand and stool parameters were surveyed. To allow a comparison with our previous study, the original variables were transformed to fit the definitions used in Chapter 3, as describerd in Table 4.1. Additionally annual radial growth were measured along extracted core-borings or on sawn trunk slices.

Logistic regression modeling was used to highlight the relevant predictor variables for stool uprooting, including environmental and dendrometric characteristics, which could both have a causal effect on tree stability. All the considered explanatory variables were not strongly correlated (Pearson $R \leq 0.5$) and were all evaluated in the model selection step. Using the R package *glmulti*, all the combinations of explanatory variables were evaluated (no quadratic terms nor interactions have been considered). The models were ranked on the basis of the AICc coefficient (Akaike information criterion with a second order correction for small sample size), and their goodness of fit was evaluated with the AUC value (area under the receiver operating characteristics curve). The best model was then compared to the models with reduced terms.

The distribution of the sampled trees with respect to microtopography and slope conditions were compared by means of bagplots Rousseeuw *et al.* (1999), which constitute a bivariate generalization of boxplots, in order also to discuss the range of validity of the models developed in both studies. Finally the measurements of the

Table 4.1: Dendrometric and geo-physiograhic parameters considered.

Parameter	Unit / Values	Assessment/Notes
Dendrometric parameters		
Social position	Predominant (1) Dominant (2) Co-dominant (3) Dominated (4)	calculated from the difference in heigth of the investigated tree with the mean of its 3 tallest neighbors in 8 m radius (≤ -4m Dominated; $>$-4 and $\leq$ 2m Codominant; $>$2 and $\leq$ 6m Dominant; $>$6m Predominant)
DBH	*cm*	virtual value calculated from the basal area at breast height (sum of of the living individuals of the stool)
Height	*m*	
Geo-physiographic parameters		
Aspect	transformed (Beers *et al.* , 1966)	
Elevation	*masl*	
Slope	*%*	
Rocks	*%*	% of rock visible on surface
Soil depth (cm)	*cm*	mean of 4 measures of depth assessed with a metal stick (Ø 13 mm) and hammer
Composite microtopography	[-3,3]	calculated from the original dataset as the sum of Horizontal curvature (3 classes) and Vertical curvature (3 classes), weighted after Curvature intensity (3 classes): negative values for convexity, 0 for slope, positive values for concavity

two datasets and the predictions of the models were visually overlapped.

The analysis were performed using the R statistical package version 2.14.0 (R Development Core Team, 2011).

Results

None of the predictor variables were correlated (Pearson R <0.5). Among the 256 generated models, the best result in term of AICc was given by the model with *microtopography, slope* and *tree height* as explaining variables, confirming the results of Vogt *et al.* (2006). Table 4.2 reports the best model and the subsequent best models that consider less variables. In the best model all coefficient estimates were significant (p-value < 0.003). The best model fits very well the uprooting events in terms of AUC and other performance measures (Table 4.2).

Among the models with 2 terms, the one considering only the environmental variables slope and microtopography was the best in terms of AUC, although not in terms of AICc. According to both those two variables, the distributions of the populations of standing and uprooted trees differed significantly (non parametric Wilcoxon test with p<0.001, for a set of boxplots see Conedera *et al.* , 2010b), the uprooted stools being on steeper slopes and more concave microtopographies (Figure 4.1). The distribution of the trees sampled in the preceding study (Chapter 3 *bottom*) were more similar to the standing trees concerning microtopography, but on more gentle slopes.

Overlapping the datasets from both studies (Figure 4.2) highlights how the uprooted stools correspond to microtopographic sites where chestnut trees display higher $LASA_{ground}$ values, although we should point out that data on $LASA_{ground}$ regarding marked concave sites and steep slopes are scarce.

This relationship becomes more evident if the predictions of the models from the two studies are plotted together (Figure 4.3).

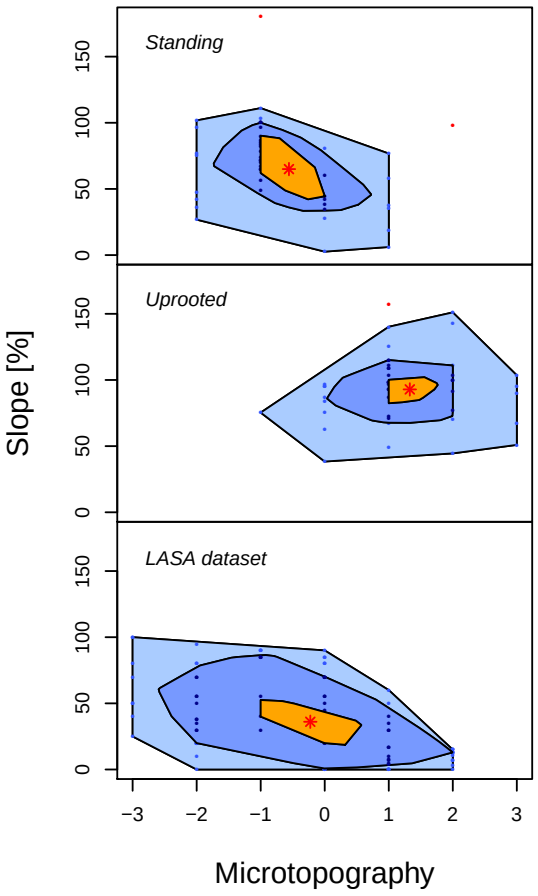

Figure 4.1: Bagplots of the site conditions (microtopography and slope) for the standing *(top)* and the uprooted *(center)* trees, and for the trees sampled in the previous study (Chapter 3, *bottom)*. The red asterisk is the bivariate median. The dark blue region is the bag, containing 50% of the observations. The outer azure region contains observations that are in the fence (the bag expanded 3 times). The orange hull center can be compared to the notches in a standard boxplot. Observations outside the fence are outliers (red dots).

The analysis of radial growth during life history of the sampled trees revealed an interesting pattern (Figure 4.4), with the uprooted stools growing faster than the standing ones in their younger phase (until the 80's), and growing slower in the last decade.

Table 4.2: Best logistic models selected. Model 1 is the best AICc ranking model, model 2 the best one with only 2 fixed effects, model 3 the best model with 2 fixed effects according to AUC, model 4 the best model with one fixed effect and model 5 is the null model with intercept only ($\beta_{0...3}$=*coefficients*).

	Model terms	log_{Lik}	AIC_c	R^2_{Nag}	AUC	$Sens.$	$Spec.$	$Prop_{corr}$	$Kappa$
1	$\beta_0 + \beta_1 Microtopography + \beta_2 Slope + \beta_3 Height$	-14.66	37.79	0.872	0.967	0.956	0.978	0.967	0.933
2	$\beta_0 + \beta_1 Microtopography + \beta_2 Height$	-24.00	54.28	0.765	0.867	0.867	0.867	0.867	0.733
3	$\beta_0 + \beta_1 Microtopography + \beta_2 Slope$	-27.90	62.09	0.714	0.878	0.867	0.889	0.878	0.756
4	$\beta_0 + \beta_1 Microtopography$	-34.14	72.42	0.622	0.822	0.800	0.844	0.822	0.644
5	β_0	-62.38	126.81	0.000	0.500	1.000	0.000	0.500	0.000

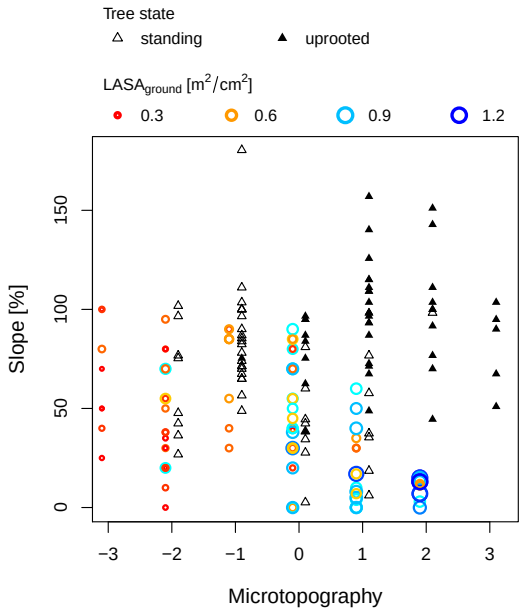

Figure 4.2: Overlapping of the site conditions of this study (triangles) and the study from Chapter 3 (circles).

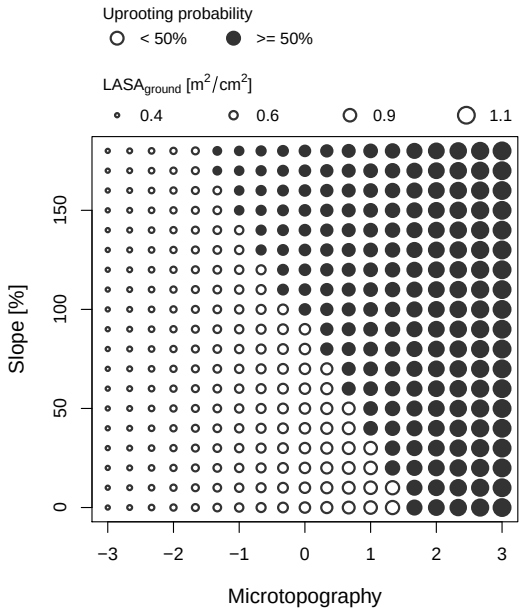

Figure 4.3: Predictions of the models of uprooting probability (filled circles represent uprooting probabilities above 50%, according to the logistic model nr. 3 in Table 4.2), and $LASA_{ground}$ (size of the circles, model nr. 3 in Table 3.4), for given ranges of microtopography and slope.

Discussion

The results of Vogt *et al.* (2006) were confirmed (same AUC values for the best model), although the explaining variables used in the model were partially modified (single ordered composite variable for microtopography, instead of various boolean variables). While windthrow risk was the main determinant in similar studies (e.g. Greenberg & McNab, 1998; McNab *et al.* , 2004; Cucchi *et al.* , 2005; Scott & Mitchell, 2005), the fact that terrain convexity is inversely correlated with uprooting occurrence, and that tree social position has not been selected in the final model (a proxy for crown exposition), confirms that the phenomena observed is probably not related to external forcing agents (hypothesis A). Mechanical stability (hypothesis C,D and partially B) seems to be a better explanation for the uprooting probability in the studied chestnut coppice stands. The selected explaining variables are of both environmental (slope and microtopography) and dendrometric (height) nature.

Microtopography is the more influential explaining variable, and a prediction based on it alone can discriminate correctly 82% of the cases of the model dataset. Since microtopography was not highly correlated with tree height, we may suppose that tree

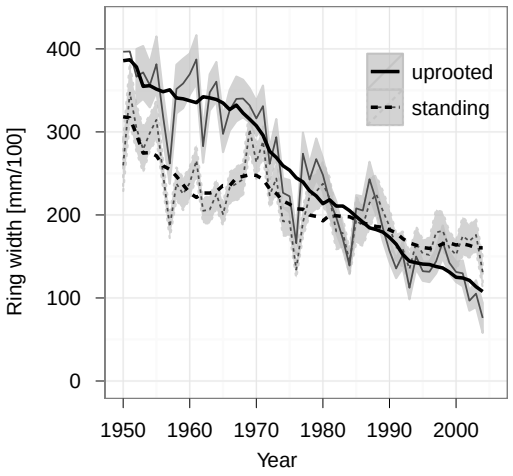

Figure 4.4: Annual radial growth of standing and uprooted stools (thin grey lines). The grey ribbons represent the standard error intervals, while black thick lines display a centered running mean over 9 years.

instability in concave sites may effectively be related to an independent effect, probably due to the unbalance of above and below ground biomasses (hypothesis D). It is known how on soils with a similar composition, microtopography can considerably affect water content and its availability to the living vegetation. In the preceding study (Chapter 3) we linked microtopography to the allometric relation between leaf and sapwood area. We may therefore assume that an highly probable functional proportionality exists between these two allometric measures ($\frac{B_{above}}{B_{below}}$ and $\frac{A_l}{A_s}$), also highlighted by the predictions of the models (Figure 4.3). However a cautionary note should be raised regarding the ranges of validity of such an assumption. In particular in future studies additional measures of $LASA$ should be taken for trees growing in steep and marked concave sites.

Steep slopes are less stable, particularly when the soil is saturated with water, and more subject to erosion and mass-movement phenomena. Moreover, as postulated in hypothesis C, trees that grow on steep slopes have a center of gravity translated downhill compared to the stem basis, and form tension (hardwoods) or compression (softwoods) wood to overcome it (Schweingruber, 2007). In this study all the uprooted stools were on slopes higher than 40%. Interestingly according to the model's predictions (Figure 4.3), slope seems to play a fundamental role in uprooting predictions for sites from light convex to light concave microtopographies (values from -1 to 1). According to Figure 3.3 in Chapter 3, we may suppose that on steeper slopes there is a reduced site water availability and consequently lower $LASA_{ground}$ values, which should favour a more balanced biomass partitioning, counteracting uprooting probability. However Figures 4.1 *bottom* and 4.2 highlight how this is probably an artifact of the lack of sampling in concave sites on marked slopes.

Finally tree height had a relevant contribution to the best logistic model, with a positive coefficient estimate, confirming hypothesis B. This is probably due to the rose baricenter of the above ground part in taller trees more than a lever effect with external agents, since it is its combined effect with slope that increase considerably model performance (from 88 to 97% of correctly predicted cases). Being in better watered microtopographies, uprooted stools showed a rapid radial growth in their young phase (there is a significant difference in DBH among the two populations, according to a non-parametric Wilcoxon-test, Conedera *et al.* , 2010b). However stem growth considerably diminished with age, being at the moment of falling even lower than the mean growth of the population of standing trees. According to the hydraulic limitation theory (Ryan & Yoder, 1997), tree height should be limited by the increasing hydraulic resistances and gravitational potential. Although trees may have developed physiological mechanisms that can partially compensate this phenomena, additional costs concur in limiting height growth (McDowell *et al.* , 2002b). When approaching the maximum size, the above ground biomass continues growing (radial growth), even if at lower rates, while root biomass remains more constant, having an higher turnover

rate. During this senescence phase the ratio of above and below ground biomasses become thus probably higher, further increasing the eventual unbalance regarding anchorage and supported mass, and finally bringing the tree in a statically unfavourable state.

Conclusions

The study of the stool uprooting phenomena confirmed the suppositions on the existing relationships between $\frac{B_{above}}{B_{below}}$ and $\frac{A_l}{A_s}$ ratios (Mazzoleni, 1990), being the leaf to sapwood area relationship and the uprooting probability both highly correlated with microtopography. This findings are coherent with the studies that demonstrated the influence of water conditions on shoot:root ratios (e.g. Monk, 1966; Bongarten & Teskey, 1987; Mazzoleni & Dickmann, 1988) and the evidences of allometric relationships between root and stem properties from one side (e.g. Kuiper & Coutts, 1992; Drexhage & Gruber, 1999; Tatarinov *et al.* , 2008; Gould & Harrington, 2008), and between stem and leaves on the other side (e.g. pipe model of Shinozaki *et al.* , 1964a,b).

References

Beers, T. W., Dress, P. E., & Wensel, L. C. 1966. Aspect transformation in site productivity research. *Journal forestry*, **64**, 691 – 692.

Bongarten, BC, & Teskey, RO. 1987. Dry-weight partitioning and its relationship to productivity in loblolly-pine seedlings from 7 sources. *Forest science*, **33**(June), 255–267.

Carlson, William C., & Harrington, Constance A. 1987. Cross-sectional area relationships in root systems of loblolly and shortleaf pine. *Canadian journal of forest research*, **17**(6), 556–558.

Conedera, M., Fonti, P., Nicoloso, A., Meloni, F., & Pividori, M. 2009. Ribaltamento delle ceppaie di castagno: Individuazione delle zone a rischio e proposte selvicolturali. *Sherwood*, **154**, 15 – 18.

Conedera, M., Pividori, M., Pezzatti, G.B., & Gehring, E. 2010b. Il ceduo come opera di sistemazione idraulica - la stabilità dei cedui invecchiati. *Pages 85–91 of:* Carraro, V, & Anfodillo, T (eds), *Gestione multifunzionale e sostenibile dei boschi cedui: criticità e prospettive. atti del 46° corso di cultura in ecologia.* San Vito: Centro Studi per l'Ambiente Alpino.

Coutts, M.P. 1987. Developmental processes in the tree root systems. *Can. j. for. res.*, **17**, 761–767.

Cucchi, V., Meredieu, C., Stokes, A., de Coligny, F., Suarez, J., & Gardiner, B.A. 2005. Modelling the windthrow risk for simulated forest stands of maritime pine (pinus pinaster ait.). *Forest ecology and management*, **213**, 184–196.

Drexhage, Michael, & Gruber, Franz. 1999. Above- and below-stump relationships for picea abies: estimating root system biomass from breast-height diameters. *Scandinavian journal of forest research*, **14**(4), 328–333.

Gould, Peter J., & Harrington, Constance A. 2008. Extending sapwood : Leaf area relationships from stems to roots in coast douglas-fir. *Annals of forest science*, **65**(8), 8–8.

Greenberg, C.H., & McNab, W.H. 1998. Forest disturbance in hurricane-related downbursts in the appalachian mountains of north carolina. *Forest ecology and management*, **104**, 179–191.

Kuiper, L.C., & Coutts, M.P. 1992. Spatial disposition and extension of the structural root system of douglas-fir. *Forest ecology and management*, **47**, 111–125.

Mazzoleni, Stefano. 1990. Relazioni tra aree fogliari e superfici di conduzione nel fusto nell'analisi di gradienti ambientali. *Linea ecologica*, 27–30.

Mazzoleni, Stefano, & Dickmann, Donald I. 1988. Differential physiological and morphological responses of two hybrid populus clones to water stress. *Tree physiol*, **4**(1), 61–70.

McDowell, N.G., Phillips, Nathan, Lunch, Claire, Bond, Barbara J., & Ryan, Michael G. 2002b. An investigation of hydraulic limitation and compensation in large, old douglas-fir trees. *Tree physiology*, **22**, 763–774.

McNab, W.H., Greenberg, C.H., & Berg, E.C. 2004. Landscape distribution and characteristics of large hurricaine-related canopy gaps in a southern appa- lachian watershed. *Forest ecology and management*, **196**, 435–447.

Monk, Carl. 1966. Ecological importance of Root/Shoot ratios. *Bulletin of the torrey botanical club*, **93**(6), 402–406.

Putz, F.E., Coley, K.L., Montalvo, A., & Aiello, A. 1983. Uprooting and snapping of trees: structural determinants and ecological consequences. *Can. j. for. res.*, **13**, 1011–1020.

R Development Core Team. 2011. *R: A language and environment for statistical computing.* R Foundation for Statistical Computing, Vienna, Austria. ISBN 3-900051-07-0.

Richardson, Andrew D., & zu Dohna, Heinrich. 2003. Predicting root biomass from branching patterns of douglas-fir root systems. *Oikos*, **100**, 96–104.

Rousseeuw, P. J., Ruts, I., & Tukey, J. W. 1999. The bagplot: a bivariate boxplot. *The american statistician*, **53**(4), 382–387.

Ryan, Michael G., & Yoder, Barbara J. 1997. Hydraulic limits to tree height and tree growth. *Bioscience*, **47**(4), 235–242.

Schaetzl, R.J., Johnson, D.L., Burns, S.F., & Small, T.W. 1989. Tree uprooting: review of terminology, process, and environmental implications. *Can. j. for. res.*, **19**, 1–11.

Schweingruber, Fritz Hans. 2007. *Wood structure and environment*. Springer series in wood science. Springer.

Scott, R.E., & Mitchell, S.J. 2005. Empirical modelling of windthrow risk in partially harvested stands using tree, neighbourhood, and stand attributes. *Forest ecology and management*, **218**, 193–209.

Shinozaki, K, Yoda, K, Hozumi, K, & Kira, T. 1964a. A quantitative analysis of plant form – the pipe model theory i. basic analyses. *Japanese journal of ecology*, **14**(3), 97–105.

Shinozaki, K, Yoda, K, Hozumi, K, & Kira, T. 1964b. A quantitative analysis of plant form – the pipe model theory ii. further evidence of the theory and its application in forest ecology. *Japanese journal of ecology*, **14**(4), 133–139.

Tatarinov, Fyodor, Urban, Josef, & Cermák, Jan. 2008. Application of "clump technique" for root system studies of quercus robur and fraxinus excelsior. *Forest ecology and management*, **255**, 495–505.

Vogt, Juliane, Fonti, Patrick, Conedera, Marco, & Schröder, Boris. 2006. Temporal and spatial dynamic of stool uprooting in abandoned chestnut coppice forests. *Forest ecology and management*, **235**(1-3), 88–95.

Chapter 5

Theoretical modeling of dynamic biomass partitioning in plants

With Giannino Francesco[1], Mazzoleni Stefano[1]

[1]University of Naples Federico II, Dip. di Arboricoltura, Botanica e Patologia vegetale, via Università 100 I-80055 Portici, Naples Italy

Keywords: C allocation, plasticity, water relations, disturbance recovery, system dynamics

"Teleonomic or apparently goal-seeking models can be highly attractive : simplicity, a useful range of application, and an evolutionary interpretation. However, this attractiveness is deceptive. The approach is a cul-de-sac. There are many possible goals. The choice of goal is inevitably subjective. The parameters can only be obtained by fitting responses at the system level. When the teleonomic model fails, as all models invariably do, there is nowhere to go, nowhere to seek the cause of failure in other than the most superficial terms. This is not to deny the importance of evolved constraints, or the value of a teleonomic viewpoint. Only if the teleonomic criteria are built into a mechanistic framework can they be properly considered in a progressive modelling endeavour."
Thornley, 1998

Abstract

Biomass allocation processes play a central role in shaping species distribution and dominance. Diverse approaches have been used to model allocation, ranging from mere empirical coefficients and goal-seeking models, to more mechanistic source-sink and transport-resistance models. Recent works have implemented very detailed and realistic representation of plant structure, but they are still lacking to achieve a full dynamic integration of functional processes. A new transport resistance mathematical model is proposed making use of system dynamic modular approach. A fairly simple model of biomass partitioning, based on the interactions between water and carbon transport processes with assimilation and growth, is presented. The simulated plants show a dynamic biomass allocation according to environmental conditions (light and water availability) and the capability to recover after disturbances (e.g. recover after pruning or fire). According to species-specific parameters, the model is able to reproduce consistent deviations from the allometric trajectory, allowing to highlight the relationships between allocation and both water and carbon transport processes. The model showed qualitatively correct responses in a range of different environmental conditions (light and water) and during recovery from unbalanced biomass removal. The presented model represents a compromise, assuming significant simplifications of the processes in-

volved in biomass allocation, but still responding consistently to different environmental conditions and species specific traits. In this respect this model has the potential to be a good instrument for theoretical investigation of relations between anatomical (e.g. sclerophylly) and functional (e.g. transport resistances) characters and allocation patterns.

Introduction

Allocation is a concept of crucial importance in life history theory (Stearns, 1992), and is a relevant topic of plant plasticity expression (Weiner, 2004). The phenotypic variation and the diverse responses to various environments have been characterized in many studies, but the underlying mechanisms of such plasticity are still largely unknown (Sultan, 2004). In particular, regarding carbon allocation there is no generally accepted theory on its basic processes (Allen *et al.* , 2005).

Typically many allocation patterns are a function of plant size and follow their allometric trajectories (the so called "passive" or "apparent" plasticity, Weiner, 2004). On the other hand, according to the optimal allocation theory, a plant should invest more in the organs that exploit the most limiting resource and less in the others (Bloom *et al.* , 1985). Concerning water availability, it is well known how plants grown in drier conditions display lower leaf/root biomass ratios than plants of wet sites. Cacti and other succulents, without or with reduced leaves, compared to algae without roots, are extreme examples of adaptation to opposite environmental conditions. Each plant shows a specific biomass allocation pattern, allowing the growth within a certain range of environments, but also a dynamic plasticity, making possible the adaptation to changing conditions and the recovery after disturbances. In this view, allocation strategies play a central role in shaping species distribution and dominance in variable or disturbed environments (Mazzoleni & Spada, 1992).

The formulation of allocation in models still remains a weak point of current plant modeling (Roux *et al.* , 2001; Minchin & Lacointe, 2005). Different approaches have been used to represent biomass partitioning in plant models (Wilson, 1988a; Dewar, 1993; Cannell & Dewar, 1994; Lacointe, 2000; Mäkelä *et al.* , 2000; Prusinkiewicz *et al.* , 2007), including empirical coefficients, functional balance, allometric relationships, transport resistance (TR) and source-sink models (Roux *et al.* , 2001). Additionally, some works claim a partitioning control by plant-growth regulators, with root producing hormones that control the shoot and vice versa (cited in Wilson, 1988a). However, this does not explain the question of the control of hormone synthesis, whose regulation remains dependent on the local plant endogenous status (Yang & Midmore, 2005).

Allocation models based on fixed coefficients, functional balance, and allometry are of empirical nature. They have been mostly used in models with yearly timesteps, while TR and source-sink models, with their more mechanistic basis of the dynamics of carbon and water transport pathways, usually have been applied at daily timesteps Roux *et al.* (2001). In fact, the mass flow described by Münch (1927, 1930) is now widely accepted to be the mechanism of assimilate transfer and allocation (Lacointe, 2000; Minchin & Lacointe, 2005). To this respect, TR models represent a better process-based approach, with explicit (more or less simplified) mechanical functioning of the assimilate flows, by differences of potentials (or concentrations), conducting areas, transport resistance and pathway length. On the other hand, source-sink approaches in part implicitly include those processes, by relating the transport to the sink-strength (or sink ability) of an organ, considered as an estimate of potential differences between sources and sinks. Because of this simplification, the source-sink approach has been more widely used in the case of models with fine-grained organs scale (plant models with an explicit architec-

ture, e.g. L-system-based models), while the more mechanistic TR design has been applied with bulk-compartments, presumably due to the difficulty of estimating local transport parameters (Roux *et al.* , 2001; Minchin & Lacointe, 2005). However, more recently the TR approach has been successfully applied also to more fine-grained models, using analogies with electrical circuits. Examples are the work by Daudet (2002) that developed a model coupling allocation to a detailed representation of the Munch flow and Da Silva *et al.* (2010) that included a water circuit into L-Peach, in order to link water stress effects to carbon partitioning.

The high computational needs of these models do not allow applications at the community scale. To this purpose, an approach with larger modules or with a simplification of the mechanistic process is still needed (Minchin & Lacointe, 2005). At this scale, only few models have been focused on the response of biomass allocation to water stress (e.g. see Dewar, 1993; Chen & Reynolds, 1997), being more focused on interactions of growth and nutrient availability (e.g. Thornley, 1972a,b).

In this paper a fairly simple model for biomass partitioning with a dynamic biomass allocation according to environmental conditions (light and water availability) and disturbances (e.g. recover after pruning or fire) is presented. It aims to be a minimal representation of the crucial processes involved in above and belowground resource partitioning.

The required inputs have been restricted to light and water conditions, factors involved in plant competition and shaping plant forms. Neither temperature (and its effects on kinetics of photosynthesis and maintenance, on fluid viscosity, etc.) nor nutrient status have been considered, although evidences of impact of the latter on biomass allocation exists an have been implemented in several other models (Cannell & Dewar, 1994). Rather we opted for a minimal plant representation, focusing on a mechanistic implementation of water and carbon transport dynamics and the influence of the plant internal water status on assimilation, growth and tissue death. Decreased water potentials in leaf cells limit leaf elongation at first, and only at lower levels affect photosynthesis and transpiration (Kramer, 1983). Dewar (1993) worked to include the effects of water potentials on growth in the model of Thornley (1972a), but its representation of water fluxes considered transpiration as simply proportional to shoot mass, without any feedback by air water status and stomatal control. The latter however is a crucial characteristic of plant ability to survive water-stressed environments and it has been implemented in our model as a function of leaf water potentials.

The developed model, which can be included in the transport-resistance models category, is tested for growth in a range of environmental conditions, and for reaction to unbalanced biomass removal. The results of the simulations are analysed in terms of deviance from the allometric trajectory (Weiner, 2004), rather then of partitioning ratios, thus unveiling patterns of plasticity and their relations with functional and structural plant properties.

Material and methods

The developed model represents simplified structures of plants, corresponding to different growth forms (herb, palm, shrub, tree, illustrated in Figures 5.1 and 5.2), including leaves, roots and woody parts (branches, stem, coarse roots).

The model is structured into 3 tightly coupled submodels:

geometry: represents implicitly the architecture of the plant from the masses of structural carbon (leaves, roots and woody parts). This module does not include fluxes or compartments.

carbon: represents the carbon fluxes, with the compartments being pools of either structural or solute carbon.

water: represents the water fluxes along the soil-atmosphere continuum through the xylem of the plant.

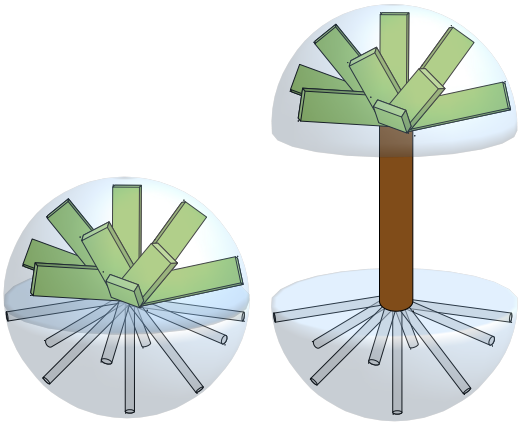

Figure 5.1: Considered implicit geometry for herb *(left)* and palm *(right)*. Leaves are represented by laminae and stem and roots by cylinders.

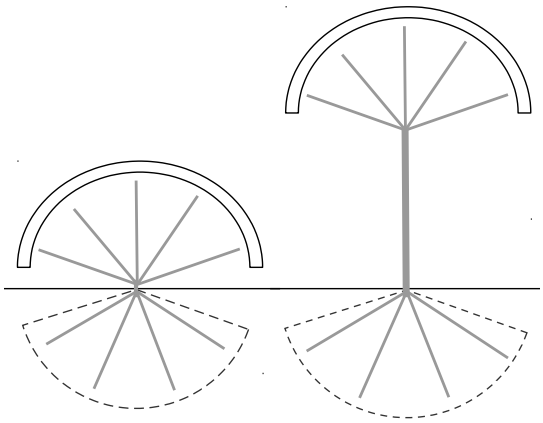

Figure 5.2: Considered implicit geometry for shrub *(left)* and tree *(right)*. Leaves are represented by a lamina on the surface of a semi-sphere (plain line), and fine roots are cylinders (not shown) occupying the soil in a semi-spherical space (region delimited by the dashed-line polygons). Woody parts are represented by grey lines on the figure, corresponding to cylindrical shapes.

Environmental inputs are soil water potential (ψ_{soil}, MPa), air water potential (ψ_{air} , MPa) and light (expressed as a fraction of maximum light incidence - from 0 to 1). In Figure 5.3 the simplified model for an herbaceous plant is presented, showing the influences of solute carbon concentrations and the feedbacks from external and internal water potentials. Figure 5.4 shows the model including woody parts, with compartments for branches, stem and coarse roots. In Table 5.1 are reported the symbols used in the description of the model. The model has been adjusted for a daily timestep and has been implemented using both the system dynamic software Simile (Muetzelfeldt & Massheder, 2003) and the R statistical package version 2.14.0 (R Development Core Team, 2011), with the *deSolve* library (Soetaert *et al.* , 2010a,b).

Geometry

Simplified plant geometries have been considered so far (Fig. 5.1 and 5.2).

Herb

Leaves are described as a rectangular lamina of a given thickness. Leaf width is not defined, so that it could be visualized as few folded leaves (like an algae or salad) or multiple leaves (like a pineapple). Roots are represented by cylinders of a given diameter. Both leaves and roots occupy semi-spherical spaces, according to a certain space filling volume fraction, that is the volume of plant tissue (V_L, V_R) divided by the space delimited by the surface enveloping the shoots or the roots respectively (the volume fraction is a concept used in fire ecology to describe plants as fuels). The meristematic active area is considered equal to the base area of the laminas for the leaves (A_L) and the sum of the cylinders bases for the roots (A_R). The plant basal area (A), which is the reference area for xylematic and phloematic fluxes, is considered as the smaller between the base area of the lamina and the sum of the cylinders bases. The transport pathways are expressed as fixed section fractions of the basal area ($fract_{xylem}$, $fract_{phloem}$). From the above mentioned parameters and the leaf and root masses of structural carbon, it is possible to determine basal area, uptake (cylinder surface without bases, A_{uptake}) and photosynthetic (one face of the lamina, A_{photo}) surface and transport pathways length (h).

Palm

It is a basic plant form similar to e.g. palms, yuccas or tree ferns. Leaves and roots are defined as in the herbaceous form. Additionally the stem dimension is calculated from its biomass, according to a fixed ratio between stem length and stem diameter. The stem meristematic area (A_S) is considered to be proportional to the stem lateral surface. For calculating the total transport pathways length (h), stem length is added to leaf and root lengths. Stem transport pathways are calculated as a fraction of the stem basal area (no cambium), and are finally averaged with those for leaf and roots, weighted on lengths.

Shrub

Leaves are described as a lamina of a given thickness on the surface of a semi-sphere (A_{photo}). Fine roots are represented by cylinders of a given diameter, similarly as defined in the herbaceous form. Branches and coarse roots are represented by cylinders of variable diameter, and their distribution in space is specified by a constant density of path length for a given volume (m m^{-3}). In this implicit geometry, the characteristics of active xylem and phloem are calculated uniquely from the woody parts (branches and coarse roots), neglecting their fractions in leaves and fine roots. The cambial areas (A_B and A_{Rc}) are considered to be proportional to the lateral surface of the cylinders. For calculating the total transport pathways length (h), branch length is added to coarse root length. Active xylematic (sapwood) and phloematic cross-sectional areas are calculated as outer ring portions of a given thickness of the basal area (inside and outside of cambium, respectively), and are finally averaged (weighted on lengths).

Tree

Leaves, branches, coarse and fine roots are represented like in the the shrub form. Stem dimension is calculated from its biomass, according to a fixed ratio between stem length and stem diameter. Cambium, active xylem and phloem are calculated as already described for branches and coarse roots. For the calculation of the transport pathways characteristics, stem length is added to branch and coarse root lengths, and active xylem and phloem cross-sectional areas are taken into account to calculate weighted mean values over the three compartments (branches, stem, coarse roots).

Carbon

The carbon submodel represents the carbon cycle of the plant, having photosynthesis as carbon source and maintenance and tissue death as carbon sinks. State variables are structural carbon mass (L and R, kg), solute carbon mass (CL and CR, kg) and concentration ($[C_L]$ and $[C_R]$, kg m^{-3}). Inputs to this submodel are light and the xylematic water potentials (ψ_L and ψ_R, MPa), the latter being calculated by the water submodel. Since the water pathway from the xylem into the plant cells has not been formalized, all the feedbacks of the water status on assimilation, growth and turnover processes have been expressed as function of the xylematic water potentials (in leaves or roots), instead of the cellular water potentials near turgor values. Similarly water contents in the xylem

Concentrations are expressed as mass of solute carbon on water mass:

$$[C_L] = \frac{C_L}{V_L \cdot \theta_L} \quad ; \quad [C_R] = \frac{C_R}{V_R \cdot \theta_R}$$

where V (m^3) is the leaf or root volume and θ (dimensionless) is the relative water content.

Photosynthesis is considered to be proportional to photosynthetic area (A_{photo}, m), leaf gas diffusion (through the two parts: cuticula $kCuticular$, and stomata $f_{stomata}$), and is inhibited by high concentrations of solute carbon and lower water potentials in the (photosynthetic) cells. These limiting functions, f_{PS_C} and f_{PS_W} are considered to reduce photosynthesis

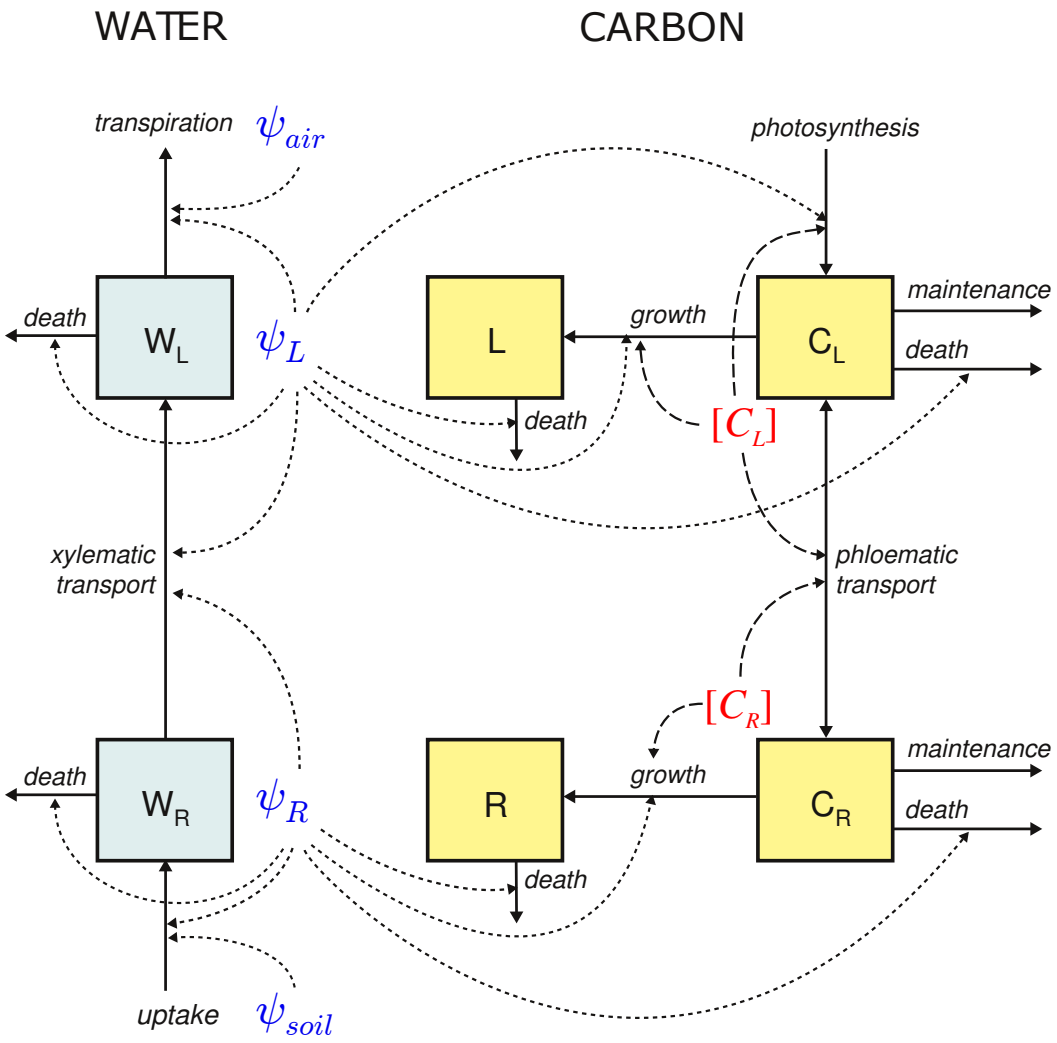

Figure 5.3: Diagram of the model for herbaceous plant, representing the carbon and water submodels with their respective above and below ground compartments (boxes) and fluxes (plain lines). Carbon in leaves and roots is divided into structural (L and R) and solute carbon (CL and CR). Dotted lines represent the influences of environmental (ψ_{air} , ψ_{soil}) and xylematic (ψ_L, ψ_R) water potentials on water and carbon processes. Dashed lines represent the influences of solute concentrations ($[C_L]$, $[C_R]$) on assimilation, growth and phloematic flux. Influences of compartments and of the related implicit geometry on different fluxes are not shown.

linearly between 2 threshold values (no photosynthesis and unlimited photosynthesis) and they are function of leaf carbon concentration and leaf water potential respectively. Stomata opening is also driven by leaf water potentials with a similar approach. So, we can write:

$$PS = kPS \cdot (f_{stomata}(\psi_L) + kCuticular) \cdot A_{photo} \cdot light \cdot f_{PSC}([C_L]) \cdot f_{PSW}(\psi_L)$$

where PS (kg d-1) is the photosynthesis production, light (dimensionless) is real number in [0,1], kPS (kg d^{-1} m^{-2}) is the photosynthesis rate.

Maintenance for structural carbon m_L and m_R (kg d^{-1}) is proportional to structural carbon (maintenance request) but with a maximum set by the available solute carbon (requests exceeding the availability will result in starving).

$$m_L = kM_L \cdot L \quad ; \quad m_R = kM_R \cdot R$$

where kML and kMR are the leaf and root maintenance rates (d^{-1}).

Growth is determined by the meristematic active area (A_L and A_R, m^2) and the local compartment concentrations of solute carbon, and is limited by lower water potentials. Water potentials are considered to reduce growth linearly between 2 threshold values (no growth and unlimited growth).

$$g_L = kG_L \cdot [C_L] \cdot A_L \cdot f_{growth}(\psi_L)$$
$$g_R = kG_R \cdot [C_R] \cdot A_R \cdot f_{growth}(\psi_R)$$

where g_L and g_R are the leaves and root growths (kg d^{-1}), kG_L and kG_R the growth rates (m d^{-1}), $f_{growth}(\psi)$ is the limitation of growth (dimensionless), due to threshold values of leaves or root water potentials ψ_L and ψ_R (see Appendix B for the mathematical formulation).

Phloematic flux $phloem$ (kg d^{-1}) has been modeled as a mass-flow process, proportional to the difference of the solute carbon concentrations and the conducting area. It is also inversely proportional to the length of transport (h, meter), and limited by a maximum flux velocity.

$$phloem = kPhloem \frac{A \cdot fract_{phloem}}{h} \cdot g_{phloem}([C_R] - [C_L])$$

where $kPhloem$ (m^2 d^{-1}) is rate of phloematic transport, A (m^2) is basal calculated as $min(A_L, A_R)$, g_{phloem} (kg m^{-3}) is an empirical function returning the "effective" driving concentration difference, taking into account the limitation of flux velocity according to a maximum driving concentration difference (see Appendix B for the mathematical formulation). Maintenance has been given priority over growth and phloematic fluxes, so that the sucrose pathway from photosynthetic cells to meristems or phloem loading points is implicitly considered.

Tissue death (d_L and d_R, kg d^{-1}) is triggered by extreme low water potentials or it occurs when maintenance can not be satisfied ($starvingL$ and $starvingR$, d^{-1}), then a dismissal of a part of the compartment is applied proportionally to the uncovered demand. A constant leaf and root turnover rate is considered. (kD_L and kD_R , d^{-1}), so it is possible write:

$$d_L = (kD_L + max(starving_L, f_{dess}(\psi_L))) \cdot L$$
$$d_R = (kD_R + max(starving_R, f_{dess}(\psi_R))) \cdot R$$

and starving being defined as the ratio of uncovered maintenance request

$$starving_L = 1 - \frac{min(kM_L \cdot L, C_L)}{kM_L \cdot L}$$
$$starving_R = 1 - \frac{min(kM_R \cdot R, C_R)}{kM_R \cdot R}$$

and $f_{dess}(\psi_L)$, $f_{dess}(\psi_R)$ being the portion (ratio, d^{-1}) of tissues dying as a consequence of low water potentials, in particular ψ_L or ψ_R, which increase the death rate linearly (f_{dess}) between 2 threshold values (complete death and no effect on death).

Structural carbon of woody parts in the tree form is divided into branches (B),

stem (S) and coarse roots (Rc). For the palm form model, only the stem compartment is considered, while for the shrub model only branches and coarse roots. No explicit representation of cambial tissues, phloem, sapwood or heartwood has been implemented, and the related maintenance costs ignored. Levels of solute carbon concentrations ($[C_B]$,$[C_S]$ and $[C_{Rc}]$) corresponding to those structures have been approximated according to a specified gradient between $[C_L]$ and $[C_R]$, that is

$$\begin{aligned}[C_B] &= [C_R] + \alpha_b([C_L] - [C_R]) \\ [C_S] &= [C_R] + \alpha_S([C_L] - [C_R]) \\ [C_{Rc}] &= [C_R] + \alpha_{Rc}([C_L] - [C_R])\end{aligned}$$

with e.g. $\alpha_B = 3/4$, $\alpha_S = 1/2$ and $\alpha_{Rc} = 1/4$ for the tree model.

Similarly to leaf and fine root growth, the growth of wood is influenced by solute concentrations and limited by water potential:

$$\begin{aligned}g_B &= kG_W \cdot [C_B] \cdot A_B \cdot f_{growth}(\psi_B) \\ g_S &= kG_W \cdot [C_S] \cdot A_S \cdot f_{growth}(\psi_S) \\ g_{Rc} &= kG_W \cdot [C_{Rc}] \cdot A_{Rc} \cdot f_{growth}(\psi_{Rc})\end{aligned}$$

with A_B, A_S and A_{Rc} being the cambial areas (m^2), and kG_W the growth rate of the woody parts (m d^{-1}). According to the direction of phloematic flux, solute carbon for the growth of woody parts is drawn from the leaves (C_L) or the fine roots (C_R) pools.

Water

The water submodel represents the water fluxes through the xylem of the plant. State variables are water mass in the xylem (W_L and W_R , kg), water content (θ_L and θ_R , dimensionless) and xylematic water potential (ψ_L and ψ_R). Water content is calculated as the fraction of the actual water volume to the volume of the xylem:

$$\begin{aligned}\theta_L &= \frac{W_L}{V_L \cdot fract_{xylem} \cdot \rho_{H_2O})} \\ \theta_R &= \frac{W_R}{V_R \cdot fract_{xylem} \cdot \rho_{H_2O}}\end{aligned}$$

where $fract_{xylem}$ is the xylematic fraction (dimensionless) and ρ_{H_2O} (kg m^{-3}) is water density. Xylematic water potentials (root and leaf) are directly calculated from water content values (θ_L and θ_R) according to following empirical functions:

$$\begin{aligned}\psi_L &= min(0, 200[tan(\theta_L + \tfrac{\pi}{2}) + 0.64]) \\ \psi_R &= min(0, 200[tan(\theta_R + \tfrac{\pi}{2}) + 0.64])\end{aligned}$$

All the water fluxes are limited by a maximum flux velocity, according to a maximum driving water potential difference. Those empirical functions are indicated with g_{uptake} , g_{xylem} , $g_{transpiration}$ (MPa). Water uptake ($uptake$, kg d^{-1}) in the roots has been set proportional to the difference of water potentials (in soil and roots) and to the uptake area (A_{uptake}, m^2).

$$\begin{aligned}uptake &= kUptake \cdot A_{uptake} \\ &\quad \cdot g_{uptake}(\psi_{soil} - \psi_R)\end{aligned}$$

where g_{uptake} (ψ_{soil} - ψ_R) (MPa) is the "effective" driving difference in water potentials and $kUptake$ (d m^{-1}) is the water uptake rate. Xylematic water transport ($xylem$ kg d^{-1}) is driven by water potential differences and is proportional to the conducting area A and inversely proportional to the length h of transport.

$$\begin{aligned}xylem &= kXylem \cdot \frac{A \cdot fract_{xylem}}{h} \\ &\quad \cdot g_{xylem}(\psi_L - \psi_R)\end{aligned}$$

where g_{xylem} (MPa) is the "effective" driving difference in water potentials, and $kXylem$ (d m^{-1}) is water transport rate. Transpiration ($transpiration$, kg d^{-1}) has been set proportional to the difference of the water potentials, the photosynthetic area (A_{photo}, m), cuticular conductance and stomata opening.

$$\begin{aligned}transpiration &= kTranspiration \\ &\quad \cdot (f_{stomata}(\psi_L) + kCuticular) \\ &\quad \cdot A_{photo} \cdot g_{transpiration}(\psi_{air} - \psi_L)\end{aligned}$$

where $g_{transpiration}$ (ψ_{air} - ψ_L) (MPa) is the "effective" driving difference in water

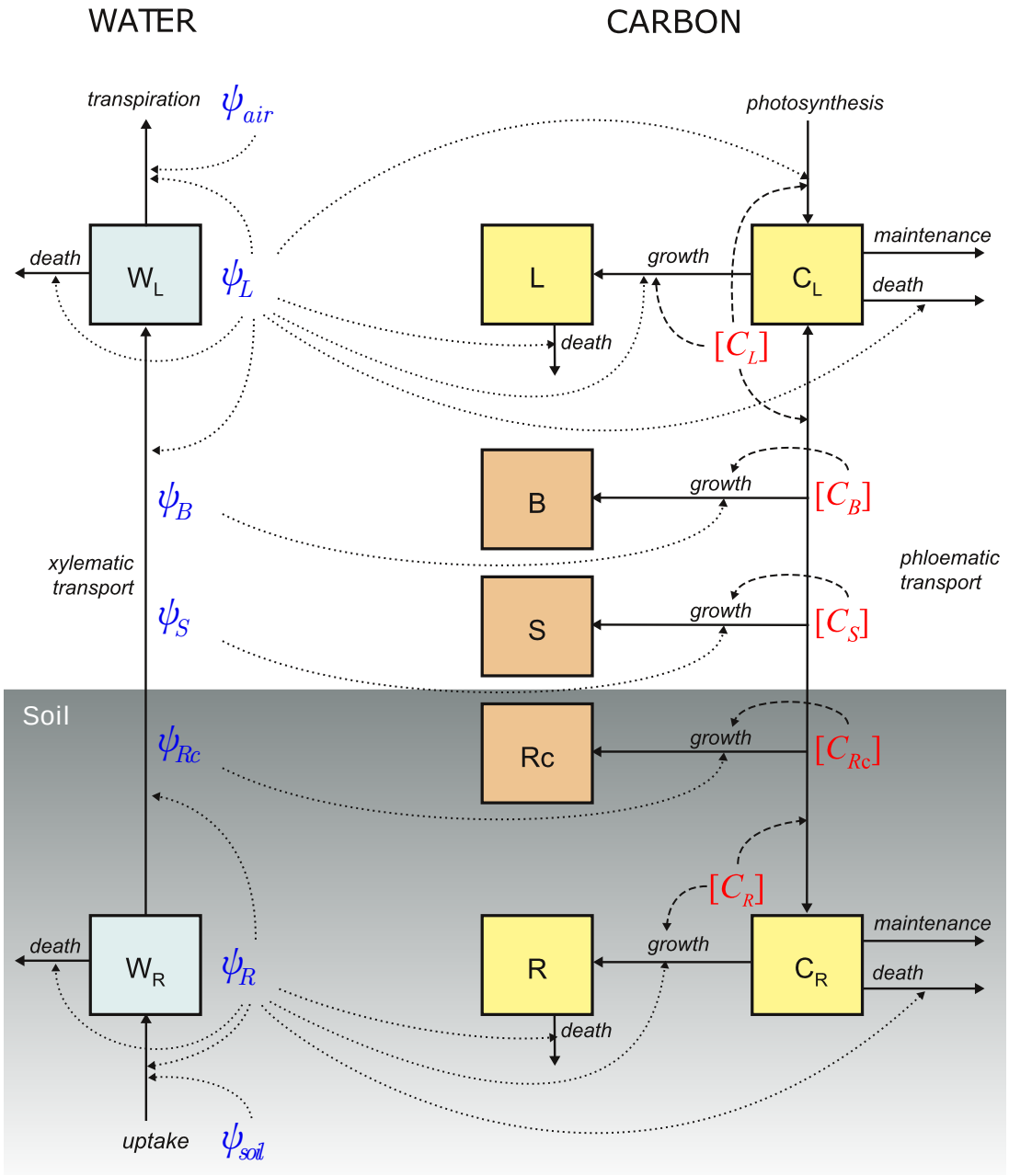

Figure 5.4: Diagram of the model for woody plant, representing the carbon and water submodels with their respective above and below ground compartments (boxes) and fluxes (plain lines). Carbon in leaves and roots is divided into structural (L and R) and solute carbon (CL and CR). Carbon in woody parts in a tree is divided into branches (B), stem (S) and coarse roots (Rc) (for the palm implicit geometry, only the stem compartment is present, while for the shrub form only the branches and coarse roots). Dotted lines represent the influences of environmental (ψ_{air} , ψ_{soil}) and xylematic (ψ_L, ψ_R, ψ_B, ψ_S and ψ_{Rc}) water potentials on water and carbon processes. Dashed lines represent the influences of solute concentrations ($[C_L]$, $[C_R]$,$[C_B]$,$[C_S]$ and $[C_{Rc}]$) on assimilation, growth and phloematic flux. Influences of compartments and of the related implicit geometry on different fluxes are not shown.

Table 5.1: Model variables and parameters, with symbol definitions and units

Symbol	Description	Unit
CARBON AND WATER MODEL		
L, R, B, S, Rc	Mass of structural carbon of leaves, fine roots, branches, stem and coarse roots	kg
C_L, C_R	Mass of solute carbon	kg
W_L, W_R	Mass of water in the xylem	kg
θ_L, θ_R	Relative water content (fraction of maximum possible water content)	-
ψ_L, ψ_R, ψ_B, ψ_S, ψ_{Rc}	Xylematic water potential	MPa
$[C_L], [C_R], [C_B], [C_S], [C_{Rc}]$	Solute carbon concentration	kg m^{-3}
PS	Photosynthesis	kg d^{-1}
m_L, m_R	Maintenance	kg d^{-1}
$phloem$	Phloematic flux	kg d^{-1}
d_L, d_R	Tissue death	kg d^{-1}
$uptake$	Water uptake	kg d^{-1}
$xylem$	Xylematic water transport	kg d^{-1}
GEOMETRY MODEL		
$V_L, V_R, V_B, V_S, V_{Rc}$	Volume	m^3
h	total transport pathways length	m
$A_L, A_R, A_B, A_S, A_{Rc}$,	Meristematic active area	m^2
A	Basal area	m^2
A_{photo}, A_{uptake}	Photosynthetic / uptake area	m^2
ENVIRONMENTAL INPUTS		
ψ_{air} , ψ_{soil}	Air and Soil water potential	MPa
$light$	Light factor	[0,1]
PARAMETERS		
f_{dess}	portion (ratio) of tissues dying as a consequence of low water potentials	d^{-1}
f_{growth}	limitation of growth, due to threshold values of water potential	-
f_{PS_W}	limitation of photosynthesis due to low water potentials	-
f_{PS_C}	limitation of photosynthesis due to high concentrations of sucrose	-
$f_{stomata}$	stomata opening (from 0 to 1)	-
g_{phloem}	empirical function returning the "effective" driving difference in solute carbon concentrations, limiting it to a maximum value	kg m^{-3}
$g_{transpiration}$, g_{uptake}, g_{xylem}	empirical functions calculating an "effective" driving difference in water potentials, limiting it to a maximum value	MPa
$frac_{xylem}, fract_{phloem}$	Xylematic and phloematic fraction	-
kPS	Photosynthesis rate	kg d^{-1} m^{-2}
kG_L, kG_R, kG_W	Leaf, root and wood growth rate	m d^{-1}
kM_L, kM_R	Leaf and root maintenance rate	d^{-1}
kD_L, kD_R	Leaf and root turnover rate	d^{-1}
$kPhloem$	Rate of phloematic transport (specific conductivity)	m^2 d^{-1}
$kTranspiration$	Water transpiration rate (specific conductance through stomata)	d m^{-1}
$kXylem$	Water transport rate (specific conductivity)	d
$kUptake$	Water uptake rate (specific conductance)	d m^{-1}
$kCuticular$	gas conductance through leaf cuticle (for PS and transpiration), expressed as proportion of conductance of completely open stomata	-

potentials and $kTranspiration$ is water transpiration rate (d m^{-1}). Impact of tissue death on the xylematic compartments is the same as in the carbon submodel.

No explicit compartments have been defined for the woody parts in the water submodel. Similarly to the calculation of the solute concentrations related to the woody parts, water potentials have been approximated according to a specified gradient between ψ_L and ψ_R, that is

$$\begin{aligned} \psi_B &= \psi_R + \beta_B(\psi_L - \psi_R) \\ \psi_S &= \psi_R + \beta_S(\psi_L - \psi_R) \\ \psi_{Rc} &= \psi_R + \beta_{Rc}(\psi_L - \psi_R) \end{aligned}$$

with e.g. $\beta_B = 3/4$, $\beta_S = 1/2$ and $\beta_{Rc} = 1/4$ for the tree model.

Coupling of the submodels

Biomass allocation results from the coupling of water and carbon cycles inside the plant: no specific partitioning functions and driving coefficients were introduced. The main feedbacks between the water and carbon submodels are:

- plant water potentials have a limiting effect on photosynthesis and growth; and can trigger plant desiccation
- θ_L and θ_R influences the concentrations of solute carbon in the above and below ground compartments ($[C_L]$, $[C_R]$), which have an effect on photosynthesis, growth and phloematic flux
- the growing biomass is increasing the xylematic volume and thus changing the water contents (θ_L and θ_R), finally affecting water transport.

Results

Effects of species specific properties

The model, despite its simplicity, is able to reproduce consistent growth patterns. Plant growth displays a logistic behaviour (Fig. 5.5a,d,g), which is the result of growth rates and growth and photosynthesis limitations according to the levels of water potential. In these theoretical simulations we implemented growth limitation as a linear decrease between -4 and -8 MPa in foliar xylematic water potentials, and photosynthesis limitation as a linear decrease between -6 and -10 MPa. Figures 5.5c,f,i show leaf water potentials (ψ_L) under constant soil (ψ_{soil}) and air conditions (ψ_{air}). The behaviour in the first 20 timesteps is an artefact due to model initialization.

The allometric trajectories (Fig. 5.5b,e,h) show increasing leaf to root ratios during growth which are consistent with generally observed trends in plants, more "rooty" in their early development and relatively "shooty" in mature stages (Weiner, 2004). The model, according to its parameterization, is able to cover a wide range of allometric trajectories therefore representing different specific strategies. According to different growth rates the plant can reach different weights. For instance increasing leaf growth rates results in faster growth, higher steady-state weights (Fig. 5.5a) and different allocation patterns (Fig. 5.5b). Such different allocation patterns, reflect consistently variations of xylematic leaf water potentials (ψ_L) (Fig. 5.5c).

While the observed patterns with changing growth rate are quite obvious, it is interesting to analyse the different allocation strategies that the model reproduces when changing the parameterization of the transport pathways of water and carbon. In fact, increasing the xylematic conductivity results in a higher steady state weight, with a biomass partitioning in favour of the above ground biomass. On the contrary, a reduced xylematic transport rate produced a more stressed water situation with lower ψ_L and consequent reduced growth (Fig. 5.5 d,e,f). Simulations on changing the root uptake rate ($kUptake$) gave the same patterns, while changing the transpiration rate ($kTranspiration$) had opposite results with higher transpiration lowering ψ_L and thus enhancing growth limitation

(data not shown).

On the other hand, increased phloematic conductivity ($kPhloem$), as expected, results in an allometric trajectory in favour of roots, by allowing more carbon solutes allocation to below ground parts (Fig. 5.5h). Interestingly, at equilibrium, the plants allocating more to roots reach an higher plant biomass (Fig. 5.5g) and a better ψ_L (Fig. 5.5i), reversing the consequence of the changes in water transport rates, where the "rooty" version is smaller and with lower ψ_L (Fig. 5.5e, h). This observed benefit in plants with high phloem transport capability, is due to the greater capacity of water uptake by the larger root system, with a consequently better water condition in the leaves.

Effects of environment and disturbances

The simulated plant reflects the environmental changes with a reduction of biomass under both limiting light and reduced water availability (Fig. 5.6a). The model is also able to react to such reduced resource levels by increasing the relative allocation to the plant parts needed for counteracting the limiting factors, as postulated by the optimal allocation theory (Bloom *et al.* , 1985). This is shown in Figure 5.6b by the higher allocation to leaves under limiting light conditions and the higher allocation to roots under limiting water levels. In particular, the deviation from the allometric trajectory under optimal conditions depends on the intensity of the limitation of either light or water indicated by the labels in Figure 5.6c. In case of excessive stressing conditions (50% of shading and -6MPa of soil water potential) the plants will progressively loose its biomass and then die.

A strength of the model is its capability of consistent reaction to disturbance such as leaf and root removal (e.g. by grazing, fire and pathogen effects). In fact, the simulated plant is able to change the relative allocation between above and below ground structures when an unbalanced partitioning condition is created by the occurrence of a disturbance (Fig. 5.6d). Following a biomass removal the plants recover a balanced partitioning by a dynamic reallocation of growth to the damaged parts. Interestingly, during recovery of leaf removal, the root turnover is initially increased to facilitate the rebalancing process (Fig. 5.6d).

The model is also able to reproduce qualitatively correct allocation patterns considering wood compartments, as shown in Figure 5.7 for a shrub form. With decreasing levels of water availability, the model allocates proportionally more resources to below ground compartments, namely to fine (Fig. 5.7 *a*) and coarse roots (Fig. 5.7 *b*). The allometric trajectory between the aerial parts (leaves and branches, Fig. 5.7 *c*) bends towards wood biomass with time, following a volume to surface proportionality rule. Instead, if branch sapwood area is plotted against leaf area (Fig. 5.7 *d*), a more linear behaviour is observed, which is coherent with the pipe model principle. Assuming a linear relationship, the behaviour of the leaf area to sapwood area coefficient *(LASA)* produced by the model is consistent with the experimental observations of the previous studies (Chapters 3 and 4) regarding water availability, confirming the hypothesized underlying hydraulic mechanisms.

Discussion

The description of hydraulic architecture of plants in recent decades has been integrating the cohesion-tension theory, explaining the physics of sap movement, with an electrical analogy used to model the water flow in the soil-plant continuum (Cruiziat *et al.* , 2002). According to this theory, evaporation of water vapour from leaves originates high tensions (low negative pressures) in the xylem vessels, pulling water upwards. Our model of the soil-atmosphere continuum is similar to a simple "water pump" driven by water potentials: a pipe (xylem) with a membrane at the soil (uptake) and one at the air interface (transpiration). Recently, Wheeler & Stroock (2008)

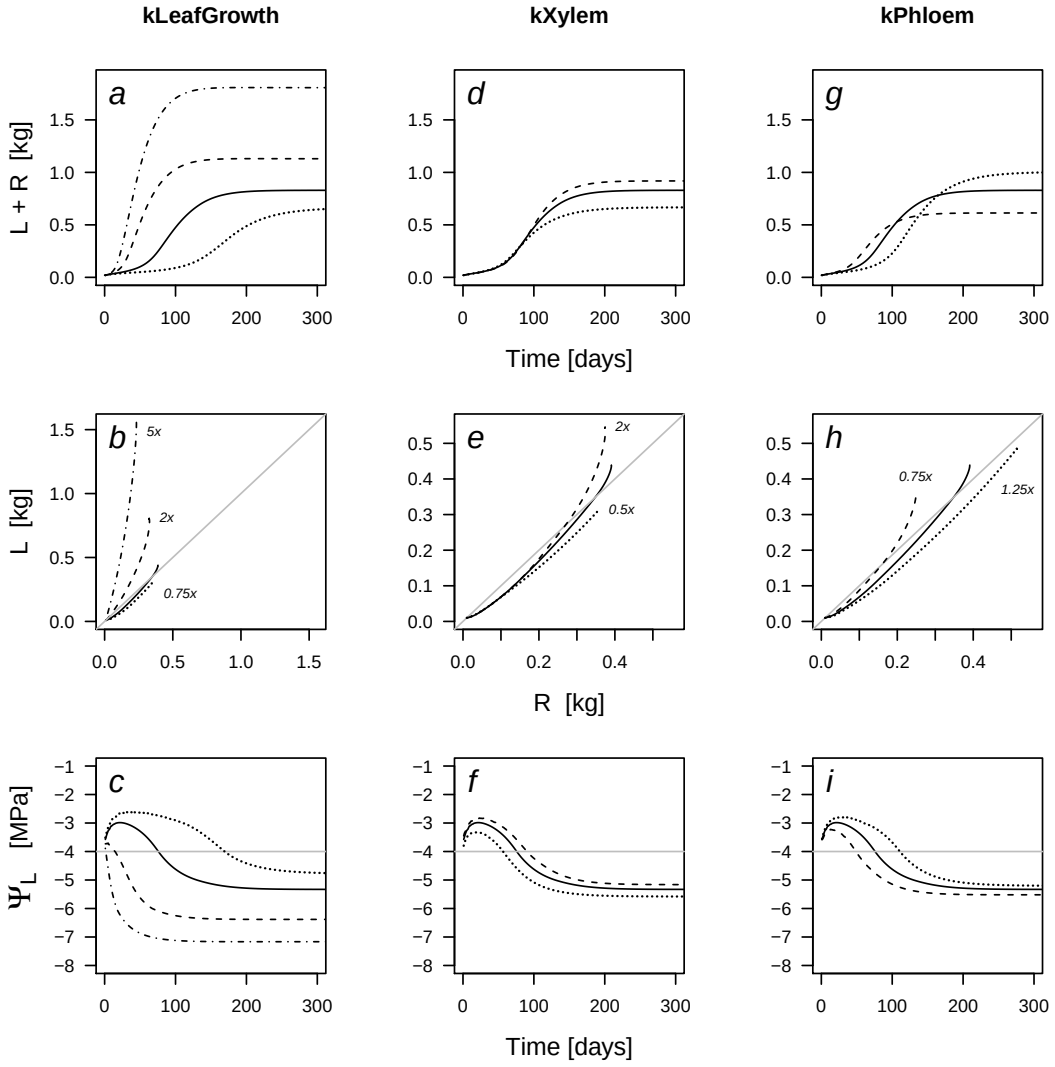

Figure 5.5: Model simulations of plant biomass development (a, d, g), allometric trajectories (b, e, h) and xylematic leaf water potential development (c, f, i), according to different leaf growth rates kGL (a,b,c), xylematic specific conductivities $kXylem$ (d,e,f) and phloematic specific conductivities $kPhloem$ (g,h,i). Plain lines represent a simulation with a standard parameterization, while dotted, dashed and dot-dashed lines represent simulations operated with alternate coefficients. The different scales applied in the simulations are specified, relatively to the standard ones in the allometric trajectories plots (b, e, h). The horizontal grey lines in the plots of xylematic water potentials represent the limit below which limitation of growth occurs (-4 MPa)

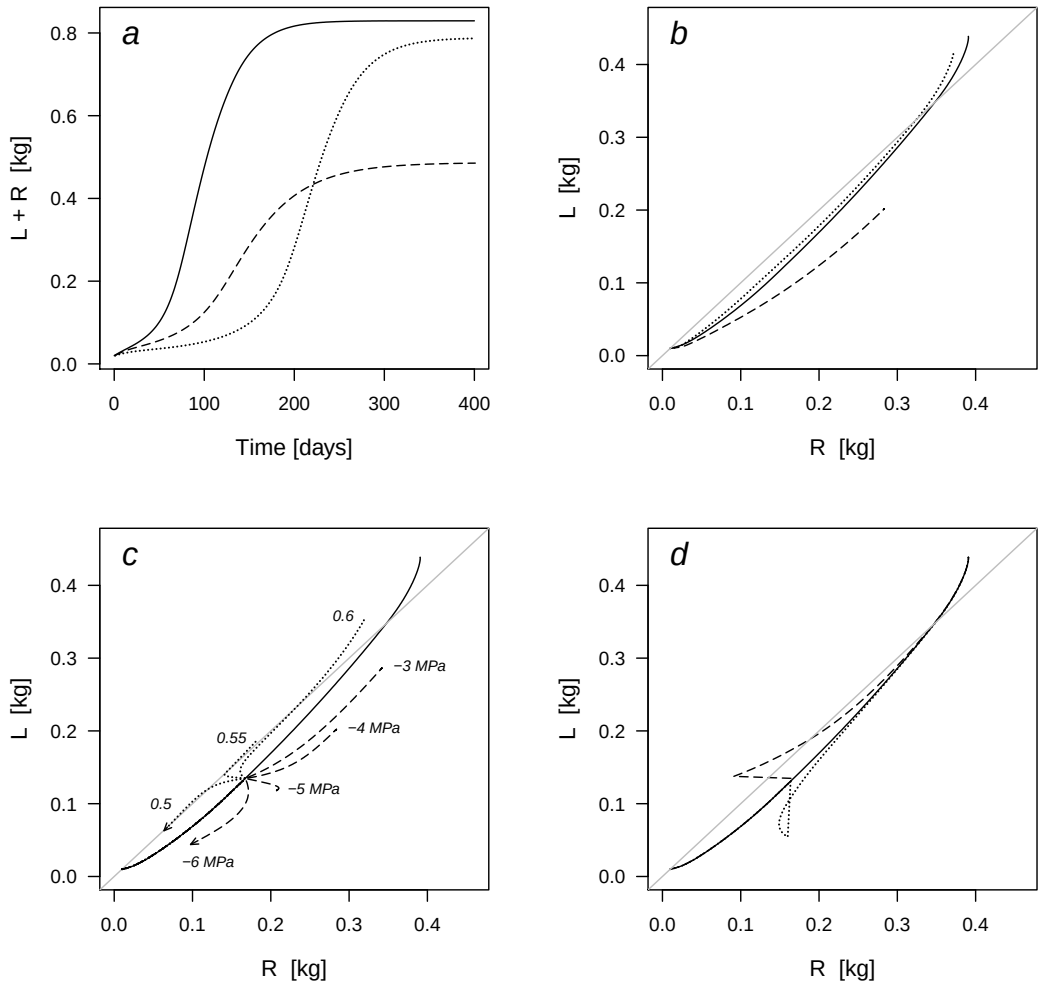

Figure 5.6: Model simulations of plant biomass development (a) and allometric trajectories (b,c,d) according to different environmental conditions or disturbances. Plain lines represent a simulation with a standard parameterization, that is -1 MPa of soil water potential and full light factor (1).
(a, b) - Growth in different but constant environments: $light = 0.8$ (dotted lines) and soil water potential ψ_{soil} = -4 MPa (dashed lines).
(c) - Growth in changing environments, starting with a standard parameterization and changing at day 80. Arrows indicate trajectories ending into plant death.
(d) - Effects of a cut of 60% of leaves (dotted line) or 50% of roots (dashed lines) at day 80

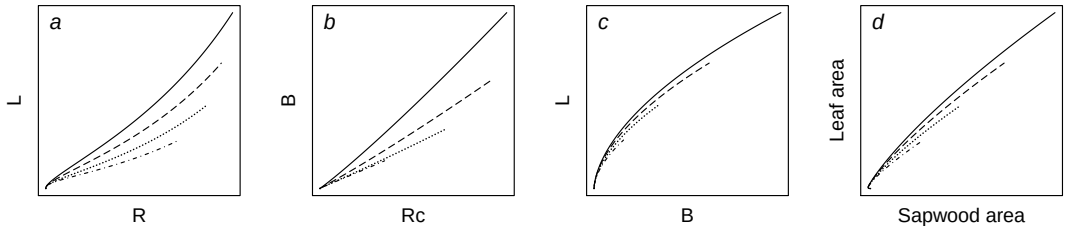

Figure 5.7: Model simulations of woody plant biomass development, according to the shrub implicit geometry. The line types represent simulations at decreasing soil water potentials, namely -1 MPa (plain lines), -2 MPa (dashed lines), -3 MPa (dotted lines) and -4 MPa (dot-dashed lines).

could capture for the first time this basic view in a synthetic tree using hydrogel membranes, supporting the cohesion-tension mechanism of transpiration. Decrease in xylematic conductivity due to xylem wall collapse (Cochard *et al.* , 2004) or xylem cavitation, with air entering to pores (Sperry *et al.* , 2002), has been indirectly considered, allowing the flow to reach a maximum speed. This was formalized by setting a maximum driving water potential gradient, above which the bulk flow does not increase. Near to this values water stress on leaves is amplified, increasing the sensitivity of stomatal response to drought, which may promote drought survival (Sperry, 2000). Increases in soil-root and leaf-air resistances along with decreasing water potentials (Cruiziat *et al.* , 2002) have been simulated with a similar approach. Similarly to Dewar (1993), in our model phloem water flow has been considered neglectable in comparison to transpiration.

Assimilate fluxes through the phloem have been considered as a bulk flow proportional to the concentration gradient between leaves and roots, considering this to be a proxy for the osmotic pressure gradient. This imply that conductivity can not be derived from anatomical investigation of the vascular tissues (Minchin & Lacointe, 2005), but it should be estimated as a diffusive parameter implicitly simulating a mass-flow process. The same author considered unlikely that specific details of generation of the sieve-tube pressure gradient (phloem apoplastic and symplastic loading) would be important in modelling plant growth. However, there are evidences that the region of highest flow resistance is within the symplastic pathway of the receiver cells (Gould *et al.* , 2004), determining a saturable kinetics of phloem unloading (Minchin & Lacointe, 2005). This has been considered by introducing into the model a limitation of phloem flow speed, setting a maximum driving concentration gradient, above which the flow does not increase. Changes in viscosity due to sugar content have not been considered. Among the represented fluxes, a priority was given to maintenance over growth and phloem flux, implicitly considering the distance of assimilate transport to meristem and phloem loading.

So far we also did not consider reserves dynamics, water soil depletion (which is depending from the soil type) and water vapour dynamics at the leaf surface, light quality (e.g. red/far red ratio), self shading and root competition.

The model showed in a consistent way, how by changing few species-specific parameters, like growth or flow rates, a wide palette of diverse allometric relationships could be produced. The model also reproduced different consistent allometric trajectories according to the different environmental conditions, fulfilling the expectations of the optimal allocation theory (Bloom *et al.* , 1985), thus increasing the relative allocation of the part which is responsible for the acquisition of the limiting factor. Confirming the results of Thornley (1998), the TR framework delivered a sur-

prising variety of realistic responses, arising from simple phenomenological assumptions belonging to the two significant types of processes involved in allocation: transport and chemical/biochemical conversion. Early models (Thornley, 1972a,b, a and b) could already reproduce qualitatively consistent allometric responses according to carbon and nitrogen substrates (Wilson, 1988a). However these and successive works (e.g. Dewar, 1993) did not consider a coupling with a sufficiently realistic representation of the water fluxes through the soil-atmosphere continuum, depending on both soil and air water status.

Moreover even if such models simulated the general dynamics of growth partitioning, the evaluation has been mainly performed according to an exponential growth pattern (Dewar, 1993), excluding for instance the complexity arising from changing substrate concentrations or the changes in the importance of the driving processes during plant life span. Since we hypothesized that changes of water conditions during plant development due to hydraulic architecture are of crucial importance, our analysis could not be restrict to the exponential growth phase. In this case we avoided the use of shoot:root ratios, since they could mask important biological phenomena (Jasienski & Bazzaz, 1999), typically size related processes. To this scope the analysis of our results as deviance from allometric relationships (Weiner, 2004) proved to be adequate, allowing the detection of "true" patterns of plasticity.

Logistic growth pattern can arise as the result of different processes, like self shading, root competition, unequal increase of mass and surface related processes. In our model this was mainly the result of attaining growth and assimilation limitation due to the lowering water potentials in the above ground part with the increasing size (water transport is inversely proportional to the length of the pathway), and to the additional photosynthesis limitation due to concentration saturation. This assumptions may also explain the changes between early "rooty" and mature "shooty" phases of plants, without assuming different turnover (litter) rates in above and below ground parts (Thornley, 1998).

Given its sound functional behavior in basic physiological process, the model capability of correct reaction to disturbance of both above and below ground parts is remarkable. This will be the basis for further applications where the model will be integrated at the community scale to analyze the competitive advantages of different allocation strategies and the related anatomical (e.g. sclerophylly) and functional (e.g. transport resistances) constrains.

References

Allen, M, Prusinkiewicz, P, & DeJong, T M. 2005. Using l-systems for modeling source-sink interactions, architecture and physiology of growing trees: the l-peach model. *New phytologist*, **166**, 869–880.

Bloom, A J, Chapin, F S, & Mooney, H A. 1985. Resource limitation in plants-an economic analogy. *Annu. rev. ecol. syst.*, **16**(1), 363–392.

Cannell, M. G. R., & Dewar, R. C. 1994. Carbon allocation in trees: a review of concepts for modelling. *Advances in ecological research*, **25**, 59–104.

Chen, JL, & Reynolds, JF. 1997. A coordination model of whole-plant carbon allocation in relation to water stress. *Annals of botany*, **80**(1), 45–55.

Cochard, Hervé, Froux, Fabienne, Mayr, Stefan, & Coutand, Catherine. 2004. Xylem wall collapse in water-stressed pine needles. *Plant physiology*, **134**(January), 401–408.

Cruiziat, P., Cochard, H., & Ameglio, T. 2002. Hydraulic architecture of trees: main concepts and results. *Annals of forest science*, **59**(7), 723–752.

Da Silva, D, Favreau, R, Auzmendi, I, & DeJong, T. 2010 (September 12-17). Linking water stress effects on carbon partitioning by introducing a xylem circuit into l-peach. *In: Proceedings of the 6th international workshop on functional-structural plant models*. University of California, Davies.

Daudet, F. 2002. Generalized münch coupling between sugar and water fluxes for modelling carbon allocation as affected by water status. *Journal of theoretical biology*, **214**(3), 498, 481.

Dewar, R. C. 1993. A root-shoot partitioning model based on carbon-nitrogen-water interactions and munch phloem flow. *Functional ecology*, 356–368.

Gould, N, Thorpe, MR, Minchin, PEH, Pritchard, J, & White, PJ. 2004. Solute is imported to elongating root cells of barley as a pressure-driven flow of solution. *Functional plant biology*, **31**, 391–397.

Jasienski, M., & Bazzaz, Fakhri A. 1999. The fallacy of ratios and the testability of models in biology. *Oikos*, **84**(2), 321–326.

Kramer, Paul Jackson. 1983. *Water relations of plants*. Academic P.,U.S.

Lacointe, André. 2000. Carbon allocation among tree organs: A review of basic processes and representation in functional-structural tree models. *Annals of forest science*, **57**(5-6), 13 pages.

Mazzoleni, S., & Spada, F. 1992. *Responses of forest ecosystems to environmental changes*. Elsevier Applied Science,London and New York. Chap. Deciduous broadleaved versus evergreen sclerophyllous forests. Disturbance and local shifting dominance in Mediterranean environments., page 839?840.

Minchin, P. E. H., & Lacointe, A. 2005. New understanding on phloem physiology and possible consequences for modelling long-distance carbon transport. *New phytologist*, **166**(3), 771–779.

Muetzelfeldt, R, & Massheder, J. 2003. The simile visual modelling environment. *European journal of agronomy*, **18**, 345–358.

Mäkelä, Annikki, Landsberg, Joe, Ek, Alan R., Burk, Thomas E., Ter-Mikaelian, Michael, Agren, Goran I., Oliver, Chadwick D., & Puttonen, Pasi. 2000. Process-based models for forest ecosystem management: current state of the art and challenges for practical implementation. *Tree physiol*, **20**(5-6), 289–298.

Münch, E. 1927. Dynamik der saftströmungen. *Bericht der deutschen botanischen gesellschaft*, **44**, 69–71.

Prusinkiewicz, P, Allen, M, Escobar-Gutierrez, A, & DeJong, TM. 2007. *Functional-structural plant modelling in crop production*. Wageningen: Frontis. Chap. Numerical methods for transport- resistance sink-source allocation models, pages 123–138.

R Development Core Team. 2011. *R: A language and environment for statistical computing*. R Foundation for Statistical Computing, Vienna, Austria. ISBN 3-900051-07-0.

Roux, XL, Lacointe, A, Escobar-Gutiérrez, A, & Dizès, SL. 2001. Carbon-based models of individual tree growth: A critical appraisal. *Annals of forest science*, **58**, 469–506.

Soetaert, Karline, Petzoldt, Thomas, & Setzer, R Woodrow. 2010a. Solving differential equations in r. *The r journal*, **2**(2), 5–15.

Soetaert, Karline, Petzoldt, Thomas, & Setzer, R Woodrow. 2010b. Solving differential equations in r: Package desolve. *Journal of statistical software*, **33**(9), 1–25.

Sperry, J. S. 2000. Hydraulic constraints on plant gas exchange. *Agricultural and forest meteorology*, **104**(1), 13–23.

Sperry, J. S., Hacke, U. G., Oren, R., & Comstock, J. P. 2002. Water deficits and hydraulic limits to leaf water supply. *Plant cell and environment*, **25**(2), 251–263.

Stearns, SC. 1992. *The evolution of life histories*. Oxford: Oxford University Press.

Sultan, SE. 2004. Promising directions in plant phenotypic plasticity. *In: Perspectives in plant ecology, evolution and systematics*.

Thornley, J. H. M. 1972a. A balanced quantitative model for root: Shoot ratios in vegetative plants. *Ann bot*, **36**(2), 431–441.

Thornley, J. H. M. 1972b. A model to describe the partitioning of photosynthate during vegetative plant growth. *Ann bot*, **36**(2), 419–430.

Thornley, JHM. 1998. Modelling shoot [ratio] root relations: the only way forward? *Annals of botany*, **81**(2), 165.

Weiner, J. 2004. Allocation, plasticity and allometry in plants. *In: Perspectives in plant ecology, evolution and systematics*.

Wheeler, Tobias D., & Stroock, Abraham D. 2008. The transpiration of water at negative pressures in a synthetic tree. *Nature*, **455**(7210), 208–212.

Wilson, J. Bastow. 1988a. A review of evidence on the control of shoot: Root ratio, in relation to models. *Ann bot*, **61**(4), 433–449.

Yang, Zongjian, & Midmore, David J. 2005. Modelling plant resource allocation and growth partitioning in response to environmental heterogeneity. *Ecological modelling*, **181**(1), 59–77.

Chapter 6

Concluding remarks

In the frame of this work, plant responses in biomass allocation to environmental conditions and disturbances were investigated, elaborating both empirical and process-based models.

After having gained a basic understanding of specific peculiarities of the studied tree species *Castanea sativa*, we proved that the pipe model approach is an effective instrument for assessing plant plasticity ranges and for gaining an insight into plant water relations. This work contributes to the establishment of a methodological basis for future research on plant plasticity according to the leaf area to sapwood area relationship.

It would now be important to extend the assessment of the plasticity ranges to other tree species, gaining a more complete picture of possible inter-specific competition dynamics, that can arise in case of changing environmental conditions.

Furthermore, it would be particularly interesting to study the temporal dynamics of partitioning, by analysing the same branches in subsequent years. This measure, being tightly allied with plant water relations, would provide an integrative instrument of phenological observations. In particular the investigation of the relationships of this temporal dynamic with climatic variables and explicit measurements of soil water content, should allow the formulation of sounder hypothesis and predictions of ecosystem responses to climate change.

The theoretical system dynamics model developed during this thesis was able to simulate complex dynamic behaviours of biomass partitioning in plants. The model included a simplified, although mechanistic, representation of water and carbon fluxes, whose integration was able to reproduce consistent deviations from the allometric trajectory, both in a range of different environmental conditions and during recovery from unbalanced biomass removal.

In this respect this model has the potential to be a good instrument for future theoretical investigation of relations between anatomical (e.g. sclerophylly) and functional (e.g. transport resistances) characters and allocation patterns.

Priority in future developments should be given to a comprehensive sensitivity analysis and to the determination of the model's domains, according to specific parameters and to different plant geometries. This would allow the exploration of the role of specific conductivities or metabolic rates, on the extent of the ranges of plastic allocation behaviour.

The coupling with a soil model, in order to include the concept of water depletion, would allow the investigation of the effect of soil specific characteristics on allocation. Moreover, it would then be possible to run individual-based community exercises. In fact, with an explicit implementation of competition for water and light (through water depletion and shading), it should be possible to test the success of species with diverse allocation strategies. In particular, simulations in changing or disturbed environments could highlight the selection of different partitioning strategies, e.g. according to disturbance regime.

Finally, it would be interesting to adapt the functional engine of this partitioning model as a module in larger integrated models at global scale, verifying how this more dynamic representation of biomass allocation would affect global carbon fluxes and storage, in the scenario of the ongoing climate change.

Appendix A

Methods of the experimental part

Data collection

Figure A.1: Pictures of data collection by Eric Gehring, during his master thesis (author Franco Fibbioli)

Figure A.2: Pictures of branch preparation and dissection (author Eric Gehring)

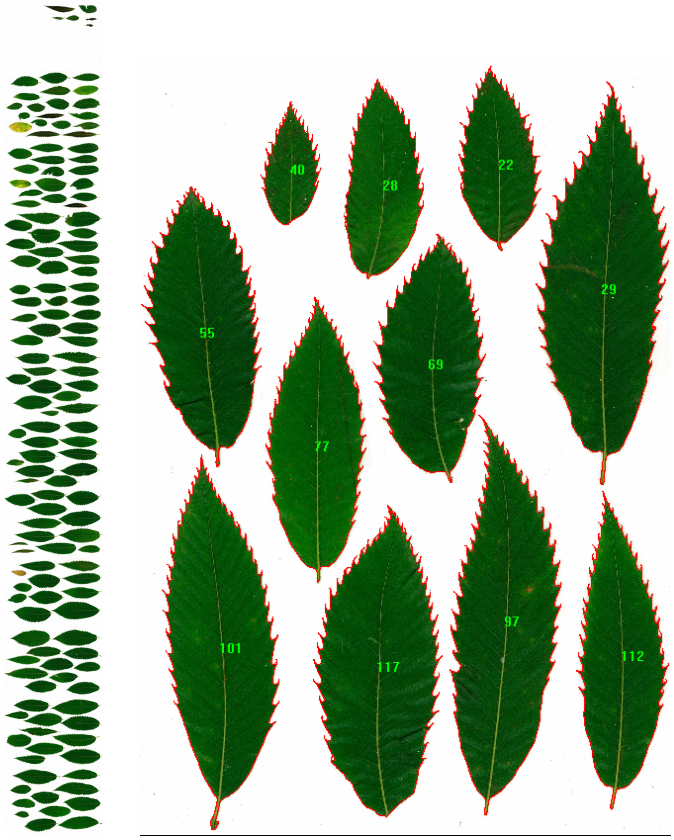

Figure A.3: Pictures of scanned leaves and image processing

Database

A relational database has been developed on a PostGreSQL server version 8.4, in order to store all the collected and processed data. The tables were conceived in a hierarchical path, from tree to leaf (FigureA.4). The *individual* level was conceived to represent the single trunks for trees in a coppice, originating from basal reiterations of the same tree.

Data entry masks have been implemented with MsAccess (Figure A.5), and allows an easy browsing of the data structure along the different levels.

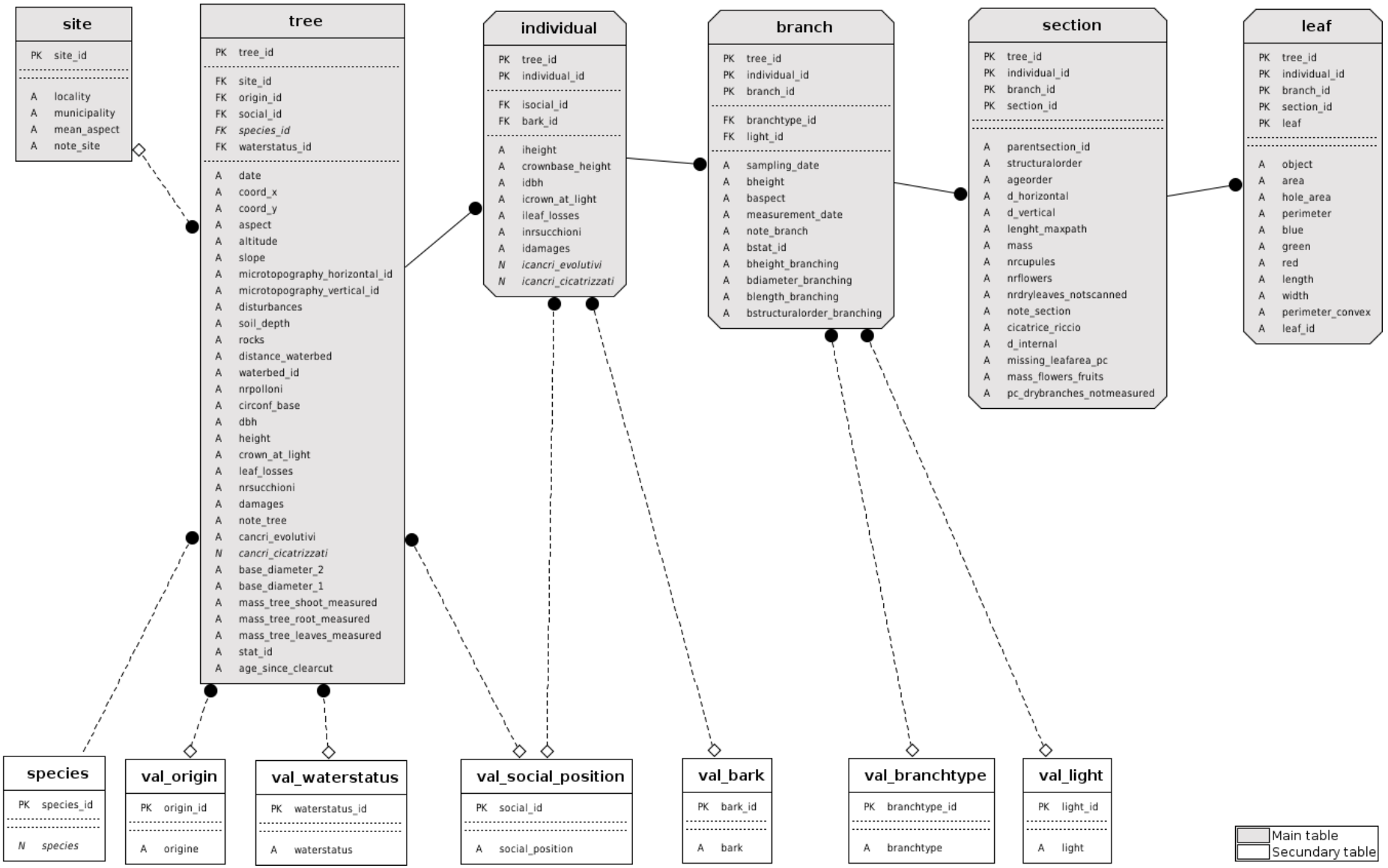

Figure A.4: Database structure with the table and field names (*PK* primary key, *FK* foreign key, *A* attribute)

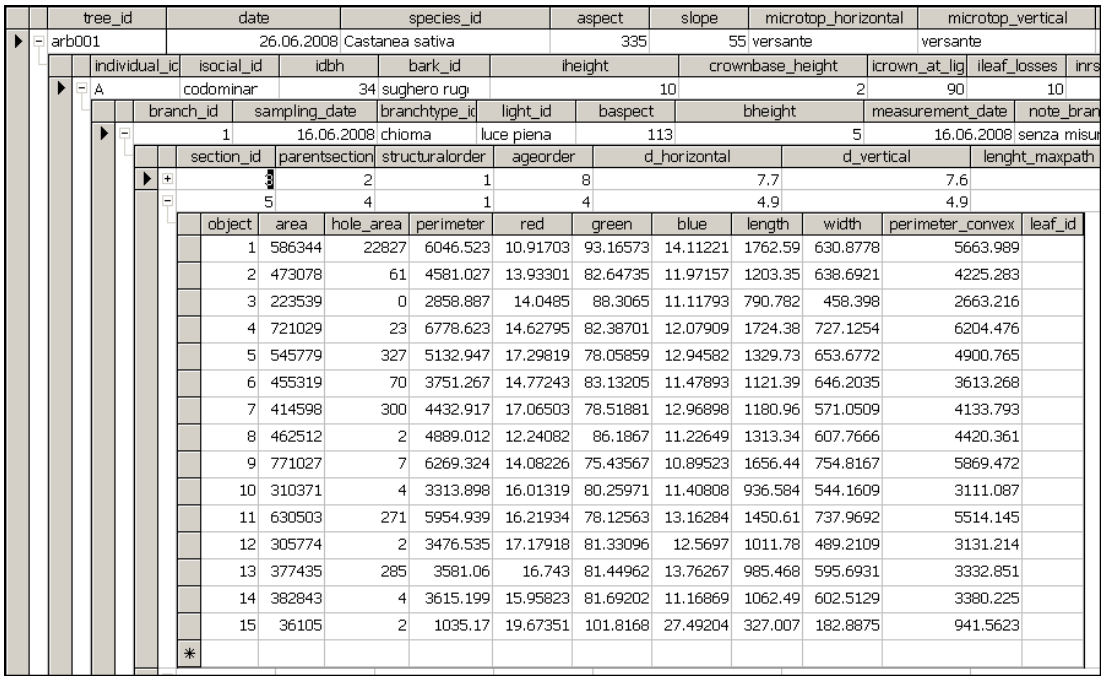

tree_id	date	species_id	aspect	slope	microtop_horizontal	microtop_vertical
arb001	26.06.2008	Castanea sativa	335	55	versante	versante

individual_ic	isocial_id	idbh	bark_id	iheight	crownbase_height	icrown_at_lig	ileaf_losses	inrs
A	codominar	34	sughero rug	10	2	90	10	

branch_id	sampling_date	branchtype_ic	light_id	baspect	bheight	measurement_date	note_bran
1	16.06.2008	chioma	luce piena	113	5	16.06.2008	senza misur

section_id	parentsection	structuralorder	ageorder	d_horizontal	d_vertical	lenght_maxpath
3	2	1	8	7.7	7.6	
5	4	1	4	4.9	4.9	

object	area	hole_area	perimeter	red	green	blue	length	width	perimeter_convex	leaf_id
1	586344	22827	6046.523	10.91703	93.16573	14.11221	1762.59	630.8778	5663.989	
2	473078	61	4581.027	13.93301	82.64735	11.97157	1203.35	638.6921	4225.283	
3	223539	0	2858.887	14.0485	88.3065	11.11793	790.782	458.398	2663.216	
4	721029	23	6778.623	14.62795	82.38701	12.07909	1724.38	727.1254	6204.476	
5	545779	327	5132.947	17.29819	78.05859	12.94582	1329.73	653.6772	4900.765	
6	455319	70	3751.267	14.77243	83.13205	11.47893	1121.39	646.2035	3613.268	
7	414598	300	4432.917	17.06503	78.51881	12.96898	1180.96	571.0509	4133.793	
8	462512	2	4889.012	12.24082	86.1867	11.22649	1313.34	607.7666	4420.361	
9	771027	7	6269.324	14.08226	75.43567	10.89523	1656.44	754.8167	5869.472	
10	310371	4	3313.898	16.01319	80.25971	11.40808	936.584	544.1609	3111.087	
11	630503	271	5954.939	16.21934	78.12563	13.16284	1450.61	737.9692	5514.145	
12	305774	2	3476.535	17.17918	81.33096	12.5697	1011.78	489.2109	3131.214	
13	377435	285	3581.06	16.743	81.44962	13.76267	985.468	595.6931	3332.851	
14	382843	4	3615.199	15.95823	81.69202	11.16869	1062.49	602.5129	3380.225	
15	36105	2	1035.17	19.67351	101.8168	27.49204	327.007	182.8875	941.5623	

Figure A.5: Screenshot of the graphical interface for data entry

In order to compute all the necessary calculations at the section level (summing up the relevant values of the child sections, e.g. for leaf area), ad hoc functions in pgSQL have been developed. Those functions, through the use of temporary tables, allow the creation of the table *v_section* with all the needed calculated values at the section level, which can be further exported for statistical analysis. The main function is *create_hierarchy_tables* (Listing A.1), which calls some specific subfunctions.

Listing A.1: Code of function *create_hierarchy_tables*

```
1  -- Function: create_hierarchy_tables(integer)
2
3  -- DROP FUNCTION create_hierarchy_tables(integer);
4
5  CREATE OR REPLACE FUNCTION create_hierarchy_tables(nrlevels integer)
6    RETURNS void AS
7  $BODY$
8  declare
9    prevtable text;
10   nexttable text;
11   i integer;
12   j integer;
13   limit integer;
14   tablename text;
15   tooDeep integer;
16   dropstmt text;
17   viewstmt text;
18 begin
19
20 /* by boris.pezzatti@wsl.ch
21  *
22  * this function creates first temporary tables of sections to reconstruct the hierarchy
23  * the created tables are checked if they can resolve the hierarchy dept, if not an exception
24  * is raised and the user should increase the nrlevels (input)
25  * then  the informations are grouped to calculate parameters for parent sections
26  *
27  * the table v_section is the output, and summarize all informations for the whole sections
28  * the view v_section_noSingleSection is provided, in order to discard branches with a sigle section
29  * (no regression possible) and to add some statistics (nr of section in branch, individual, tree)
30  */
31
32
33   prevtable:='section';                                          --create tables s0_x = section without
       roots of x level
34   for i in 1..nrlevels loop
35         nexttable:='s0_'||i::text;
36         perform create_base_hierarchy_table(nexttable,prevtable);
37         prevtable:=nexttable;
38   end loop;
39
40   for j in 1..nrlevels+1 loop                                    --create hierarchy tables sx_y
41         limit:=nrlevels+1 - j;
42         for i in 0..limit loop
```

```
                nexttable:='s'||j||'_'||i::text;
                prevtable:='s'||j-1||'_'||i::text;
                if j=1 then
                        if i=0 then prevtable:='section'; end if;     /*only for the first table*/
                        perform create_first_hierarchy_table(nexttable,prevtable);
                else
                        perform create_next_hierarchy_table(nexttable,prevtable);
                end if;
        end loop;
  end loop;

  dropstmt:='';                                                   --drop tables s0_x
  for i in 1..nrlevels loop
        dropstmt:=dropstmt||'s0_'||i::text||',';
  end loop;
  for j in 1..nrlevels loop                                     --drop not relevant tables sx_y
        limit:=nrlevels - j;
        for i in 0..limit loop
                dropstmt:=dropstmt||'s'||j||'_'||i::text||',';
        end loop;
  end loop;
  dropstmt:='DROP TABLE '||trim(trailing ',' from dropstmt);
  execute dropstmt;

                                                                --the remaining tables are checked if they
                                                                     can
                                                                --resolve the hierarchy dept
  for i in 1..nrlevels+1 loop
        tablename:='s'||i::text||'_'||(nrlevels+1-i)::text;
        execute 'select count(newparentsection_id)  from '||tablename into tooDeep;
        if tooDeep>0 then raise exception 'dept scanning level is not enough: % child sections were found
             in table %',tooDeep,tablename;end if;
  end loop;

                                                                --build the necessary queries
  viewstmt:='CREATE OR REPLACE VIEW summary_leaf AS
 SELECT min(leaf.tree_id::text) AS tree_id, min(leaf.individual_id::text) AS individual_id, min(leaf.
      branch_id) AS branch_id, min(leaf.section_id) AS section_id, count(leaf.tree_id) AS nr_leaves, sum(
      leaf.area) AS larea, sum(leaf.hole_area) AS lhole_area, sum(leaf.length) AS llength, sum(leaf.width)
      AS lwidth, sum(leaf.perimeter) AS lperimeter, sum(leaf.perimeter_convex) AS lperimeter_convex, sum(
      leaf.blue * leaf.area) AS blue, sum(leaf.green * leaf.area) AS green, sum(leaf.red * leaf.area) AS
      red
   FROM leaf
  GROUP BY leaf.tree_id, leaf.individual_id, leaf.branch_id, leaf.section_id;

ALTER TABLE summary_leaf OWNER TO pipe;


CREATE OR REPLACE VIEW summary_single_sections AS
 SELECT tree_id, individual_id, section.branch_id, section.section_id, section.parentsection_id, section.
      structuralorder, section.ageorder, section.d_horizontal, section.d_vertical, section.cicatrice_riccio
      , section.lenght_maxpath, section.mass, section.nrcupules, section.nrflowers, section.
      nrdryleaves_notscanned, section.note_section AS note, COALESCE(summary_leaf.nr_leaves, 0::bigint) AS
      nr_leaves, COALESCE(summary_leaf.larea, 0::double precision) AS larea, COALESCE(summary_leaf.
      lhole_area, 0::double precision) AS lhole_area, COALESCE(summary_leaf.llength, 0::real) AS llength,
      COALESCE(summary_leaf.lwidth, 0::double precision) AS lwidth, COALESCE(summary_leaf.lperimeter, 0::
      double precision) AS lperimeter, COALESCE(summary_leaf.lperimeter_convex, 0::double precision) AS
      lperimeter_convex, COALESCE(summary_leaf.blue, 0::double precision) AS blue, COALESCE(summary_leaf.
      green, 0::double precision) AS green, COALESCE(summary_leaf.red, 0::double precision) AS red
   FROM section
   LEFT JOIN summary_leaf USING (tree_id, individual_id, branch_id, section_id);

ALTER TABLE summary_single_sections OWNER TO pipe;


  CREATE OR REPLACE VIEW summary_section_part AS
 SELECT s.tree_id, s.individual_id, s.branch_id, s.section_id, s.count,s.mass,s.nrcupules, s.nrflowers,s.
      nrdryleaves_notscanned, s.nr_leaves, s.larea, s.lholearea, s.llength, s.lwidth, s.lperimeter, s.
      lperimeter_convex, s.blue, s.green, s.red
   FROM (';

  for i in 1..nrlevels+1 loop
        viewstmt:=viewstmt||part_view_summary_section_part('s'||i::text||'_'||(nrlevels+1-i)::text)||'
             UNION ';
  end loop;

  viewstmt:=  trim(trailing 'UNION ' from viewstmt)||'  ) s
ORDER BY s.tree_id, s.individual_id, s.branch_id, s.section_id;
ALTER TABLE summary_section_part OWNER TO pipe;

CREATE OR REPLACE VIEW summary_section AS
 SELECT tree_id, section.individual_id, section.branch_id, section.section_id, section.parentsection_id,
      section.structuralorder, section.ageorder, section.d_horizontal, section.d_vertical, section.
      d_internal, section.cicatrice_riccio, section.lenght_maxpath, ssp.mass, ssp.nrcupules, ssp.nrflowers,
       ssp.nrdryleaves_notscanned, section.note_section AS note, ssp.nr_leaves, ssp.larea, ssp.lholearea,
      ssp.llength, ssp.lwidth, ssp.lperimeter, ssp.lperimeter_convex, case when ssp.larea=0 then null else
      ssp.blue/ssp.larea end AS blue, case when ssp.larea=0 then null else ssp.green/ssp.larea end AS green
      , case when ssp.larea=0 then null else ssp.red/ssp.larea end AS red
   FROM section
   LEFT JOIN summary_section_part ssp USING (tree_id, individual_id, branch_id, section_id);

ALTER TABLE summary_section OWNER TO pipe;
';

  execute viewstmt;
                                                                        --build the output table and view
  viewstmt:='

DROP TABLE v_section CASCADE;
```

```
117
118  CREATE TABLE v_section AS
119   SELECT species.species, tree.site_id, summary_section.tree_id, individual_id, summary_section.branch_id,
        summary_section.section_id, summary_section.parentsection_id, summary_section.structuralorder,
        summary_section.ageorder, summary_section.d_horizontal, summary_section.d_vertical, summary_section.
        cicatrice_riccio, summary_section.lenght_maxpath, summary_section.mass, summary_section.nrcupules,
        summary_section.nrflowers, summary_section.nrdryleaves_notscanned, summary_section.note,
        summary_section.nr_leaves, summary_section.larea, summary_section.lholearea, summary_section.llength,
         summary_section.lwidth, summary_section.lperimeter, summary_section.lperimeter_convex,
        summary_section.blue, summary_section.green, summary_section.red, branch.sampling_date, branch.
        branchtype_id, branch.bheight, branch.baspect, branch.light_id, branch.measurement_date, branch.
        note_branch, branch.bstat_id, branch.bheight_branching, branch.bdiameter_branching, branch.
        blength_branching, branch.bstructuralorder_branching, individual.iheight, individual.crownbase_height
        , individual.idbh, individual.isocial_id, individual.bark_id, individual.icrown_at_light, individual.
        ileaf_losses, individual.inrsucchioni, individual.icancri_evolutivi, individual.icancri_cicatrizzati,
         individual.idamages, tree.date,  tree.coord_x, tree.coord_y, tree.aspect, tree.altitude, tree.slope,
         tree.microtopography_horizontal_id, tree.microtopography_vertical_id, tree.disturbances, tree.
        soil_depth, tree.rocks, tree.distance_waterbed, tree.waterbed_id, tree.origin_id, tree.nrpolloni,
        tree.circonf_base, tree.dbh, tree.height, tree.social_id, tree.crown_at_light, tree.leaf_losses, tree
        .nrsucchioni, tree.cancri_evolutivi, tree.cancri_cicatrizzati, tree.damages, tree.note_tree, tree.
        mass_tree_leaves_measured, tree.mass_tree_leaves_measured+tree.mass_tree_shoot_measured as
        mass_tree_shoot,tree.mass_tree_root_measured as  mass_tree_root, tree.waterstatus_id, tree.stat_id,
        tree.age_since_clearcut, site.locality, site.municipality, site.mean_aspect, site.note_site
120     FROM summary_section
121     LEFT JOIN branch USING (tree_id, individual_id, branch_id)
122     LEFT JOIN individual USING (tree_id, individual_id)
123     LEFT JOIN tree USING (tree_id)
124     LEFT JOIN site USING (site_id)
125     LEFT JOIN species USING (species_id);
126
127  ALTER TABLE v_section OWNER TO pipe;
128
129
130  CREATE OR REPLACE VIEW "v_section_noSingleSection" AS
131   SELECT v.species, v.site_id, v.tree_id, v.individual_id, v.branch_id, v.section_id, v.parentsection_id, v.
        structuralorder, v.ageorder, v.d_horizontal, v.d_vertical, v.cicatrice_riccio, v.lenght_maxpath, v.
        mass, v.nrcupules, v.nrflowers, v.nrdryleaves_notscanned, v.note, v.nr_leaves, v.larea, v.lholearea,
        v.llength, v.lwidth, v.lperimeter, v.lperimeter_convex, v.blue, v.green, v.red, v.sampling_date, v.
        branchtype_id, v.bheight, v.baspect, v.light_id, v.measurement_date, v.note_branch, v.bstat_id, v.
        bheight_branching, v.bdiameter_branching, v.blength_branching, v.bstructuralorder_branching, v.
        iheight, v.crownbase_height, v.idbh, v.isocial_id, v.bark_id, v.icrown_at_light, v.ileaf_losses, v.
        inrsucchioni, v.icancri_evolutivi, v.icancri_cicatrizzati, v.idamages, v.date, v.coord_x, v.coord_y,
        v.aspect, v.altitude, v.slope, v.microtopography_horizontal_id, v.microtopography_vertical_id, v.
        disturbances, v.soil_depth, v.rocks, v.distance_waterbed, v.waterbed_id, v.origin_id, v.nrpolloni, v.
        circonf_base, v.dbh, v.height, v.social_id, v.crown_at_light, v.leaf_losses, v.nrsucchioni, v.
        cancri_evolutivi, v.cancri_cicatrizzati, v.damages, v.note_tree,  v.mass_tree_leaves_measured, v.
        mass_tree_shoot,v.mass_tree_root, v.waterstatus_id, v.stat_id, v.age_since_clearcut,v.locality, v.
        municipality, v.mean_aspect, v.note_site, t.nr_sections4tree, i.nr_sections4individual, b.
        nr_sections4branch
132     FROM v_section v
133     LEFT JOIN ( SELECT min(v_section.tree_id::text) AS tree_id, count(*) AS nr_sections4tree
134             FROM v_section
135            GROUP BY v_section.tree_id) t USING (tree_id)
136     LEFT JOIN ( SELECT min(v_section.tree_id::text) AS tree_id,
137                        min(v_section.individual_id::text) AS individual_id , count(*) AS
                               nr_sections4individual
138              FROM v_section
139             GROUP BY v_section.tree_id, v_section.individual_id) i USING (tree_id, individual_id)
140     LEFT JOIN ( SELECT min(v_section.tree_id::text) AS tree_id,
141                        min(v_section.individual_id::text) AS individual_id ,
142                        min(v_section.branch_id) AS branch_id ,count(*) AS nr_sections4branch
143              FROM v_section
144             GROUP BY v_section.tree_id, v_section.individual_id, branch_id) b USING (tree_id, individual_id,
                    branch_id)
145    WHERE b.nr_sections4branch > 1
146    ORDER BY v.species,v.tree_id, v.individual_id, v.branch_id, v.section_id;
147
148  ALTER TABLE "v_section_noSingleSection" OWNER TO pipe;
149  ';
150
151    execute viewstmt;
152
153    dropstmt:='';                                                --drop remaning tables sx_y and temporary
          views
154    for i in 1..nrlevels+1 loop
155          dropstmt:=dropstmt||'s'||i::text||'_'||(nrlevels+1-i)::text||',';
156    end loop;
157    dropstmt:='DROP VIEW summary_leaf CASCADE;
158               DROP TABLE '||trim(trailing ',' from dropstmt)||' CASCADE;';
159
160    execute dropstmt;
161
162
163
164  end;
165  $BODY$
166    LANGUAGE plpgsql VOLATILE
167    COST 100;
168  ALTER FUNCTION create_hierarchy_tables(integer)
169    OWNER TO pipe;
```

Listing A.2: Code of function *create_ base_ hierarchy_ table*

```
1  -- Function: create_base_hierarchy_table(text, text)
2
3  -- DROP FUNCTION create_base_hierarchy_table(text, text);
4
5  CREATE OR REPLACE FUNCTION create_base_hierarchy_table(newtable text, sourcetable text)
```

```
  RETURNS void AS
$BODY$
declare
  statm varchar;
begin
  statm := 'CREATE TABLE '|| quote_ident(newtable)||' AS
 SELECT tree_id, individual_id, branch_id, section_id,
        CASE
            WHEN ((((((tree_id::text || '||quote_literal('-')||'::text) || individual_id::text) || '||
                 quote_literal('-')||'::text) || branch_id::text) ||  '||quote_literal('-')||'::text) ||
                 parentsection_id::text IN ( SELECT (((((tree_id::text || '||quote_literal('-')||'::text)
                 || individual_id::text) || '||quote_literal('-')||'::text) || branch_id::text) || '||
                 quote_literal('-')||'::text) || section_id::text
               FROM '|| quote_ident(sourcetable)||'
              WHERE parentsection_id > 0)) THEN parentsection_id
            ELSE NULL::integer
        END AS parentsection_id
   FROM '|| quote_ident(sourcetable)||'
  WHERE parentsection_id > 0 ;
  ALTER TABLE '||newtable||' OWNER TO pipe;';

  execute statm;
end;
$BODY$
  LANGUAGE plpgsql VOLATILE
  COST 100;
ALTER FUNCTION create_base_hierarchy_table(text, text)
  OWNER TO pipe;
```

Listing A.3: Code of function *create_first_hierarchy_table*

```
-- Function: create_first_hierarchy_table(text, text)

-- DROP FUNCTION create_first_hierarchy_table(text, text);

CREATE OR REPLACE FUNCTION create_first_hierarchy_table(newtable text, sourcetable text)
  RETURNS void AS
$BODY$
declare
  statm varchar;
begin
  statm := 'CREATE TABLE '|| quote_ident(newtable)||' AS
 SELECT section.tree_id, section.individual_id, section.branch_id, section.section_id, section.
      parentsection_id,
        coalesce(section.parentsection_id, section.section_id) AS newsection_id,
        (SELECT s.parentsection_id FROM '|| quote_ident(sourcetable)||' s
          WHERE s.tree_id::text = section.tree_id::text AND s.individual_id::text = section.individual_id::
               text
          AND s.branch_id = section.branch_id AND s.section_id = section.parentsection_id) AS
               newparentsection_id,
        (EXISTS ( SELECT sec.tree_id FROM '|| quote_ident(sourcetable)||' sec
          WHERE sec.tree_id::text = section.tree_id::text AND sec.individual_id::text = section.
               individual_id::text
          AND sec.branch_id = section.branch_id AND sec.parentsection_id = section.section_id)) AS isparent
   FROM '|| quote_ident(sourcetable)||' section;
   ALTER TABLE '||newtable||' OWNER TO pipe;';

  execute statm;
end;
$BODY$
  LANGUAGE plpgsql VOLATILE
  COST 100;
ALTER FUNCTION create_first_hierarchy_table(text, text)
  OWNER TO postgres;
```

Listing A.4: Code of function *create_next_hierarchy_table*

```
-- Function: create_next_hierarchy_table(text, text)

-- DROP FUNCTION create_next_hierarchy_table(text, text);

CREATE OR REPLACE FUNCTION create_next_hierarchy_table(newtable text, sourcetable text)
  RETURNS void AS
$BODY$
declare
  statm varchar;
begin
  statm := 'CREATE TABLE '|| quote_ident(newtable)||' AS
 SELECT section.tree_id, section.individual_id, section.branch_id, section.section_id, section.
      parentsection_id,
        coalesce(section.newparentsection_id,section.newsection_id) AS newsection_id,
        (SELECT s.parentsection_id FROM '|| quote_ident(sourcetable)||' s
          WHERE s.tree_id::text = section.tree_id::text AND s.individual_id::text = section.individual_id::
               text
           AND s.branch_id = section.branch_id AND s.section_id = section.newparentsection_id) AS
                newparentsection_id,
        (EXISTS ( SELECT sec.tree_id FROM '|| quote_ident(sourcetable)||' sec
          WHERE sec.tree_id::text = section.tree_id::text AND sec.individual_id::text = section.
               individual_id::text
           AND sec.branch_id = section.branch_id AND sec.parentsection_id = section.newsection_id)) AS
                isparent
   FROM '|| quote_ident(sourcetable)||' section;
   ALTER TABLE '||newtable||' OWNER TO pipe;';

  execute statm;
end;
```

```
$BODY$
  LANGUAGE plpgsql VOLATILE
  COST 100;
ALTER FUNCTION create_next_hierarchy_table(text, text)
  OWNER TO postgres;
```

Listing A.5: Code of function *part_view_summary_section_part*

```
-- Function: part_view_summary_section_part(text)

-- DROP FUNCTION part_view_summary_section_part(text);

CREATE OR REPLACE FUNCTION part_view_summary_section_part(tablename text)
  RETURNS text AS
$BODY$
declare
  statm varchar;
begin
  statm := 'SELECT min(tree_id::text) AS tree_id, min('||quote_ident(tablename)||'.individual_id::text) AS
       individual_id, min('||quote_ident(tablename)||'.branch_id) AS branch_id, min('||quote_ident(
       tablename)||'.newsection_id) AS section_id, count(*) AS count, sum(summary_singlesections.mass) AS
       mass, sum(summary_singlesections.nrcupules) AS nrcupules, sum(summary_singlesections.nrflowers) AS
       nrflowers, sum(summary_singlesections.nrdryleaves_notscanned) AS nrdryleaves_notscanned, sum(
       summary_singlesections.nr_leaves) AS nr_leaves, sum(summary_singlesections.larea) AS larea, sum(
       summary_singlesections.lhole_area) AS lholearea, sum(summary_singlesections.llength) AS llength, sum
       (summary_singlesections.lwidth) AS lwidth, sum(summary_singlesections.lperimeter) AS lperimeter, sum
       (summary_singlesections.lperimeter_convex) AS lperimeter_convex, sum(summary_singlesections.blue) AS
        blue, sum(summary_singlesections.green) AS green, sum(summary_singlesections.red) AS red
     FROM '||quote_ident(tablename)||'
     LEFT JOIN summary_single_sections summary_singlesections USING (tree_id, individual_id, branch_id,
          section_id)
     GROUP BY tree_id, '||quote_ident(tablename)||'.individual_id, '||quote_ident(tablename)||'.branch_id,
          '||quote_ident(tablename)||'.newsection_id
     ';

  return statm;
end;
$BODY$
  LANGUAGE plpgsql VOLATILE
  COST 100;
ALTER FUNCTION part_view_summary_section_part(text)
  OWNER TO pipe;
```

Appendix B

Methods of the system dynamics modeling part

Limiting functions

For convenience, two generic functions have been formulated to describe the influence of a limiting or activating factor. These functions return a value in the range [0,1].

If the needed limiting or activating influence appear to be reversed (Z shape instead of a S shape), $1 - f(x)$ should be used.

Linear function $f_{lim}(x)$

This function represents a linear limiting function.

$$f_{\text{lim}}\left(x, x_{lower}, x_{upper}\right) = \begin{cases} 0 & if\ x \leq x_{lower} \\ \dfrac{x - x_{lower}}{x_{upper} - x_{lower}} & if\ x \in]x_{lower}, x_{upper}[\\ 1 & if\ x \geq x_{upper} \end{cases}$$

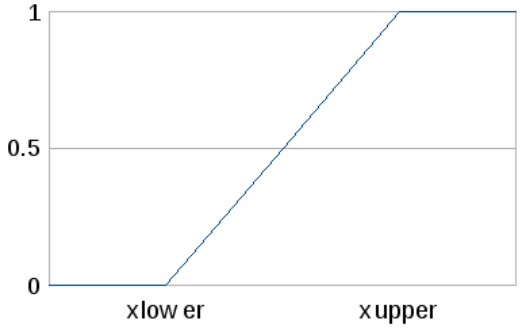

Sigmoid function $g_{lim}(x)$

This function behaves like a sigmoid function, truncated in the application range.

As a basis, the classical sigmoid function was used, in the form

$$sigm(x) = \frac{1}{1 + e^{-r(x - x_{shift})}}$$

which returns a shifted (x_{shift}) sigmoid function, with variable slope (depending from r).

This function was enhanced:

- to allow the control of the left and right truncation of the sigmoid shape, x_{shift} and r have been calculated from x_{lower}, x_{upper}, tr_{lower} and tr_{upper} (determining the degree of truncation of the sigmoid function). The last two parameters (tr_{lower} and tr_{upper}) correspond to the values of the general sigmoid function when cut at x_{lower} and x_{upper}:

$$\begin{aligned} tr_{lower} &= sigm(x_{lower}) \\ tr_{upper} &= sigm(x_{upper}) \end{aligned}$$

- to be scaled exactly from 0 to 1 for a given application range, so that $g_{lim}(x_{lower}) = 0$ and $g_{lim}(x_{upper}) = 1$

The resulting function is

$$g_{\text{lim}}(x, x_{lower}, x_{upper}, tr_{lower}, tr_{upper}) = \begin{cases} 0 & if\, x \leq x_{lower} \\ \dfrac{\dfrac{1}{1+e^{-r(x-x_{shift})}} - tr_{lower}}{1 - tr_{upper} - tr_{lower}} & if\, x \in]x_{lower}, x_{upper}[\\ 1 & if\, x \geq x_{upper} \end{cases}$$

with

$$x_{shift} = \frac{x_{lower} \ln\left(\frac{tr_{upper}}{1-tr_{upper}}\right) - x_{upper} \ln\left(\frac{1-tr_{lower}}{tr_{lower}}\right)}{\ln\left(\frac{tr_{upper}}{1-tr_{upper}}\right) - \ln\left(\frac{1-tr_{lower}}{tr_{lower}}\right)}$$

and

$$r = -\frac{\ln\left(\frac{1-tr_{lower}}{tr_{lower}}\right)}{x_{lower} - x_{shift}}$$

Following figure shows three curves drawn with this function (in brackets are the values used for the parameters tr_{lower} and tr_{upper}).

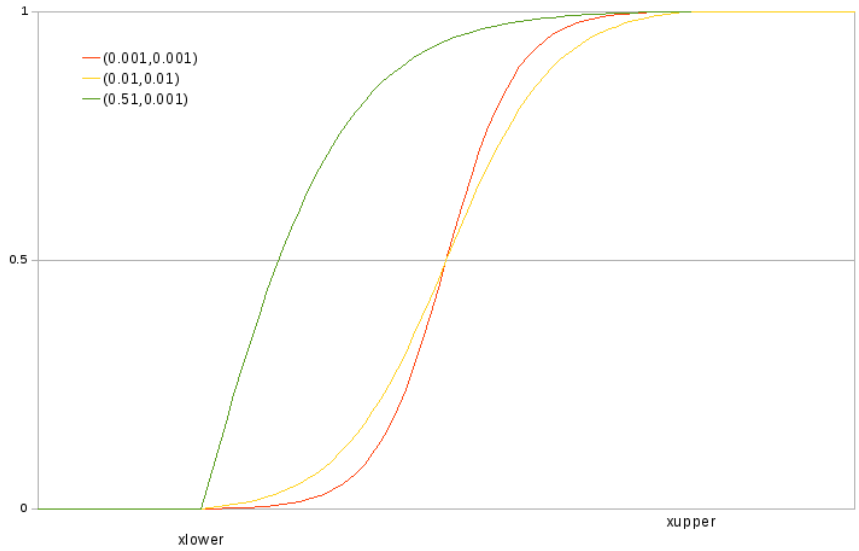
1
0.5
0
(0.001,0.001)
(0.01,0.01)
(0.51,0.001)
xlower
xupper

Implementation of the system dynamics models

The model development phase has been initially done with the Simile system dynamics simulation software (Muetzelfeldt & Massheder, 2003) of Simulistics Ltd (http://www.simulistics.com/). The possibility to specify formally and visually the models with simple drawing tools, to control model runs according to a play/pause/stop principle, and to display the model outputs through easily created plot or table monitors, gave the maximum flexbility for an agile and cooperative model development.

In a second phase the models have been implemented with the open source statistical program R-Cran (http://cran.r-project.org/), using the package *deSolve* (Soetaert *et al.* , 2010a,b), which allows a Matlab-like specification for solving differential equations. Although a steeper learning curve is needed, this allowed faster runtime execution and more flexibility compared to Simile, regarding the choice of ODE solvers and the availability of the huge amount of libraries available. I specified each model organizing the code into to five separate R files, namely *model.r* with the model definition, *params.r* with the parameters, *events.r* to handle specific events at certain time steps (e.g. biomass removal), *functions.r* for support functions, and *run.r*, containing the specification of initial values, the integration details and the output plotting instructions.

As an example, here following we add some details on the implementations of the generic model for herbaceous plants. A set of activation switches for growth, limitations (on flux speed, growth and photosynthesis), stomata, dessiccation were implemented, allowing a piecewise testing of the model, and a better understanding of the role and influence of the involved processes. Moreover the generic parameters kW and kC were defined, as multipliers of selected metabolic and transport rates in the water and carbon submodels, respectively. This allowed us to investigate the effects of a relative increase or decrease of the rates of a given submodel on the partitioning behaviour .

References

Muetzelfeldt, R, & Massheder, J. 2003. The simile visual modelling environment. *European journal of agronomy*, **18**, 345–358.

Soetaert, Karline, Petzoldt, Thomas, & Setzer, R Woodrow. 2010a. Solving differential equations in r. *The r journal*, **2**(2), 5–15.

Soetaert, Karline, Petzoldt, Thomas, & Setzer, R Woodrow. 2010b. Solving differential equations in r: Package desolve. *Journal of statistical software*, **33**(9), 1–25.

Simile

Simile model diagrams of the generic model of herbaceous plant, without interactions.

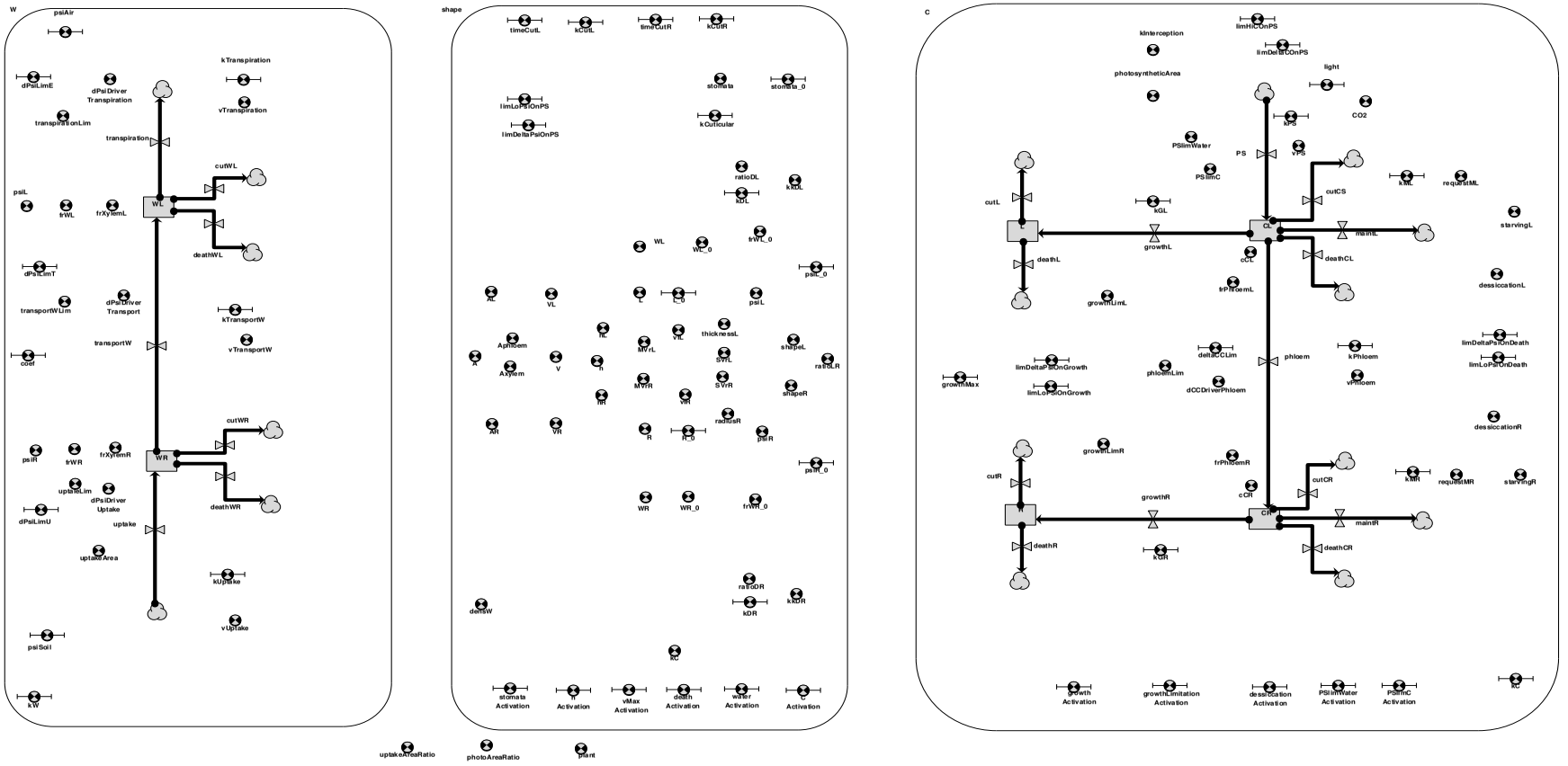
W
psiAir
kTranspiration
dPsiLimE
dPsiDriver Transpiration
vTranspiration
transpirationLim
transpiration
cutWL
psiL
frWL
frXylemL
WL
deathWL
dPsiLimT
transportWLim
dPsiDriver Transport
kTransportW
transportW
vTransportW
coef
cutWR
psiR
frWR
frXylemR
WR
uptakeLim
dPsiDriver Uptake
deathWR
dPsiLimU
uptake
uptakeArea
kUptake
vUptake
psiSoil
kW
shape
timeCutL
kCutL
timeCutR
kCutR
stomata
stomata_0
limLoPsiOnPS
limDeltaPsiOnPS
kCuticular
ratioDL
kDL
kdDL
WL
WL_0
frWL_0
psiL_0
AL
VL
L
L_0
psiL
thickressL
Aphloem
hL
MVrL
VrL
shapeL
A
AXylem
V
h
SVrL
ratioLR
MVrR
SVrR
shapeR
hR
VR
AR
VR
R
R_0
radiusR
psiR
psiR_0
WR
WR_0
frWR_0
deltaW
kDR
kdDR
kV
stomata Activation
lA Activation
vMax Activation
death Activation
water Activation
C Activation
uptakeAreaRatio
photoAreaRatio
plant
C
kInterception
limHiCOnPS
limDeltaCOnPS
photosyntheticArea
light
CO2
kPS
PSlimWater
PS
vPS
PSlimC
kML
requiredML
cutL
kGL
cutCS
starvingL
L
growthL
CL
mainL
deathL
cCL
deathCL
frPhloemL
dessiccationL
growthLimL
limDeltaPsiOnDeath
limLoPsiOnDeath
deltaCCLim
phloem
kPhloem
limDeltaPsiOnGrowth
phloemLim
vPhloem
growthMax
limLoPsiOnGrowth
dCCDriverPhloem
dessiccationR
growthLimR
frPhloemR
cutR
kMR
requiredMR
starvingR
cCR
cutCR
growthR
R
CR
mainR
deathR
kdR
deathCR
growth Activation
growthLimitation Activation
dessiccation Activation
PSlimWater Activation
PSlimC Activation
kV

R-Cran

Here following the codes of the model specification and the relative files. Note that some of the functions specified in *functions.r* are described in Section B.

Listing B.1: Code of script *model.r*

```

ipm <- function(t, state, parameters){

with(as.list(state),{



##shape
  VL = L/MVrL   #m^3
  VR = R/MVrR

  spaceL =VL / vfL    #m^3
  spaceR =VR / vfR
  hL = (3 * spaceL*2 / (4 * pi)) ^ (1/3)  #m  #equivalent radius of an half sphere
  hR = (3 * spaceR*2 / (4 * pi)) ^ (1/3)      #equivalent radius of an half sphere

  h = if (h_Activation==1) hL+hR else 1     #m

  AL = VL/hL     #m^2
  AR = VR/hR

  V = VL + VR     #m^3
  A = min(AL, AR) #m^2

  Aphloem = min(AL * frPhloemL, AR * frPhloemR)  #m^2
  Axylem  = min(AL * frXylemL, AR * frXylemR)

  photosyntheticArea = (VL*SVrL / 2 )^kInterception  #m^2
  uptakeArea         = VR*SVrR                       #m^2

  kCuticular =  kCuticular_0

##water
  frWL =  WL/(densW*VL*frXylemL)
  frWR =  WR/(densW*VR*frXylemR)

  psiL =  psi4theta(frWL,coef)    #MPa
  psiR =  psi4theta(frWR,coef)



  stomata = if (stomata_Activation==1) limit_lin_s(psiL,limLoPsiOnPS,limLoPsiOnPS+limDeltaPsiOnPS) else
       stomata_0

## carbon
  cCL = CL/(VL*frWL)    #kg/m^3
  cCR = CR/(VR*frWR)

  dCCDriverPhloem = (if (vMax_Activation==1) limit_sigm_s(abs(cCR-cCL),0*deltaCCLim,deltaCCLim/0.27, 0.51,
       0.001) else 1) *deltaCCLim*sign(-(cCR-cCL))  #kg/m^3

#       - Fluxes ########################################################################
## carbon

  limPS_W = if (limPS_W_Activation==1) limit_lin_s(psiL,limLoPsiOnPS,limLoPsiOnPS+limDeltaPsiOnPS) else 1
  limPS_C = if (limPS_C_Activation==1) limit_sigm_z(cCL, (limHiCOnPS-limDeltaCOnPS),limHiCOnPS,0.001,0.51)
       else 1

  PS= light*photosyntheticArea*kPS*(stomata+kCuticular)*limPS_C*limPS_W*CO2   #kg/day

  requestML     = kML*L    #kg/day
  requestMR     = kMR*R
  maintL        = requestML   #kg/day
  maintR        = requestMR
  starvingL     = if ((!is.na(maintL)) & requestML>maintL) 1-maintL/requestML else 0     #ratio
  starvingR     = if ((!is.na(maintR)) & requestMR>maintR) 1-maintR/requestMR else 0
  desiccationL  = desiccation_Activation*limit_lin_z(psiL,limLoPsiOnDeath,limLoPsiOnDeath+
       limDeltaPsiOnDeath)   #ratio
  desiccationR  = desiccation_Activation*limit_lin_z(psiR,limLoPsiOnDeath,limLoPsiOnDeath+
       limDeltaPsiOnDeath)
  ratioDL       = 0
  ratioDR       = 0
  kkDL          = if (death_Activation==1) kDL + ratioDL else 0    #1/day
  kkDR          = if (death_Activation==1) kDR + ratioDR else 0


  deathCL = CL*kkDL   #kg/day
  deathCR = CR*kkDR

  deathL = L*kkDL     #kg/day
  deathR = R*kkDR
  deathP = ratioP * deathL  #P*kkDL

  deathWL = WL*kkDL  #kg/day
  deathWR = WR*kkDR  #kg/day


  maxGrowthL = AL*growthMax
  maxGrowthR = AR*growthMax
```

```
86
87
88    limPhloem = if (is.na(cCL) | is.na(cCR) | cCR==cCL) 0 else dCCDriverPhloem/abs(cCR-cCL)
89
90    tmpflux=kPhloem*Aphloem/h*dCCDriverPhloem
91    signFlux = if (is.na(tmpflux)) 0 else sign(tmpflux)
92    phloem = tmpflux
93
94    limGrowthL = if (limGrowth_Activation==1) limit_lin_s(psiL,limLoPSiOnGrowth,limLoPSiOnGrowth+
          limDeltaPsiOnGrowth) else 1
95    limGrowthR = if (limGrowth_Activation==1) limit_lin_s(psiR,limLoPSiOnGrowth,limLoPSiOnGrowth+
          limDeltaPsiOnGrowth) else 1
96
97
98    growthL = growth_Activation * max(0, min(maxGrowthL, kGL*limGrowthL*cCL*AL))
99    growthR = growth_Activation * max(0, min(maxGrowthR, kGR*limGrowthR*cCR*AR))
100
101 ## water
102
103   dPsiDriverTranspiration = (if (vMax_Activation==1) limit_sigm_s(abs((psiAir-psiL)*(stomata+kCuticular))
          ,0,dPsiLimE/0.27, 0.51, 0.001) else 1) * dPsiLimE *sign(-(psiAir-psiL)) #MPa
104   dPsiDriverTransportW    = (if (vMax_Activation==1) limit_sigm_s(abs(psiL-psiR),0,dPsiLimT/0.27, 0.51,
          0.001) else 1) *dPsiLimT *sign(-(psiL-psiR))
105   dPsiDriverUptake        = (if (vMax_Activation==1) limit_sigm_s(abs(psiR-psiSoil),0,dPsiLimU/0.27, 0.51,
          0.001) else 1) *dPsiLimU *sign(-(psiR-psiSoil))
106
107   limTranspiration = dPsiDriverTranspiration /(abs(psiAir-psiL)*(stomata+kCuticular))
108   limTransportW    = dPsiDriverTransportW/abs(psiL-psiR)
109   limUptake        = dPsiDriverUptake/abs(psiR-psiSoil)
110
111   transpiration =  max(0, dPsiDriverTranspiration *kTranspiration* photosyntheticArea/ 100)
112   transportW    =  max(0, kTransportW* Axylem/h*dPsiDriverTransportW)
113   uptake        =  max(0, dPsiDriverUptake* kUptake* uptakeArea)
114
115
116
117 # - Monitor
118   vTranspiration = transpiration/densW/photosyntheticArea   #m/day
119   vTransportW    = transportW/densW/A                       #m/day
120   vUptake        = uptake/densW/AR
121   vPhloem        = phloem/A                                 #kg/day/m^2
122
123   vPS            = PS/photosyntheticArea                    #kg/day/m^2
124
125
126
127 #       - System ###################################################################
128
129   dWL <- transportW - transpiration - deathWL
130   dWR <- uptake - transportW - deathWR
131
132   dCL <- PS - phloem - maintL - growthL - deathCL
133   dCR <- phloem -maintR - growthR - deathCR
134   dP  <- growthP - deathP
135   dL  <- growthL - deathL
136   dR  <- growthR - deathR
137
138 list(
139         c(dL, dR, dCL, dCR, dWL, dWR),
140         c(psiAir= psiAir, psiL=psiL, psiR=psiR, psiSoil=psiSoil),
141   c(growthL=growthL, growthR=growthR),
142   c(maintL=maintL, maintR=maintR),
143   c(deathL=deathL, deathR=deathR),
144   c(starvingL=starvingL, starvingR=starvingR),
145   c(desiccationL=desiccationL, desiccationR=desiccationR),
146   c(PS = PS, phloem=phloem, uptake=uptake, transportW=transportW,transpiration=transpiration),
147   c(frWL=frWL, frWR=frWR, cCL=cCL, cCR=cCR),
148   c(dPsiDriverTranspiration=dPsiDriverTranspiration, dPsiDriverTransportW=dPsiDriverTransportW,
          dPsiDriverUptake=dPsiDriverUptake),
149   c(dCCDriverPhloem=dCCDriverPhloem),
150   c(limPhloem=limPhloem, limGrowthL=limGrowthL, limGrowthR=limGrowthR),
151   c(limTranspiration=limTranspiration, limTransportW=limTransportW, limUptake=limUptake),
152   c(stomata=stomata,limPS_C=limPS_C, limPS_W=limPS_W),
153   c(vTranspiration=vTranspiration, vTransportW=vTransportW, vUptake=vUptake),
154   c(VL=VL, VR=VR)
155   )
156
157         })
158 }
```

Listing B.2: Code of script *params.r*

```
1
2  #constants
3    densW = 1000  #kg/m3
4
5
6  ## global
7    kC      = 40
8    kW      =  1000
9
10 ## activation
11   growth_Activation      = 1
12   limGrowth_Activation   = 1
13   desiccation_Activation = 1
14   limPS_W_Activation     = 1
15   limPS_C_Activation     = 1
16
```

```
  stomata_Activation     = 1
  h_Activation           = 1
  vMax_Activation        = 1
  death_Activation       = 1
  water_Activation       = 1
  C_Activation           = 1


# Parameters

## input (environment)
  CO2     = 1       #kg
  light   = 1       #-
  psiAir  = -8      #MPa
  psiSoil = -1      #MPa

## carbon

  kPS       = kC*0.004   #1/day/m^2

  kGL       = kC*0.2 /0.05    #m/day
  kGR       = kC*1   /0.05    #m/day
  growthMax = kC*1000    #kg/d/m2

  kML       = kC*0.001       #1/day
  kMR       = kC*0.001       #1/day

  kDL       = kC*0.001#0.001       #1/day
  kDR       = kC*0.001#0.001       #1/day
  kStarving = 0.4

  ratioP  = 0. # 0.1

  kPhloem =  kC*4 /0.05    #m^2/day
  deltaCCLim = 44*2     #kg/m^3

  kInterception = 1

## water

  kTranspiration = kW*0.4     #day/m
  kTransportW    = kW*10      #day
  kUptake        = kW*0.002   #day/m

  dPsiLimE = 30   #MPa
  dPsiLimT = 30   #MPa
  dPsiLimU = 30   #MPa

  coef = 200


## anatomy
  frXylemL  = 0.1
  frXylemR  = 0.1
  frPhloemL = 0.05
  frPhloemR = 0.05

  thicknessL = 0.001  #m
  radiusR    = 0.0005 #m

  MVrL  = 600  #kg/m3
  MVrR  = 600  #kg/m3

  vfL = 0.01   # volume fraction
  vfR = 0.01   # volume fraction

  SVrL = 2/thicknessL    #1/m
  SVrR = 2/radiusR       #1/m



## limitations
  limLoPsiOnPS = -10     #MPa
  limDeltaPsiOnPS = 4

  limLoPsiOnDeath = -20
  limDeltaPsiOnDeath = 8

  limLoPSiOnGrowth = -8
  limDeltaPsiOnGrowth = 4

  limHiCOnPS = 0.08   #kg/m3
  limDeltaCOnPS = 0.04


## cut
  timeCutL = 0
  kCutL = 0.5
  timeCutR = 0
  kCutR = 0.4


#activation related

  kCuticular_0 = 0.1
  stomata_0 = 1
```

Listing B.3: Code of script *events.r*

```
eventfun <- function(t, y, parms){
  with (as.list(y),{
    if (t %in% timeCutL){
      L <- L * (1-kCutL)
      P <- P * (1-kCutL)
      WL <- WL * (1-kCutL)
      CL <- CL * (1-kCutL)
    }
    if (t %in% timeCutR){
      R <- R * (1-kCutR)
      WR <- WR * (1-kCutR)
      CR <- CR * (1-kCutR)
    }
    return(c(L, R, P, CL, CR, WL, WR))
  })
}
```

Listing B.4: Code of script *functions.r*

```
limit_lin_s   <- function(x,lower,upper) {ifelse(x<=lower,0,ifelse(x>=upper, 1, (x-lower)/(upper-lower)))}

limit_lin_z   <- function(x,lower,upper) {ifelse(x<=lower,1,ifelse(x>=upper, 0, -(x-upper)/(upper-lower)))}

limit_sigm_s   <- function(x,lower,upper,ltrunc,utrunc) {
  utruncReal =1-utrunc
  transX = (lower*log((1-utruncReal)/utruncReal)-upper*log((1-ltrunc)/ltrunc))/(log((1-utruncReal)/
       utruncReal)-log((1-ltrunc)/ltrunc))
  r = -log((1-ltrunc)/ltrunc)/(lower-transX)

  ifelse(x<=lower, 0, ifelse(x>=upper, 1, ((1/(1+exp(-r*(x-transX))))-ltrunc)/(utruncReal-ltrunc)))
}

limit_sigm_z   <- function(x,lower,upper,ltrunc,utrunc) {
  ltruncReal =1-ltrunc
  transX = (upper*log((1-ltruncReal)/ltruncReal)-lower*log((1-utrunc)/utrunc))/(log((1-ltruncReal)/
       ltruncReal)-log((1-utrunc)/utrunc))
  r = -log((1-ltrunc)/ltrunc)/(lower-transX)

  ifelse(x<=lower, 1, ifelse(x>=upper, 0, ((1/(1+exp(+r*(x-transX))))-utrunc)/(ltruncReal-utrunc)))
}
#% returns an effect [between 0 and 1] for a limiting factor (e.g. psi on photosysthesis)

topped   <- function(x,slope){(2/(1+exp(-2*slope*x))-1)}
#~ % returns a sigmoid starting from the turning point (returns 0) with a certain slope

psi4theta   <- function(theta,coef){(min(0,coef*(tan(theta - pi/2)+0.64)))}
theta4psi   <- function(psi,coef) {(atan(psi/coef-0.64) + pi/2)}
```

Listing B.5: Code of script *run.r*

```
# ipm model with protection
require(deSolve)

source('functions.r')
source('params.r')
source('events.r')
source('model.r')

#specify initial values of compartements
L. = 0.01
R. = 0.01
P. = L. * ratioP
CL. = L./600*0.05   * 10
CR. = R./600*0.05   * 10
VL. = L./MVrL
VR. = R./MVrR
WL. = VL.*frXylemL*densW * 0.98
WR. = VR.*frXylemR*densW * 0.99

state <- c(
  L = L.,
  R = R.,
  P = P.,
  CL = CL.,
  CR = CR.,
  WL = WL.,
  WR = WR.
)

#specify time step and interval
dt <- 1
times <- seq(0,500, by=dt)
eventtimes <- unique(nearestEvent(times,c(timeCutL,timeCutR)))
eventtimes <- eventtimes[eventtimes!=0]
solver = 'lsoda'

# solve ode
out <-as.data.frame(ode(state, times, ipm, parms=0, verbose=FALSE, method=solver,
                        events=list(func=eventfun,time=eventtimes)))
```

```
40
41
42
43  #plotting function
44  plotOut <- function (d,indices){
45    matplot(out[,1],out[,indices], type='l', lty=1, col=c('green', 'orange','brown','red'), xlab='Time (days)
          ', ylab = '')#'Biomass (KgC)')
46    legend('topleft', indices, col=c('deepskyblue', 'orange','brown','red'), bty='n', pch='_')
47  }
48
49
50  #plot results
51  out <- out[-1,]
52
53  pdf("plot_mass_conc.pdf",10,6)
54  par(mfrow=c(3,2))
55  par(mar=c(4,3,1,1))
56  plotOut(out,c('L','R'))
57  plotOut(out,c('CL','CR'))
58  plotOut(out,c('WL','WR'))
59  plotOut(out,c('psiAir','psiL','psiR','psiSoil'))
60  plotOut(out,c('frWL','frWR'))
61  plotOut(out,c('cCL','cCR'))
62
63  plotOut(out,c('transpiration','transportW','uptake'))
64  plotOut(out,c('PS','phloem'))
65  plotOut(out,c('vTranspiration','vTransportW','vUptake'))
66  plotOut(out,c('limGrowthL','limGrowthR','limPhloem'))
67  plotOut(out,c('limTranspiration','limTransportW','limUptake'))
68  plotOut(out,c('stomata','limPS_W','limPS_C'))
69
70  plotOut(out,c('growthL','growthR'))
71  plotOut(out,c('maintL','maintR'))
72  plotOut(out,c('deathL','deathR'))
73  plotOut(out,c('starvingL','starvingR'))
74  plotOut(out,c('desiccationL','desiccationR'))
75  plotOut(out,c('VL','VR'))
76
77  dev.off()
78
79  pdf("plot_allocation.pdf",6,6)
80  plot(L~R,data=out)
81  dev.off()
```